Modulating anxiety with extrasynaptic inhibition

Inauguraldissertation

Zur Erlangung der Würde eines Doktor der Philosophie vorgelegt der
Philosophisch-Naturwissenschaftlichen Fakultät der Universität Basel
von

Paolo Botta

aus Cagliari, Italien

Basel 2014

Genehmigt von der Philosophisch - Naturwissenschaftlichen Fakultät auf Antrag von

Prof. Dr. Andreas Lüthi
(Fakultätsverantwortlicher und Dissertationsleiter)

Prof. Dr. Thomas Mrsic-Flogel
(Korreferent)

Prof. Dr. Jörg Schibler
(Dekan)

Basel, den 20.05.2014

“The only thing we have to fear is fear itself”

Franklin D. Roosevelt

Abbreviations.. 11

Abstract.. 13

Introduction.. 15

Fear and Anxiety.. 18

Models.. 20

Fear models.. 20

Anxiety models.. 21

Role of inhibition in fear and anxiety.. 23

Phasic inhibition.. 24

Tonic inhibition.. 25

GABA_A receptor trafficking.. 28

Brain structures involved in fear and anxiety.. 31

Amygdala.. 31

General structure.. 32

Basolateral amygdala.. 33

Central amygdala.. 34

Microcircuitry.. 36

Plasticity.. 38

Aim of the study.. 41

Material and Methods.. 43

Animals.. 45

Slice electrophysiology.. 45

Morphological reconstruction.. 46

Combined single unit recording and in vivo pharmacology.. 46

Behavior.. 48

Auditory fear conditioning... 48

Open field paradigm... 49

Elevated plus maze... 49

Virus injection... 49

Optogenetic experiments... 50

Immunohistochemistry... 50

Cre regulated knockdown of alpha5 subunit... 51

Results

Results... 53

Tonic firing on anxiety and fear generalization.................................... 55

Physiological control of the tonic firing... 59

Fear-induced specific extrasynaptic plasticity.. 64

The α_5GABA$_A$R on anxiety and fear generalization..................................67

Supplementary material... 71

CEA microcircuitry... 73

Morphology of CEA neurons... 73

Connectivity of CEA neurons... 75

Pharmacology of GABAergic inhibition of CEA neurons............................ 78

Extrasynaptic inhibition in CEA...78

GABAergic synaptic events of PKCδ$^+$ neurons.................................... 81

Role of spillover on the extrasynaptic inhibition...................................... 81

Spontaneous gating of the GABAAR-mediated extrasynaptic inhibition................ 82

Role of central amygdala GABAergic inhibition on fear and anxiety................ 84

Associative learning on the GABAergic inhibition of CEA neurons.................. 84

Extrasynaptic inhibition is not affected in constitutive alpha5 KO.................. 85

Associative learning on GABAergic synaptic events……………………………………….... 86

Role of α_5GABAR mediated inhibition in CEA on anxiety……………………………..… 87

Tonic firing on tone responsiveness………………………………………………..88

Discussion…………………………………………………………………...91

References………………………………………………………………... 101

Acknowledgements………………………………………………………….111

Curriculum Vitae……………………………………………………….... 113

Abbreviations

BLA	Basolateral amygdala
BNST	Bed nucleus of the stria terminalis
CEA	Central amygdala
CEl	Central lateral amygdala nucleus
$\mathrm{CEl}_{\mathrm{off}}$	CS^+ -inhibited CEl neuron
$\mathrm{CEl}_{\mathrm{on}}$	CS^+ -excited CEl neuron
CEm	Central medial amygdala nucleus
CFP	Cyan fluorescence protein
CRH	Corticotrophin-releasing hormon
CS^-	Acoustic cue unpaired with the US
CS^+	Acoustic cue paired with the US
EPI	Epi-fluorescence
GABA	γ-aminobutyric acid
$\mathrm{GABA}_{\mathrm{A}}\mathrm{R}$	GABA A type receptor
GFP	Green fluorescent protein
IR DIC	Infrared
LTP	Long term potentiation
NMDAR	N-methyl-D-aspartate
PKA	Protein kinase A
$\mathrm{PKC}\delta^-$	Protein kinase Cδ not expressing neurons in CEl
$\mathrm{PKC}\delta^+$	Protein kinase Cδ expressing neurons in CEl
SOM^-	Somatostatin not expressing neurons
SOM^+	Somatostatin expressing neurons
US	unconditional stimulus (shock)
*vl*PAG	ventral lateral periacqueductal gray matter

Abstract

Traumatic experiences and stress can lead to complex behavioral adaptations, including increased levels of anxiety and fear generalization. The neuronal mechanisms underlying such maladaptive behavioral changes are, however, poorly understood. Numerous studies have indicated that, in both animals and humans, the amygdala is a key brain structure encoding for fear and anxiety. Further, it was recently hypothesized, and indeed is still a matter of discussion, that the role of protein kinase Cδ (PKCδ) isoform-expressing neurons in the lateral nucleus of the central amygdala is specific to encoding for fear generalization to an unconditional stimulus.

Classically, sensory cortico-thalamic information is processed and transferred from the basolateral to the central nucleus of the amygdala; the latter of which is considered this circuit's primary output structure. Central amygdala neurons thereby project to brain regions involved in the expression of fear and anxiety. Interestingly, it was recently found that fear conditioning induced cell-type-specific plasticity in three distinct neuronal subtypes of the central amygdala. In addition to a phasic change response, the spontaneous firing of defined neuronal populations was changed and predicted fear generalization of behavioral responses to an unconditional cue.

Yet, the direct involvement of particular neuronal classes on anxiety and fear generalization to an unconditioned sensory stimulus remains elusive. Further, mechanisms underlying such changes in tonic activity in central amygdala followed by a traumatic experience are not known. It has been shown in other brain areas that tonic activity can be modulated by GABAergic inhibition. In particular, GABAergic tonic currents are well-suited for this task because they exert a continuous dampening of cell-excitability and reduce the integration of excitatory inputs within neurons.

My PhD research focused predominantly on causally defining a specific physiological mechanism by which the change in tonic activity of defined neuronal CEA subtypes control behavioral emotional responses. To gain genetic access to these particular neuronal populations, a transgenic mouse line was used in combination with an array of *state-of-the-art* techniques.

Here, we identify a specific cell-type located in the central nucleus of the amygdala as a key mediator of stress-induced anxiety and fear generalization. Moreover, we show that acute stress regulates the activity of these cells by tuning extrasynaptic inhibition mediated by specific alpha5 subunit containing $GABA_A$ receptors. Our findings demonstrate that the neuronal circuitries of fear and anxiety overlap in the central amygdala and indicate that complex changes in fear and anxiety behavior can be driven by discrete molecular mechanisms in distinct neuronal cell types.

INTRODUCTION

Animals must adopt the right defense in order to survive. These defenses can be innate, or are learned upon life experience and adapted to discriminate different environmental conditions to evaluate risks and benefits. Emotions have been hypothesized to be a biological strategy for rapidly integrating previously recorded data (weighted for significance), assigning a motivational value to the stimulus, and orchestrating an appropriate behavioral response (Tooby and Cosmides 1990; Nieh, Kim et al. 2013). Undeniably, emotions are physiological, cognitive, and behavioral response patterns, shaped by natural selection, that engender selective advantages in particular situations and increase the ability to cope with threats or to seize opportunities.

One peculiarity is that emotions are shaped and elicited by life experiences. In order to learn and memorize emotions, the animal's brain is equipped with multiple, specialized areas. These are subsequently divided into smaller regions composed of micro-circuits involved in coding, acquisition, and short- and long-term storing of neuronal information. Damage of particular brain areas, caused by degenerative processes or physical insults, can result in the impairment of certain learning tasks and normal cognitive function.

In general, learning and memory storage occurs on both molecular and cellular scales. Changes in the strength of synapses have been repeatedly suggested as the cellular mechanism underlying memory formation (Cajal 1909 - 1911; Hebb 1949)(Eccles 1965; Kandel and Spencer 1968). Furthermore, *Hebbian cell assembly theory* (Hebb 1949) proposes an explanation for the adaptation of neurons during the learning process. It hypothesizes that the assemblage of neurons that are co–activated during the learning process undertake plastic changes to strengthen their connections, thereby becoming the engram of that memory (Citri and Malenka 2008).

The description of long - term potentiation (LTP) of synaptic transmission (Bliss and Lomo 1973) and its inverse counterpart, long - term depression (LTD) (Lynch, Dunwiddie et al. 1977), provided the necessary physiological support for the basis of memory formation in synaptic plasticity (Citri and Malenka 2008). Considerable progress has been made since these salient findings, such that the mechanisms of synaptic plasticity at excitatory synapses and their involvement in memory formation are now well understood (Martin, Grimwood et al. 2000; Malenka and Bear 2004; Sjostrom, Rancz et al. 2008). However, functional plasticity at inhibitory synapses is more poorly characterized, but it is believed to play an important role in adaptation of neural excitability in the central nervous system. Indeed, physiological dysfunctions in this form of plasticity are known to underlie various emotional disorders, including anxiety (Luscher and Keller 2004).

Fear and anxiety

Dangerous or potentially threatening situations trigger defensive, conditioned and unconditioned responses such as fear and anxiety. Ethological analyses of defensive behaviors in rodents suggest that fear and anxiety are two separate entities elicited by dissimilar threat predictability and behavioral outcome. Fear is considered an acute, stimulus-specific emotional response to a known or discrete threat (or cue). Fear rises and dissipates rapidly with the occurrence of imminent or sudden danger that elicits active defensive behaviors, such as freezing and flight. On the other hand, anxiety is a sustained, generalized emotional response to an unknown or less predictable threat. Anxiety is the negative prediction of a potential threat and often results in an apprehensive mood. This is typically accompanied by increased arousal and vigilance, which may last for extended periods (days to weeks) (Davis, Walker et al. 2010).

Evolutionary theories support the hypothesis that fear and anxiety increase Darwinian fitness under adverse situations which may threaten reproductive resources. Despite the importance of these two emotional states, it is essential that they fit adaptive challenges without negatively impacting daily activity (Marks and de Silva 1994; Davis, Walker et al. 2010). It is striking then that, according to recent reports, 28% of U.S. inhabitants experience some form of anxiety-related disorders throughout their lifetime. These conditions often dramatically impair individual quality of life and can incur high financial costs of treatment.

Anxiety disorders in humans are common, yet complex, pathologies associated with unnecessary fear and avoidance in response to specific objects or situations but also to unknown dangers (Shin and Liberzon 2010). There are six types of anxiety disorders that are classified by the *Diagnostic and Statistical Manual of Mental Disorders* (*DSM)*: post-traumatic stress disorder (PTSD), panic disorder, social phobia, specific phobia, obsessive-compulsive disorder, and generalized anxiety disorder.

Interestingly, of these disorders, PTSD is triggered by a particular traumatic experience, such as combat, rape, natural disorders, torture, and more. It is important to note that the intensity and duration of the trauma are not the only risk factors since individual predisposition (e.g., preexisting traits and pre- or posttraumatic life events) dictates the basis and strength of the condition.

PTSD is associated with three main symptoms that occur for a minimum of one month and impair social, occupational or interpersonal function. They are *re-experiencing* (traumatic memory), *avoidance* (generalized emotional and social withdrawal), and *hyperarousal* (insomnia, impaired concentration, increase startle responses) (Yehuda and LeDoux 2007).

It is thought that PTSD is a sign of strong associative learning, analogous to models that include Pavlovian fear conditioning where a neutral stimulus elicited a strong fear response only after being associated with a noxious stimulus. Interestingly, associative fear-learning paradigms trigger high but variable levels of anxiety that are associated to the traumatic experience. It is clear that inter-individual variability also plays a role (Davis, Walker et al. 2010).

Models

It is fundamental to understand the functioning of brain systems during different emotional states in order to develop treatments to ameliorate negative side effects induced by these pathologies.

However, we are still far from appreciating the nature of these physiological perturbations in specific micro-circuitries in the human brain due to the technical limitations of modern non-invasive systems. Animal models, on the other hand, remain an integral system to understand disorder etiology and to evaluate potential treatments for predictive efficacy in humans. Mouse models are most commonly used owing to comparable anatomy and physiology, with respect to humans. Moreover, genetic manipulation of mice is now commonplace. Consequently, many novel experimental approaches have been developed to powerfully study precise neuronal subclasses and the physiological and pathological ways impinging on them.

Given that the key component of anxiety is excessive fear, it is not surprising that the search for the neuro-circuitry of anxiety disorders is frequently combined with animal models.

Fear models

PTSD and fear can be powerfully modeled, at least by some aspects, using a Pavlovian fear conditioning paradigm in which a specific cue (tone, light or context) elicits the fear response. This simplistic model of fear acquisition is becoming recognized for its use in the study of certain aspects of post-traumatic stress disorders and phobias (Shin and Liberzon 2010). It is improbable that simple fear conditioning alone provides a sufficient model of the complexities of PTSD. Nevertheless, one significant aspect of PTSD is that an asymptomatic patient (that had previously undergone to a strong traumatic experience) may become symptomatic again by exposure to a new stressor (Yehuda and LeDoux 2007).

Classically, in fear conditioning, the subject is exposed to the conditioned stimulus (CS), which is initially neutral, paired with an unconditioned, noxious stimulus (US). In mice, a common US is delivery of an electrical footshock. Thus, after multiple pairings between the CS and US, the CS gains aversive properties and, on subsequent presentation, triggers fear reactions in the absence of the US. In rodents, fear responses comprise changes in blood pressure and heart rate, release of stress hormones, analgesia and facilitation of reflexes (LeDoux 2000; Fanselow and Poulos 2005). A range of active and passive defensive behaviors can also be triggered by fearful stimuli, depending on their timing, proximity, context, and intensity (Adolphs 2013). Aversive stimuli presented in innocuous environments mainly trigger freezing behavior. Freezing is an innate defensive behavior evolved to avoid detection by predators (LeDoux 2000; Fanselow and Poulos 2005). Since freezing is marked as an immobile posture due to the strong muscle contraction, it is easily measured and is considered the principal experimental readout to quantify fear responses (LeDoux 2000; Fanselow and Poulos 2005). The ability to precisely control stimuli in combination with a robust behavioral response makes classical fear conditioning a reliable and physiologically relevant model system.

It is fundamental for the animal survival to discriminate between cues predicting danger or safety signals. Experimentalists overcome this potential confound by use of a *discriminatory auditory fear conditioning paradigm* (Ciocchi, Herry et al. 2010; Likhtik, Stujenske et al. 2014). In this case, during conditioning, a second tone is given, in addition to the tone paired with the US (CS^+), but it is not paired with a noxious stimulus (CS^-). On the retrieval day mice, tend to highly freeze to the cue predicting aversion (CS^+), but show reduced or absent freezing when presented with the CS^-. The variability of freezing to the CS^- shows that rodents, as humans, are differentially frightened and may generalize to multiple cues even if these are not associated with a threat. Generalization is considered as the inability of the test animal to distinguish between tones other than the one paired with the footshock. The variability of fear generalization in the animal population is interesting because it is associated with a range of anxiety disorders in humans (Likhtik, Stujenske et al. 2014). Risk factors for such variability are certainly reconcilable to the individual genetic background that could shape the behavioral outcome induced by single environmental experiences with different intensity and type (Yehuda and LeDoux 2007).

Fear conditioning triggers not only fear learning association but also awareness to unpredictable threats resulting in high levels of anxiety that depends from the genetic and previous traumatic/rewarding individual experiences (Yehuda and LeDoux 2007; Shin and Liberzon 2010).

Interestingly, anxiety levels correlates with fear generalizations in rodents and humans (Duvarci, Bauer et al. 2009).

Anxiety models

Anxiety behavior, as a separate entity from fear, can be studied using different behavioral paradigms and, as previously mentioned, be triggered by fear a conditioning paradigm. These behavioral procedures take advantage of rodents' natural tendency to display anxiety-like behavior in open spaces due to anticipated exposure to predators. Several behavioral assays are commonly used to measured anxiety states and all of them use open spaces or ambiguous contextual cues in order to elicit unpredictability. In addition, all of these paradigms are sensitive to anxiolytic drugs when delivered *in vivo* to specific brain regions (Menard and Treit 1999).

The open field paradigm, developed by Hall and Ballachey (Hall and Ballachey, 1932), is a commonly qualitative and quantitative measure of locomotor activity, willingness to explore, and subsequently anxiety (Fisher, Stewart et al. 2007). This consists of a wide arena (>40 cm^2) were the animal is placed and can freely move and explore the new context. Rodents are prone to remain close to the walls, in order to hide themselves from unpredicted predators, thus infrequently crossing the arena's center. The open field resembles an animal's approach-avoidance conflict test because the animal is forced to explore the novel surrounding (Blanchard, Lackner et al. 2008).

Open field behavior is also highly sensitive to motor impairments and must be controlled with another anxiety paradigm such as the elevated plus maze (EPM). The latter is based on a conflict between the tendency of rodents to explore a novel environment and the aversive properties of the open arms (Pellow, Chopin et al. 1985). The animal is placed on the center of a maze composed of two closed arms perpendicular to two open arms. The animal then balances exploration behavior with the tendency to hide. Mice, as do rats, generally spend more time in the closed arms, which may be considered as a safe context (Montgomery and Segall 1955).

Systemic injections of anxiolytic doses of benzodiazepines, that are comparable with human treatments, increase the time that the animal spends in the open arms of a plus maze (Handley and Mithani 1984).

Role of inhibition in fear and anxiety

Generalized anxiety disorders, panic anxiety, but also sleep disturbances and epilepsy, including status epilepticus, are pathologies ameliorated by enhancing inhibitory neurotransmission largely mediated by γ-aminobutyric acid (GABA), acting through GABA type A receptors ($GABA_A$Rs) in the central nervous system (Malizia 2002; Lydiard 2003; Rudolph and Mohler 2006).

Like other members of the cysteine-loop ligand-gated ion channel family, such as nicotinic acetylcholine, glycine and 5-hydroxytryptamine type 3 (5-HT3) receptors, $GABA_A$ receptors are pentameric assemblies of subunits that form a central ion channel that is highly permeable to chloride (Farrant and Nusser 2005; Luscher, Fuchs et al. 2011).

$GABA_A$R subunits are encoded by 19 different genes that have been grouped into eight subclasses based on sequence homology (α_{1-6}, β_{1-3}, γ_{1-3}, δ, ε, θ, π, ρ_{1-3}) (Luscher, Fuchs et al. 2011). All of these subunits share a common ancestral structure that includes an extracellular N-terminal domain, four transmembrane domains (TM1-4), and an extended cytoplasmic loop region between TM3 and TM4 mediating interactions with trafficking and signaling factors important in plasticity (Alldred, Mulder-Rosi et al. 2005) (Figure 1).

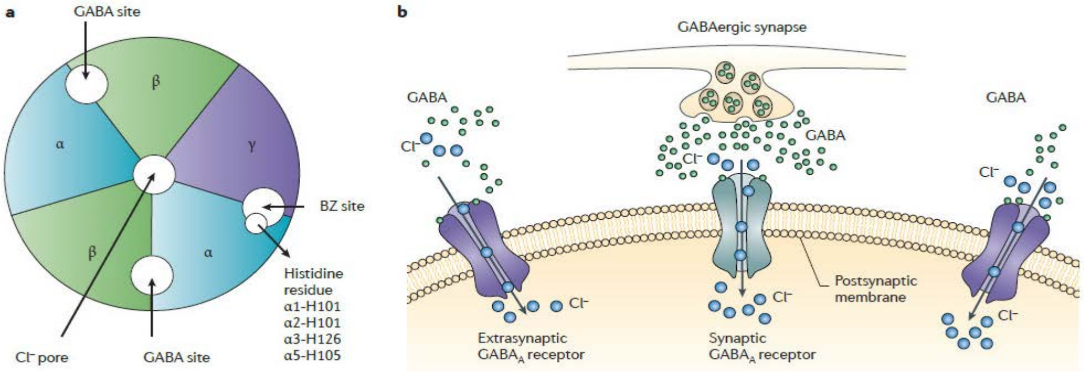

Figure 1. $GABA_A$R structure and location. a | Pentameric structure of the $GABA_A$R showing the pore permeable to chloride ions, the two GABA binding sites between α and β subunits, the benzodiazepine binding site (BZ site). In this latter site, histidine residues confer sensitivity to benzodiazepine. Importantly, a histidine to arginine mutation in the α subunit confers lack of sensitivity. **b** | Synaptic (*turquoise*) versus extrasynaptic (*violet*) location of $GABA_A$Rs (adapted from Rudolph and Knoflach, 2011).

Various kinetic schemes propose that $GABA_A$Rs transiently change their conformation from closed, to open, to a desensitized state either due to the presence of GABA or also through a spontaneous gating process (Luscher and Keller 2004). Subunit heterogeneity confers variability in kinetic properties. Further, localization of these receptors in the synaptic versus extrasynaptic space is fundamental in generating pharmacologically distinct patterns of neuronal inhibition, specifically, *the phasic* and *the tonic inhibition*.

Phasic inhibition

Phasic inhibition is important in synaptic signaling and allows a rapid and precise temporal transmission with the presynaptic input into the postsynaptic signal.

Receptors containing a γ_2 subunit in association with α_1, α_2, or α_3 subunits are the predominant receptor subtypes that mediate phasic synaptic inhibition. Freeze-fracture replica immunogold labeling indicates that α_2, α_3, and β_3 subunit-containing receptors are 50–130 times more concentrated at synapses than in the extrasynaptic membrane (Kasugai, Swinny et al. 2010). Clustering of synaptic $GABA_AR$s seems to be primarily caused by the binding of γ2 subunit with the $GABA_AR$- associated protein Gephyrin (Essrich, Lorez et al. 1998).

The action potential arriving at the presynaptic terminal triggers calcium influx causing the fusion of vesicles that liberate thousands of GABA molecules into the synaptic cleft. A small number of clustered synaptic $GABA_AR$s located in the postsynaptic side experience a rapid GABA transient that reach millimolar concentrations allowing their near-synchronous activation. Individual inhibitory postsynaptic currents (IPSCs), which arise from synaptic contacts, transiently inhibit neurons for 10–100 ms.

Single vesicle release induces a miniature inhibitory post-synaptic current (mIPSC) that have a rapid onset, a rise time of few hundred microseconds and a slower decay time (Figure 2a). The rise time is influenced by the concentration of GABA released, the distance between the release site and the post-synaptic active zone, the speed of the transition between closed to open state. The decay time is influenced by the kinetics of GABA clearance from the synapse, the transition from open to desensitized state, and the binding between GABA and its receptor (Farrant and Nusser 2005). Phasic inhibition sets rhythmic activity of neuronal networks, such as theta and gamma frequency network oscillations in different brain areas. Furthermore, rapid GABA inhibition allows high frequency synchronization of large populations of neurons in the hippocampus (Cobb, Buhl et al. 1995; Galarreta and Hestrin 2001; Jonas, Bischofberger et al. 2004; Somogyi and Klausberger 2005) and other brain regions (Perez-Orive, Mazor et al. 2002).

Spatially segregated inhibitory postsynaptic potentials (IPSPs), consisting of phasic inhibition, and originating from different GABAergic neuronal subtypes, are strongly involved in synaptic integration of excitatory inputs at the postsynaptic level. Location of the synapse, but also the timing of inhibition relative to the excitatory inputs, confers the impact of phasic GABA-mediated input on synaptic excitatory integration in a small and precise time window (Pouille and Scanziani 2001; Gulledge and Stuart 2003).

Synaptic $GABA_ARs$ seems to be involved in anxiety, sleep processes, schizophrenia, alcohol dependence and anesthesia (Rudolph and Knoflach 2011).

Tonic inhibition

As previously demonstrated, low concentrations of the $GABA_AR$ competitive antagonist SR-95331 (gabazine) completely blocked spontaneous IPSCs in hippocampal neurons without affecting a continuous GABAergic inhibition (Semyanov, Walker et al. 2003). This slower form of GABAergic signaling, called t*onic* or *extrasynaptic inhibition,* sustains constant inhibition that strongly controls cellular excitability (Mitchell and Silver 2003) (Figure 1c).

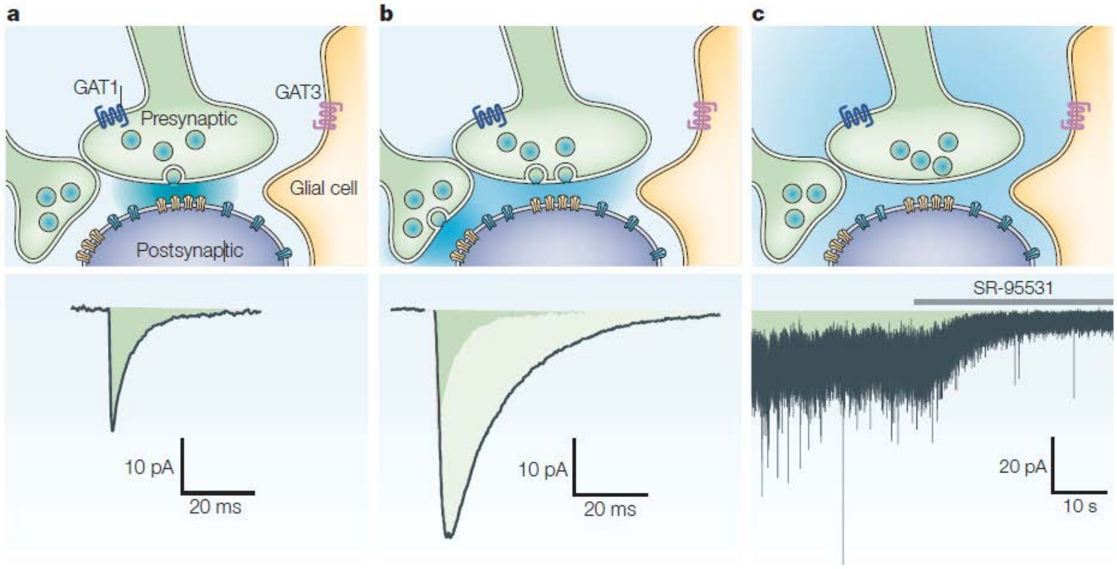

Figure 2. Types of GABAergic inhibition. a | Single vesicle release from a presynaptic terminal leads to the activation of synaptic $GABA_ARs$ clustered (*yellow*) in the postsynaptic side. GABA diffusion is indicated by the blue shading. Recording of single quantal release (mIPSC) induced by the activation of this synaptic cluster (*down the scheme*) independent by TTX application. The trace is filled with a green shadow to indicate the charge transfer. **b** | Action potential- dependent GABA release induces the fusion or more vesicles causing a bigger diffusion of GABA also to the perisomatic and extrasynaptic $GABA_ARs$ (*blue*). The recorded average trace shows larger and slower time course IPSC in comparison to the previous mIPSC. The charge transfer is indicated by the light green filling superimposed to the mIPSC charge transfer. **c** | Despite the presence of GABA transporters (GAT1 and GAT3), a low concentration of ambient GABA persists being able to constantly activate extrasynaptic $GABA_ARs$. The trace shows fast synaptic events that are superimposed to a "noisy" tonic current caused by the stochastic opening of extrasynaptic $GABA_ARs$. Application of gabazine (10 μM) causes a shift in the holding current. Green shaded filling show the massive charge transfer carried by the tonic current. Recordings were performed from cerebellar granule cells using whole-cell patch-clamp technique at -70 mV using a CsCl-based internal solution (adapted from Farrant and Nusser, 2005).

The first evidence of the existence of tonic inhibition was shown in rat cerebellar granule cells in voltage-clamp experiments. The $GABA_A$ receptor antagonists, bicuculline and gabazine, blocked spontaneously occurring IPSCs and decreased the 'holding' current that was required to clamp the cells at a given membrane potential (Kaneda, Farrant et al. 1995; Brickley, Cull-Candy et al. 1996; Wall and Usowicz 1997). Subsequently, other studies indicated that GABA-mediated tonic conductance exist in many other neuronal populations such as granule cells of the dentate gyrus (Nusser and Mody 2002; Stell and Mody 2002), CA1 pyramidal cells (Bai, Zhu et al. 2001), subtypes of inhibitory interneurons in the CA1 region of the hippocampus, striatal spiny neurons (Semyanov, Walker et al. 2003; Ade, Janssen et al. 2008), thalamocortical relay neurons of the ventral basal complex (Porcello, Huntsman et al. 2003), layer V pyramidal neurons in the somatosensory cortex (Yamada, Okabe et al. 2004), Layer IV pyramidal neurons in barrel cortex (Urban-Ciecko, Kossut et al. 2010), and *corticotrophin-releasing factor* receptors- expressing neurons in central amygdala (Herman, Contet et al. 2013).

Tonic inhibition is mediated by extrasynaptic $GABA_ARs$ containing the δ subunit (in combination with α_1, α_4, and α_6) and $\alpha_5\beta\gamma$ subunits. These do not co-localize with synaptic structural proteins, thereby occluding synaptic clustering, and are widely expressed in the dendritic, somatic and axonal compartments (Brunig, Scotti et al. 2002; Crestani, Keist et al. 2002; Caraiscos, Elliott et al. 2004; Biro, Holderith et al. 2006; Serwanski, Miralles et al. 2006; Glykys, Mann et al. 2008; Zarnowska, Keist et al. 2009).

Unlike synaptic $GABA_ARs$, the extrasynaptic forms exhibit high affinity for GABA (at nanomolar concentration), slow and low desensitization (Farrant and Nusser 2005), and in some cases exhibit spontaneous gating (McCartney, Deeb et al. 2007). These kinetic properties are well-suited for continuous activation by the low extrasynaptic GABA concentrations which arise via spillover from the synaptic cleft to the extrasynaptic space (Kaneda, Farrant et al. 1995) and GABA clearance uptake induced by GABA transporters (Rossi, Hamann et al. 2003; Farrant and Nusser 2005).

Most of the studies that clarify the role of this persistent inhibitory conductance in cellular excitability were performed in cerebellar granule cells because they express a strong extrasynaptic inhibition (Kaneda, Farrant et al. 1995) and, due to their small size, are considered single electrical compartments (Silver, Traynelis et al. 1992).

Electrophysiological experiments in slices demonstrated that tonic inhibition decreases the size and duration of excitatory postsynaptic potentials and it narrows the spatial and temporal window of synaptic integration.

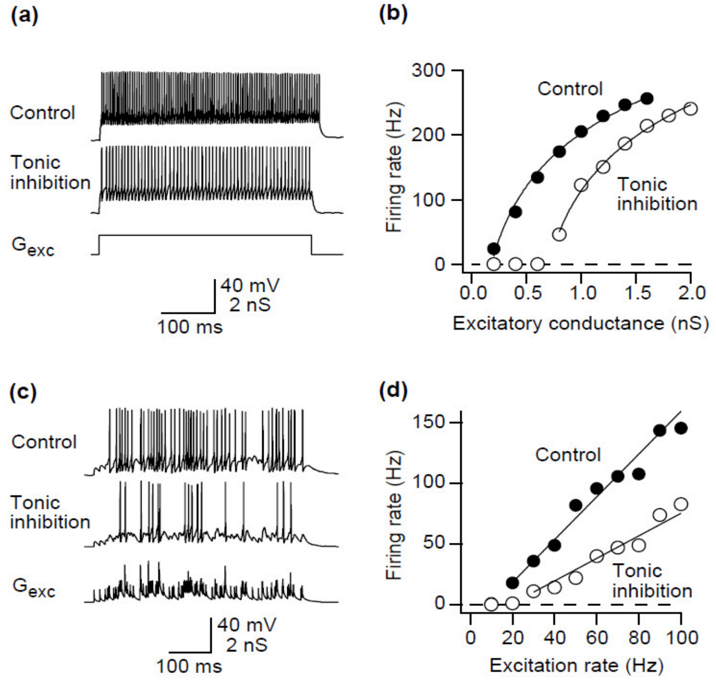

Figure 3. Tonic inhibition on neuronal output. a | Recording from a cerebellar granule cell in whole-cell patch-clamp mode. Firing is elicited by 1 nS of excitatory current step injection (G_{exc}) in absence (control) and presence of 1 nS tonic inhibition. **b** | Evoked firing rate by several excitatory conductances in absence (control) or presence of tonic inhibition. Tonic inhibition induces a subtractive operation on the input- output relationship because it causes only a shift rather than a change in slope (gain). **c** | Firing recordings elicited by four independent 50 Hz Poisson trains of excitatory synaptic conductance waveforms (G_{exc}) in control and in presence of 1 nS tonic inhibition. **d** | Input- output relationship between excitation rate and output firing frequency in control and presence of tonic inhibition. Tonic inhibition causes a multiplicative scaling on the input- output relationship decreasing its gain (adapted from Semyanov et al., 2004).

Overall, tonic inhibition is essential to modulate the input-output function of the neuron causing a subtractive and divisive mathematical operation due to excitatory input variability. Furthermore, higher frequency of excitatory inputs (considered the variance) is required to achieve a given output rate in presence of tonic inhibition (Mitchell and Silver 2003).

Recordings from granule cells in the cerebellar cortex of anaesthetized Sprague–Dawley rats showed that they exhibit low spontaneous firing rate, triggered by sparse glutamatergic mossy inputs, enforced by tonic inhibition *in vivo*. Therefore, tonic GABAergic inhibition contributes to sensory input sensitivity by modulating the signal-to-noise ratio (Chadderton, Margrie et al. 2004).

$GABA_A$Rs containing the δ subunit are shown to be involved in different neurological and psychiatric disorders including sleep disturbances, epilepsy, stress-related psychiatric disorders such as anxiety and bipolar disorders, but also in pregnancy, alcohol addiction, learning and memory (Brickley and Mody 2012).

However, it is also becoming increasingly appreciated that $GABA_A$Rs containing the α_5 subunit are involved in learning, cognition and other psychiatric diseases such as schizophrenia, depression and anxiety disorders (Rudolph and Mohler 2006; Brickley and Mody 2012).

Mice with a partial deficit of α_5- containing $GABA_A$ receptors in the hippocampus displayed an improved performance in trace fear conditioning, a hippocampus-dependent memory task, but not in delay conditioning, which is a hippocampus- independent memory task (Crestani, Assandri et al. 2002; Yee, Hauser et al. 2004). Mice lacking the α_5 subunit displayed an improved performance in a spatial learning task in the water maze (Collinson, Kuenzi et al. 2002). In the same test, α_5-selective partial inverse agonists enhanced the performance of wild-type rats (Chambers, Atack et al. 2004; Sternfeld, Carling et al. 2004; Rudolph and Mohler 2006). Following auditory fear conditioning acquisition, α_5-$GABA_A$R mRNA selectively decreased in central amygdale thus highlighting the importance of expression-regulation of this receptor in associative learning (Heldt and Ressler 2007). Interestingly, inflammation causes impairment of contextual fear memory and synaptic plasticity, at least in part, by increasing $\alpha_5$$GABA_A$Rs-mediated tonic inhibition in CA1 pyramidal neurons (Wang, Zurek et al. 2012).

Inverse agonists that partially and selectively block the α_5-$GABA_A$Rs have been developed, but the suitability for use in humans remains questionable due to their anxiogenic effects (Navarro, Buron et al. 2002). Furthermore, mice with a partial deficit in α_5-containing $GABA_A$ receptors display a mild deficit in prepulse inhibition of the acoustic startle reflex, indicating an abnormality in sensorimotor gating and anxiety (Hauser, Rudolph et al. 2005). Interestingly, high-anxiety patients presented low levels of prepulse inhibition in one study (Duley, Hillman et al. 2007). Additionally, a *mouse model of increased trait anxiety* showed decreased expression of α_5-containing $GABA_A$Rs specifically in CEA (Tasan, Bukovac et al. 2011). Finally, human studies showed that polymorphisms of the α_5-$GABA_A$R gene are associated with major affective disorders in humans (Delong 2007; Craddock, Jones et al. 2010).

$GABA_A$ Receptor trafficking

Dynamic changes in the posttranslational modification, surface accumulation, protein turnover and trafficking of $GABA_A$Rs regulate GABAergic transmission (Luscher, Fuchs et al. 2011).

Studies in rodents indicate that alterations in subunit mRNA levels are generally paralleled by corresponding changes in surface accumulation and function of $GABA_ARs$ (Shen, Gong et al. 2007; Shen, Sabaliauskas et al. 2010).

Before the fully-assembled receptor is translocated to the cell surface, *αβ* subunit heterodimers are formed in the endoplasmic reticulum (ER) and quality control is monitored through association of the subunits' N-terminus with ER-associated chaperons, such as calnexin and immunoglobulin heavy chain binding protein (Connolly, Krishek et al. 1996; Bradley, Taghibiglou et al. 2008).

The exit of the constituted $GABA_AR$ from ER is limited by ER-associated degradation (ERAD) of *α* and *β* subunits (Gallagher, Ding et al. 2007; Bradley, Taghibiglou et al. 2008). ERAD of $GABA_AR$ is enhanced by blockade of neuronal activity, mediated by the decrease in calcium influx, which causes increased ubiquitination and receptor degradation. In addition, this may cause activation of *l*inks *i*ntegrin-associated protein with the *c*ytoskeleton-1 (PLIC-1), which binds *α* and *β* subunits and causes entry into the secretory pathway (Bedford, Kittler et al. 2001).

Subsequently, the Golgi-specific DHHC zinc finger protein (GODZ) interacts and palmitoylates the γ_2 subunit, facilitating ER to Golgi translocation of γ_2 containing $GABA_ARs$ (Luscher, Fuchs et al. 2011). Another protein, brefeldin A inhibited GDP/GTP exchange factor 2 (BIG2), interacts with the *β* subunit of $GABA_ARs$ facilitating either its exit from the Golgi toward the plasma membrane or endocytic recycling.

Golgi is enriched in $GABA_AR$ associated protein (GABARAP) induces cell surface expression of $GABA_ARs$ (Chen and Olsen 2007). High levels of intracellular calcium influx through NMDA receptors could activate an ubiquitin-like protein that binds γ_2-containing $GABA_AR$ and is involved in LTP of inhibitory synapses and $GABA_AR$ autophagy in *C. elegans* (Rowland, Richmond et al. 2006; Marsden, Beattie et al. 2007). GABARAP competes with other proteins involved in endocytic trafficking of $GABA_AR$ (phospholipase C-related catalytically inactive proteins 1 and 2, PRIP1/2, and NSF).

Internalization of plasma membrane-associated $GABA_AR$ occurs via clathrin- and dynamin-dependent endocytosis mechanisms which require intracellular calcium. In particular, protein kinase A (PKA) and protein kinase C (PKC), but also calcium calmodulin dependent kinases II (CaMKII), phosphorylate the *β* subunit of the $GABA_AR$ thus causing its internalization. The clathrin protein adaptor (AP2) interacts with the phosphorylated *β* subunit starting the endocytotic process (Luscher, Fuchs et al. 2011).

The decision of whether internalized $GABA_ARs$ are recycled or degraded is regulated by the interaction of the β subunit with a variety of proteins, such as huntingtin-asssociated protein (HAP-1). These proteins facilitate recycling and surface expression of $GABA_AR$ containing the γ_2 subunit, but similar mechanisms are observed also for extrasynaptic $GABA_ARs$ (Luscher, Fuchs et al. 2011).

Brain structures involved in fear and anxiety

Decades of research in humans and animals have demonstrated the participation of different brain structures in fear and anxiety-like behavior. It is widely accepted that the brain macrostructure referred to as "extended amygdala" is directly involved in coding these two emotional responses (Dias, Banerjee et al. 2013). It is clear that the Amygdala structure is hyperactive and hyper-responsive in all the anxiety disorders in humans and this can be induced by a traumatic experience (Shin and Liberzon 2010). Other brain macroscopic areas can be differentially involved in the behavioral outcome of fear and anxiety, such as the bed nucleus of the stria terminalis (BNST) which is included in the nucleus accumbens, the medial prefrontal cortex (mPFC), the insular cortex (IC), the hippocampus, and the periaqueductal gray matter (PAG). Furthermore, amygdala function is related to acquisition and expression of fear responses in combination with downstream structures such as PAG or hypothalamus, which are important in freezing and catecholamine release, respectively, and in combination with the hippocampus to carry and evaluate contextual inputs. In addition, different amygdala sub-nuclei seem to play a role in anxiety responses as the BNST area. Importantly, complete pharmacological lesions of the amygdala decrease fear learning and anxiety (Jellestad, Markowska et al. 1986; Goosens and Maren 2001).

Neuroimaging studies in humans have revealed the importance of its structure at the macroscopic level however, these provide no resolution of the particular microcircuits involved (Shin and Liberzon 2010). Further, the precise neuroanatomical regions that store fear memory traces and their precise functioning is matter of debate and actively studied. Since Amygdala is widely recognized as the structure that computes fear and anxiety information, it is critical to understand its components which encode information on cellular network and, behavioral levels (Ehrlich, Humeau et al. 2009).

Amygdala

Amygdala (also *corpus amygdaloideum* in Latin, from Greek *ἀμυγδαλή*, *amygdalē*, "almond", "tonsil") was first described in the 19th Century by the anatomist Karl Friedrich Burdach as an almond-shaped structure located in the human temporal lobe. However, its function was first realized in 1937 by way of lesion studies conducted in monkeys by Klüver and Bucy. They found that lesion of the temporal medial lobe induced hyperphagia, associated with emotional blunting, characterized by a flat effect, weak stimuli responsiveness, and loss of fear. The amygdala was later considered to be a "fear generation station" when few studies found that its bilateral lesion made monkeys less fearful (Weiskrantz 1956), while its electrical stimulation elicited strong fear responses (Delgado, Rosvold et al. 1956).

In the same decade, its function was becoming clear due to the discovery of a rare syndrome in humans called *Hurbach-Wiethe Syndrome* that causes a bilateral amygdala calcification. Interestingly, these patients have profound social and emotional problems, in particular facial recognition of fear expression and fear conditioning are impaired (Adolphs 2013).

Clearly, the amygdala is one of the key brain structures for fear memory acquisition and storage, a notion consistently supported by a large number of studies using different experimental paradigms and measures of conditioned fear responses (LeDoux 2000; Maren 2001; Fanselow and Poulos 2005; Davis, Walker et al. 2010). In addition, the amygdala also modulates fear-related learning in other brain structures, such as the cortex and the hippocampus (McGaugh 2004).

General structure

Amygdala is a medial temporal lobe structure composed of different sub nuclei that orchestrate the processing of sensory cortico-thalamic information for the acquisition and expression of Pavlovian fear conditioning (FC) and anxiety behavior (Jellestad, Markowska et al. 1986; Goosens and Maren 2001). These anatomically and functionally distinct nuclei include the lateral (LA) and basal (BA) nuclei (jointly referred to as the basolateral amygdala, BLA) and the central nucleus (CEA) (Krettek and Price 1978; Krettek and Price 1978) (Figure 3). The CEA can be additional divided into a lateral (CEl) and a medial (CEm) part because of their spatial location and different neuronal composition (McDonald 1992). CEl has been subdivided on anatomical and immunohistochemical justifications into a lateral-capsular division (CElc), an intermediate division (CEi), and a lateral division proper (CEl) (Cassell, Gray et al. 1986; McDonald 1992; Jolkkonen and Pitkanen 1998), though from a functional view it is often considered as a single structure (Samson, Duvarci et al. 2005). It should be noted that the cytoarchitecture and organization of the amygdala nuclei are similar to those of parts of the telencephalon. While the lateral structures (BLA) are cortex-like, consisting of a majority of glutamatergic projection neurons and a minority of local GABAergic interneurons (McDonald 1992), the medial structures (CEA) are striatum-like, with a preponderance of neurons being

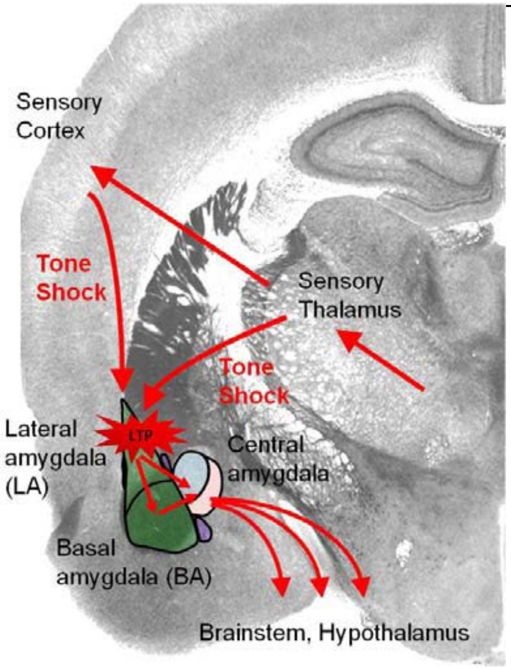

Figure 4. Flowing of sensory information in Amygdala. Tone and shock inputs are sent from the periphery to different thalamic nuclei. The thalamus directly projects to the lateral amygdala (LA) and conveys sensory information via this "low road" pathway. Simultaneously, the thalamus projects via the "high road" to sensory cortices, like the auditory cortex, where the sensory information is further processed and subsequently also conveyed to the LA. Co-activation of LA neurons by tone and shock inputs leads to long - term potentiation (LTP) at both thalamic and cortical afferents in the LA. Information is transmitted to the basal amygdala (BA), which is important for switches in the emotional state of an animal during conditioning and extinction. The LA and the BA together form the basolateral amygdala (BLA). Both the BA and the LA project to the lateral subdivision of the central amygdala (CEl), but only the BA also to its medial subdivision (CEm). The CEm is the final output nucleus of the amygdala and projects to the hypothalamus and several brainstem nuclei, where the physiological fear responses are triggered.

GABAergic (about 90%) and exhibiting medium spiny-type morphology (Cassell, Gray et al. 1986; McDonald 1992; Swanson and Petrovich 1998).

The lateral nucleus of the amygdala (LA) is the primary site for the formation and storage of the conditioned (CS) and unconditioned stimulus (US), whereas the central nucleus (CEA) is thought to be the output structure that mediates the behavioral expression of fear (Ehrlich, Humeau et al. 2009).

Basolateral amygdala

It has been demonstrated that selective lesions of BLA decreases fear levels in Monkeys and rodents (Weiskrantz 1956; Jellestad, Markowska et al. 1986; Goosens and Maren 2001; Kalin, Shelton et al. 2004) while its electrical stimulation elicited strong fear responses (Delgado, Rosvold et al. 1956). Glutamatergic neurons, or principal neurons (PNs), transmit excitatory information in BLA circuitry through axonal collaterals towards different areas involved in fear and anxiety (McDonald 1992; Herry, Ciocchi et al. 2008). PNs receives inhibitory GABAergic inputs from other cells thought to be mainly interneurons and important in feed-forward transmission and fear behavior. There is a myriad of heterogeneity among PNs due to their molecular markers, connectivity, sub-cellular targeting, cellular properties and behavioral function (Freund and Buzsaki 1996; Somogyi and Klausberger 2005; Ehrlich, Humeau et al. 2009; Pape and Pare 2010; Fishell and Rudy 2011; Spampanato, De Maria et al. 2012).

The BLA is considered the input station forming the association between CS and US during fear conditioning (LeDoux 2000). Cortical and thalamic inputs, transmitting the unfiltered sensory information, converge on the BLA (LeDoux, Farb et al. 1991). In this site, in particular the LA, it has been shown that synaptic transmission is increased after fear conditioning *ex vivo* (McKernan and Shinnick-Gallagher 1997; Tsvetkov, Carlezon et al. 2002) and *in vivo* (Quirk, Armony et al. 1997; Rogan, Staubli et al. 1997; Goosens and Maren 2001). Numerous studies demonstrated that a NMDA-dependent long term potentiation of cortico-thalamic afferents to PNs occurs at this location and is directly involved in fear learning (Rogan and LeDoux 1995; Huang and Kandel 1998; Doyere, Schafe et al. 2003).

Importantly, learning–induced plasticity could indeed be observed in extracellular recordings of LA neurons as an enhancement of short latency CS-evoked activity (Quirk, Repa et al. 1995; Quirk, Armony et al. 1997; Rogan, Staubli et al. 1997). Thalamic, but not cortical, afferents to LA neurons are likely to be the initial site of this plasticity. The thalamic component of the CS response is potentiated first in LA, and plasticity in this region is observed earlier than in cortical neurons. This plasticity is stimulus-specific, given that only CS^+, and not CS^-, responses are enhanced after a discriminative fear conditioning paradigm (Collins and Pare 2000).

Inhibitory transmission mediated by GABAergic neurons locally connected to PNs is now gaining increased attention because it seems to be fundamental in maintaining low the excitability of PNs and, consequently, both modulation of and regulation by fear-induced plasticity (Harris and Westbrook 1998; Heldt and Ressler 2007; Ehrlich, Humeau et al. 2009).

Central amygdala

CEA is part of the extended amygdala and considered the output station of the amygdaloid complex where the information coming from BLA is further processed and transferred to areas directly involved in fear and anxiety (Ehrlich, Humeau et al. 2009). CEA is not only considered a relay station for fear information but evidence is accumulating regarding its involvement in plastic changes and an active role in fear learning (Wilensky, Schafe et al. 2000; Samson, Duvarci et al. 2005; Ciocchi, Herry et al. 2010). Indeed, CEA neurotoxic lesions attenuate freezing to contextual and auditory conditional stimuli (Goosens and Maren 2001). Furthermore, acute and reversible inactivation of CEA using the $GABA_A$ receptor agonist muscimol during fear conditioning, or local blockade of NMDA receptors, caused impairment in acquisition of conditioned fear responses (Wilensky, Schafe et al. 2000; Goosens and Maren 2003). Following BLA lesions though, conditioned fear responses can still be acquired by overtraining in an associative and CEA-dependent manner (Zimmerman, Rabinak et al. 2007; Rabinak and Maren 2008). It was determined that there are morphological and electrophysiological differences in neurons located in CEA, relative to BLA, and they are differentially altered in response to emotionally-arousing stimuli produced by fear conditioning learning (Pascoe and Kapp 1985; Ciocchi, Herry et al. 2010).

Additionally, CEA is considered directly involved in anxiety behavior. Its electrolytic lesion decreases anxiety-like behavior in rats (Jellestad, Markowska et al. 1986). A human study demonstrates that BLA and CEA connectivity was less pronounced in patients suffering from generalized anxiety disorders (Etkin, Prater et al. 2009). Indeed, focal activation of BLA terminals specifically onto unidentified CEA neurons induces an acute anxiolytic effect. This was thought to be caused by an activity enhancement of CEm output neurons (Tye, Prakash et al. 2011).

Intrinsic connectivity of CEA has been identified using injection of anterograde tracers into various CEA subdivisions (Jolkkonen and Pitkanen 1998). CEl sends latero-medial unidirectional projections to CEm but also to other nuclei, such as the bed nucleus of the stria terminalis (BNST), which is also part of the extended amygdala.

External afferents of CEA originated from different nuclei and it seems there is a compartmental segregation and differential cellular targeting (Dong, Fukazawa et al. 2010; Li, Penzo et al. 2013). BLA is the major and most characterized glutamatergic afferent of CEA (in CEc) (Pitkanen, Stefanacci et al., 1995) and potentiates upon fear conditioning in CEA (Li, Penzo et al. 2013; Penzo, Robert et al. 2014). However, CEA receives a variety of extra-amygdaloid inputs (Ottersen and Ben-Ari 1979; Veinante and Freund-Mercier 1998; Dong, Fukazawa et al. 2010), suggesting that it could function in parallel or independently from the BLA (Sun, Yi et al. 1994; Balleine and Killcross 2006). Enthorinal and Insular cortex inputs target CEl while afferents from prefrontal cortex seem to target the CEc (Sun, Yi et al. 1994). While the paraventricular nucleus of the thalamus targets all CEA subdivisions, the auditory thalamus preferentially targets CEm and its input is enhanced after fear conditioning (Samson and Pare 2005). Interestingly, CEA receives visceral and nociceptive brainstem inputs from parabrachial nucleus and solitary tract (Dong, Fukazawa et al. 2010) but their function is still unknown.

Microcircuitry

Based on old and recent anatomical, morphological, molecular and physiological studies, it is accepted that CEA and its sub-nuclei contain a varied neuronal populations (Martina, Royer et al. 1999; Dumont, Martina et al. 2002; Chieng and Christie 2010; Ciocchi, Herry et al. 2010; Gozzi, Jain et al. 2010; Haubensak, Kunwar et al. 2010; Viviani, Charlet et al. 2011; Knobloch, Charlet et al. 2012).

These different neuronal subtypes are mostly GABAergic striatum-like, medium-spiny type morphology. This basic feature, together with strong dopaminergic and enkephalinergic innervations, resemble a basal ganglia-type structure (Cassell, Freedman et al. 1999).

At the physiological level, it has been shown in several studies that late-firing neurons are the majority of neurons located in CEl, followed by regular spiking and a minority of low-threshold bursting neurons, while in CEm the low-threshold bursting are the most abundant in comparison with regular spiking neurons (Martina, Royer et al. 1999; Dumont, Martina et al. 2002; Chieng and Christie 2010; Haubensak, Kunwar et al. 2010).

A variety of neuropeptides and their receptors are expressed in the CEA structure (Roberts, Woodhams et al. 1982; Veinante and Freund-Mercier 1998; Haubensak, Kunwar et al. 2010). Furthermore, many neuropeptide-containing afferents target specific divisions of CEA. *Corticotrophin-releasing factor* (*CRF*) and *CRF receptors* (Yu and Shinnick-Gallagher 1998; Bouret, Duvel et al. 2003; Nie, Schweitzer et al. 2004), *dynorphin* (Zerdetto-Smith et al., 1988), *kappa-opioid receptors, mu- opioid receptors* and *delta- opioid receptors* (Chieng, Christie et al. 2006), *enkephalin* (Gray, Cassell et al. 1984), *oxytocin*, *vasopressin* and its receptors (Veinante and Freund-Mercier 1995; Veinante and Freund-Mercier 1997), *calcitonin- gene related peptide* (*CGRP*) Honkaniemi (Honkaniemi 1992), *galanin* and its receptors Waters and Kraude (Waters and Krause 2000), *somatostatin* (*SOM*), *substance P*, *neurotensin*, *cholecystokinin* Roberts (Roberts, Woodhams et al. 1982; Ciriello, Rosas-Arellano et al. 2003), *orexin/hypocretin* and *PKCδ* (Haubensak, Kunwar et al. 2010) are all expressed in CEA neurons. Recent studies show that there are different neuronal sub-types within CEA that can be classified based on their anatomical location, the expression of precise neuropeptides or their receptors, other proteins markers (Roberts, Woodhams et al. 1982; Veinante and Freund-Mercier 1997; Huber, Veinante et al. 2005; Haubensak, Kunwar et al. 2010), and also on the basis of their role in input processing (Huber, Veinante et al. 2005; Ciocchi, Herry et al. 2010; Knobloch, Charlet et al. 2012; Li, Penzo et al. 2013; Penzo, Robert et al. 2014).

Based on anatomical and physiological evidence, neurons located in CEl are thought to inhibit the neuronal firing of CEm output neurons through $GABA_A$ receptor ($GABA_AR$) activation (Huber, Veinante et al. 2005; Ehrlich, Humeau et al. 2009; Ciocchi, Herry et al. 2010; Haubensak, Kunwar et al. 2010). Output neurons located in CEm project to the hypothalamus and various brainstem nuclei that mediate the endocrine, autonomic, and motor-related aspects of fear responses. These are mainly located in the medial part of CEA, the CEm (Hopkins and Holstege 1978; Veening, Swanson et al. 1984; Cassel, Weidenheim et al. 1986), albeit a subpopulation of CEl neurons also projects to brain stem targets that are vital for fear conditioning (Penzo, Robert et al. 2014).

Indeed, recent work showed that a subpopulation of GABAergic CEl neurons selectively expressed oxytocin receptors (Huber et al. 2005). Their activation, mediated by an agonist of these receptors, led to a phasic increase in GABAergic inhibition on the post-synaptic CEm neurons projecting to *vl*PAG. This caused a direct decrease in freezing behavior induced by contextual fear conditioning (Viviani, Charlet et al. 2011).

In combination with these physiological studies, it was shown that 90% of CEA neurons are GABAergic, expressing a variety of molecular markers (Haubensak, Kunwar et al. 2010).

Fifty percentage of the entire GABAergic population is composed of *protein kinase C delta* expressing neurons ($PKC\delta^+$ neurons) that also express *oxytocin receptors* and *Enkephalin*. *$PKC\delta^+$* neurons are mostly late-firing neurons while, aside from the $PKC\delta^-$ neuronal population, regular firing neurons seem to be predominant (Haubensak, Kunwar et al. 2010). These neurons connect within CEA (Haubensak, Kunwar et al. 2010) and with BNST (Veening, Swanson et al. 1984; Huber, Veinante et al. 2005). It seems that they receive inputs from the parabrachial nucleus, which is important in pain (Shimada, Inagaki et al. 1992). GABAergic inputs coming from CEl neurons onto $PKC\delta^+$ neurons are still poorly described. It is known that their optogenetic activation evoked a GABAergic inhibitory response in CEm output neurons projecting to *vl*PAG and $PKC\delta^-$ neurons located in CEl (putative CEl_{on} neurons).

Within the $PKC\delta^-$ neuronal population, *SOM^+* neurons were found in CEl (Haubensak, Kunwar et al. 2010; Li, Penzo et al. 2013). This neuronal subclass receives monosynaptic glutamatergic BLA inputs (Li, Penzo et al. 2013) and contacts only *SOM^-* neurons (probably $PKC\delta^+$ neurons included) located in CEl but, importantly, not to CEm *vl*PAG-projecting neurons (Li, Penzo et al. 2013).

CRH cells expressing *Dynorphin* are located within CEc/CEl and appear to form extrinsic connectivity with the parabrachial nucleus and are innervated by dopaminergic afferents (Asan 1998; Veinante and Freund-Mecier 1998; Marchant et al. 2007).

Plasticity

CEA was originally considered only a relay station between BLA and hypothalamus/brainstem areas (LeDoux 1996), leaving BLA as the only site of CS-US association during fear conditioning (Maren and Quirk 2004). Nevertheless, recent studies have shown that precise neuronal populations located in CEA are directly involved in fear and anxiety behavior and can possibly be caused by plastic changes related to fear conditioning (Henke et al. 1988, Samson and Pare 2005, Fu and Shinnick-Gallagher 2005, Ciocchi et al. 2010, Haubensak et al. 2010, Tye et al. 2011, Li et al. 2013, Penzo et al. 2014).

One study related extracellular activity with behavior showing that the firing of two CEA neuronal types selectively and differentially changed during immobilization and stress *in vivo* (Henke et al. 1988). In addition, direct activation of BLA inputs onto unidentified CEl neurons led to a decrease in anxiety (Tye et al. 2011).

Plastic changes can occur in CEA neurons causing a long-term change in the behavioral outcome. Along with this hypothesis, it was found that sensory thalamic glutamatergic afferents exhibit input-specific, NMDA receptor-dependent LTP onto CEm neurons (Turner and Herkenham 1991, Samson and Pare 2005). Input- specific LTP was also observed between BLA glutamatergic inputs to CEl neurons (Fu and Shinnick-Gallagher 2005, Li et al. 2013, Penzo et al. 2014). Specially, BLA inputs were observed to be enhanced selectively onto SOM$^+$ neurons located in CEl and to be directly involved in fear memory recall as observed for CEl$_{on}$ neurons (Li et al. 2013).

More recently, it was found that there is a differential role for CEl and CEm in fear conditioning. For instance, CEl inactivation by local application of muscimol, or CEm activation by light stimulation, directly led to freezing responses *in*

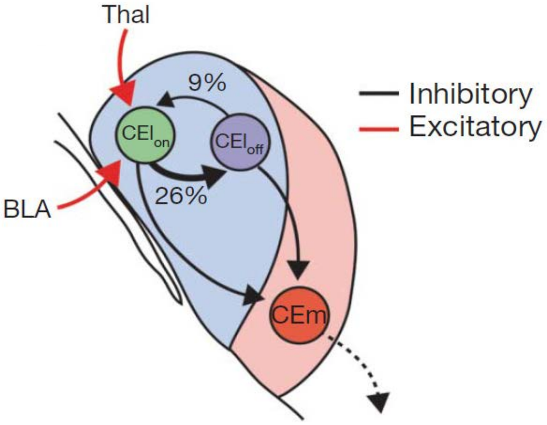

Figure 6. Fear conditioning induces cell-type-specific plasticity in CEl inhibitory circuits. Schematic illustrating the organization of CEA based on electrophysiological and morphological data. BLA and cortico-thalamic inputs carrying the CS input transiently inhibited CEl$_{on}$ neurons. Subsequently, CEl$_{off}$ neurons are phasically inhibited causing a disinhibition of CEm output neurons and the observe freezing (adapted from Ciocchi et al. 2010).

vivo (Ciocchi et al. 2010). This further suggests that CEm output neurons are under tight inhibitory control originating from CEl. Moreover, fear conditioning induced cell-type-specific plasticity in three distinct neuronal subtypes in CEA. It was found that CEl contains CEl$_{on}$ and CEl$_{off}$ neurons that are phasically activated and inactivated by the CS (acoustic tone used for conditioning the animal), respectively, while all the CEm neurons are activated by the tone. By calculating the CS-evoked spike latency, these responses likely reflect, among other mechanisms, a disinhibitory control of CEm neurons from CEl$_{off}$ neurons that are transiently inhibited by CEl$_{on}$ neurons (figure 5). Furthermore, using single unit recording combined with a pharmaco-genetic approach, it was found that CEl$_{off}$ neurons largely overlap with a genetically-defined GABAergic neuronal subtype (the PKCδ^{+} neurons) (Haubensak et al. 2010). Interestingly, the phasic change in the three neuronal populations statistically correlates with the freezing level of the mouse during the CS^{+} presentation.

In addition to a phasic change response that can be explained by direct GABAergic connectivity, it was found that the tonic firing of these three types of neurons were changed and predicted generalization of behavioral responses to the CS^{-} (a tone that was not paired with the footshock during conditioning). In particular, the tonic firing was enhanced in CEl$_{off}$ neurons while it was decreased in CEm neurons after fear conditioning, the time when the animal expressed high fear generalization (figure 6, Ciocchi et al. 2010). Furthermore, central amygdala can be considered a plastic relay brain station composed of many neuronal sub-classes important in gating sensory inputs.

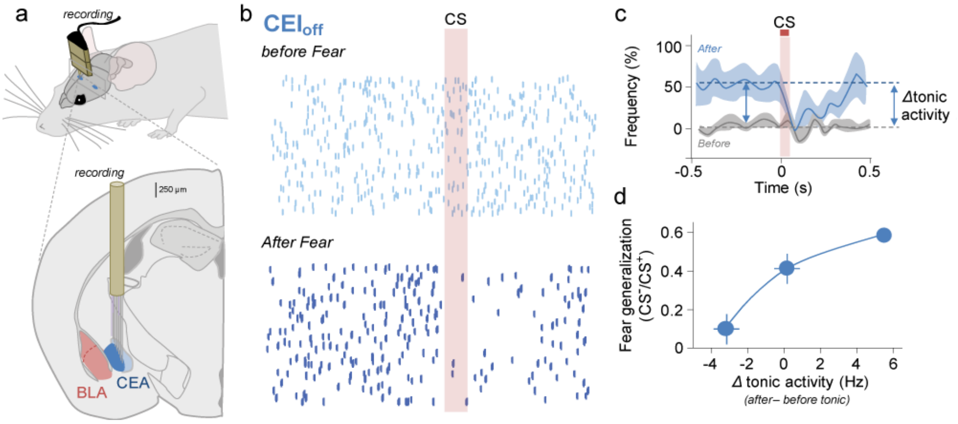

Figure 7. Fear conditioning induces plastic changes of the CEl$_{off}$ neurons tonic firing. a | schematic illustrating the single unit recording in CEA. *Down*, enlargement of a coronal section of amygdala. **b** | Example raster plot of a CEl$_{off}$ neuron tonic firing before and after fear conditioning. CS evoked a transient inhibition of CEl$_{off}$ neuron. **c** | Averaged population peristimulus time histograms from CEloff neurons before (gray) and after (blue) fear conditioning paradigm. Double arrow shows the change in tonic firing (Δtonic activity). **d** | Correlation between the fear generalization and the change in tonic firing before/after fear conditioning (adapted from Ciocchi et al. 2010).

Central amygdala contains a variety of neuronal subtypes that could directly influence fear and anxiety. However, their specific contribution on the encoding for these two emotional behaviors remains speculative.

In particular, CEl_{off} neurons expressing PKCδ isoform seems to have the unique property particularly important in gating fear generalization to an ambiguous stimulus. Indeed, CEl_{off} neurons are the sole cell type of central amygdala that overcome (what specifically does it mean here to overcome?) a specific plastic increase of the tonic firing after fear conditioning that predicts fear generalization.

The mechanism(s) underlying such changes in tonic activity in defining neuronal populations in CEA and its causal role in anxiety and fear generalization are still not known.

My thesis therefore predominantly focused on understanding whether the tonic activity of a peculiar GABAergic neuronal subclass of the central amygdala network, PKCδ positive neurons directly modulate anxiety levels. Further, I also sought a physiological mechanism that explains the observed changes to the neuronal spontaneous firing. To define such a causal relationship between this mechanism and anxiety, I undertook a multiple-technique approach.

MATERIAL AND METHODS

Animals

Male C57BL6/J, PKCδ Cre$^+$, α_5-floxed and α_5-floxed x PKCδ Cre$^+$ mice (2–3 months old; Harlan Ltd) were individually housed for 7 days before all behavioral experiments, under a 12 h light/dark cycle, and provided with food and water *ad libitum*. All animal procedures were executed in accordance with institutional guidelines and were approved by the Veterinary Department of the Canton of Basel-Stadt.

Slice electrophysiology

Standard procedures were used to prepare 300 µM thick coronal slices from 6- to 12-week-old male wild-type, PKCδ Cre$^+$, α_5-floxed and α_5-floxed x PKCδ Cre$^+$ mice. Briefly, the brain was dissected in ice-cold artificial CSF (ACSF), mounted on an agar block, and sliced with a vibratome (Leica VT 1000; Leica, Wetzlar, Germany) at 4°C. Slices were maintained for 45 min at 37°C in an interface chamber containing ACSF equilibrated with 95% O_2/5% CO_2 and containing the following (in mM): 124 NaCl, 2.7 KCl, 2 CaCl2, 1.3 MgCl2, 26 NaHCO3, 0.4 NaH2PO4, 18 glucose, 4 ascorbate. Slices were then transferred to another chamber for at least 60 min at room temperature in another physiological ACSF (pACSF) containing the following (in mM): 125 NaCl, 3.5 KCl, 1.2 CaCl2, 1 $MgSO_4$, 26 NaHCO3, 1.25 NaH2PO4, 11 D-glucose. Recordings were performed with pACSF in a recording chamber at a temperature of 35°C at a perfusion rate of 1-2 mL/min. Neurons were visually identified with infrared video microscopy using an upright microscope equipped with a 40X objective (Olympus, Tokyo, Japan). Patch electrodes (3–5MΩ) were pulled from borosilicate glass tubing. For current clamp experiments, patch electrodes were filled with a solution containing the following (in mM): 120 K-gluconate, 20 KCl, 10 HEPES, 10 phosphocreatine, 4 Mg-ATP, and 0.3 Na-GTP (pH adjusted to 7.25 with KOH, respectively, 295 mOsm). The GABAergic sIPSCs were recorded using an internal solution containing the following (in mM): 110 CsCl, 30 K-gluconate, 1.1 EGTA, 10 HEPES, 0.1 CaCl2, 4 Mg-ATP, 0.3 Na-GTP (pH adjusted to 7.3 with CsOH, 280 mOsm). For on-cell recordings, pACSF was used inside the recording pipette. To exclude glutamatergic inputs, CNQX (6-cyano-7-nitroquinoxaline-2,3-dione, 10 µM: AMPA receptor antagonist) and (R)-CPP ((*RS*)-3-(2-Carboxypiperazin-4-yl)-propyl-1-phosphonic acid, 10 µM: NMDA receptor antagonist) were added to the pACSF.

Whole cell Patch-clamp recordings were excluded if the access resistance was higher than 13 MΩ and it changed more than 20% during the recordings. Seal resistance, for on-cell recordings, was around 20 and 50 MΩ and data were excluded if it changed more that 20% from the initial value.

Data were recorded with a MultiClamp 700B, filtered at 0.2 kHz, and digitized at 10 kHz. Data were acquired and analyzed with Clampex 10.0, Clampfit 10.0 (Molecular Devices, Palo Alto, CA) and the Mini Analysis Program (Synaptosoft, Decatur, GA). Data are the mean ± SEM. *p* values are from paired t-test.

All chemicals for the internal and external solution were purchased from Fluka/Sigma (Buchs, Switzerland). Glutamatergic blockers were purchased from Tocris Bioscience (Bristol, UK). TTX was from Latoxan (Valence, France). PWZ-029 was obtained from J. Cook, University of Wisconsin.

Morphological reconstruction

Patch-clamp electrodes were filled with 1.5% biocytin (Vector Laboratories Inc.) mixed in CsCl or KGluconate-based internal solution. After completing the entire electrophysiological recording in whole cell configuration, positive DC pulses (0.1–1.0 nA, 500 ms, 1 Hz) were used to inject biocytin into the neurons while the electrode was slowly retracted. Brain slices were then incubated for an hour in physiological ACSF and, subsequently, stored in 4% paraformaldehyde and 0.5% picric acid for up to 3 days at 4°C. They were later labelled for neurobiotin using the Vectastain Elite avidin–biotin complex peroxidase kit (Vector Laboratories Inc.). Neurons were reconstructed with the Neurolucida software (Microbrightfield) (Ciocchi et al. 2010).

Combined single unit recording and in vivo pharmacology in freely behaving mice

Single unit recordings and pharmacology were performed in chronically implanted animals. Three to four-month old mice were anesthetized with isoflurane (induction: 4%, maintenance: 1.5%, Attane™, Minrad Inc., Buffalo, NY, USA) in oxygen-enriched air (Oxymat 3©, Weinmann, Hamburg, Germany) and fixed in a stereotaxic frame (Kopf Instruments, Tujunga, USA). Core body temperature was maintained at 36.5°C by a feed ‐ back controlled heating pad (FHC, Bowdoinham, ME, USA). Analgesia was provided by local injection of ropivacain (200µl of 2mg/mL, s.c., Naropin©, AstraZeneca, Switzerland) and systemic injection of meloxicam (100µl of 5mg/mL, i.p., Metacam©, Boehringer ‐ Ingelheim, Ingelheim, Germany). Mice were unilaterally implanted in the central amygdala with a custom built injectrode consisting of a multi-wire electrode attached to a guide cannula (26 gauges, with dummy screw caps, Plastics One, Roanoke, USA) and aimed at the following coordinates: 1.3 mm posterior to bregma; ±2.9 mm lateral to midline; and 4 mm to 4.1 mm deep from the cortical surface. The electrodes consisted of 16 individually insulated, gold-plated nichrome wires (13 µm inner diameter, impedance 30–100 kΩ, Sandvik, Stockholm, Sweden) contained in a 26-gauge stainless steel guide cannula and attached to a 18-pin connector (Omnetics Connector Corporation, Minneapolis, MN, USA). Implants were fixed to the skull with cyanoacrylate glue (Ultra Gel©, Henkel, Düsseldorf, Germany) and dental cement (Paladur©, Heraeus, Hanau, Germany). Mice were then given one week to recover from surgery, during which time they were daily handled to habituate them to the recording and injection procedures.

Ten minutes before injections, 33 gauge stainless steel injectors attached to 2.5mL Hamilton syringes were inserted into the guide canulae. Electrodes were connected to a head stage (Plexon Inc, Dallas, TX, USA) containing sixteen unity-gain operational amplifiers. The head stage was connected to a 16-channel computer-controlled preamplifier (gain ×100, band-pass filter from 150 Hz to 9 kHz, Plexon). Neuronal activity was digitized at 40 kHz and band-pass filtered from 250 Hz to 8 kHz, and was isolated by time–amplitude window discrimination and template matching using a Multichannel Acquisition Processor system (Plexon Inc, Dallas, TX, USA). Perfusion of Vehicle (78 ng DMSO in ACSF, AMRESCO, USA) or PWZ (10µM PWZ-029 in ACSF, Prof. James Cook, University of Wisconsin) was performed using a micro-infusion pump (Stoelting, Wood Dale, IL, USA) and consisted of an injection volume of 1µl delivered within 10-20 minutes. After completion of the experiment, recording sites were marked with electrolytic lesions before mice were transcardially perfused with 4% paraformaldehyde in phosphate - buffered saline (PFA), their brains extracted and post - fixed in PFA overnight. For histological verification of the injection site, 80 µm coronal brain sections were made on a vibratome (Leica Microsystems, Heerbrugg, Switzerland) and imaged on a stereo microscope (Leica Microsystems, Heerbrugg, Switzerland).

Single-unit spike sorting was performed using an Offline Sorter (Plexon). Principal component scores were calculated for unsorted waveforms and plotted on three-dimensional principal component spaces, and clusters containing similar valid waveforms were manually defined. A group of waveforms was considered to be generated from a single neuron if it defined a discrete cluster in principal component space that was distinct from clusters for other units and if it displayed a clear refractory period (>1 ms) in the auto-correlogram histograms. To avoid analysis of the same neuron recorded on different channels, we computed cross-correlation histograms (NeuroExplorer, Nex Technologies, Madison, AL, USA). If a target neuron presented a peak of activity at a time that the reference neuron fires, only one of the two neurons was considered for further analysis.

Behavior

Auditory discriminative Fear conditioning

Fear conditioning and fear retrieval took place in two different contexts (context A and B). The conditioning and retrieval boxes and the floor were cleaned with 70% ethanol or 1% acetic acid before and after each session, respectively. To score freezing behavior, an automatic infrared beam detection system placed on the bottom of the experimental chambers (Coulbourn Instruments) was used. Mice were considered to be freezing if no movement was detected for 2 s and the measure was expressed as a percentage of time spent freezing. To ensure that our automatic system scores freezing rather than just immobility, we previously compared the values obtained with those measured using a classical time-sampling procedure during which an experimenter blind to the experimental conditions determined the mice to be freezing or not freezing every 2 s (defined as the complete absence of movement except for respiratory movements). The values obtained were 95% identical and the automatic detection system was therefore used throughout the experimental sessions. Tones were presented as CS^+ and the CS^- (total CS duration of 30 s, consisting of 50-ms pips repeated at 0.9 Hz, 2-ms rise and fall; pip frequency: 7.5 kHz or white noise, 80 dB sound pressure level). Discriminative fear conditioning was performed on day 1 by pairing the CS^+ with a US (1-s foot shock, 0.6 mA, 5 CS^+/US pairings; inter-trial interval: 20–180 s) (CS-US group). The onset of the US coincided with the offset of the CS^+. The CS^- was presented after each CS^+/US association but was never reinforced (5 CS^- presentations, inter-trial interval: 20–180 s). The frequencies used for CS^+ and CS^- were counterbalanced across animals. On day 2, conditioned mice were submitted to fear retrieval in context B, during which they received four and four presentations of the CS^- and the CS^+, respectively. Control animals (CS only) were treated in the same manner but were not exposed to the US and they did not freeze during exposure of the tones (Fig. 3a, b).

Fear generalization index was calculated as the ratio between the freezing values during the CS^- and CS^+ presentation.

Open field paradigm

Mice were always placed on the periphery of an open field arena (50 cm^2 wide) located in a bigger box that was sound-isolated. Since the color of the mice was black, the arena had white background color to allow Viewer software to distinguish between the background and the animal. The light source was situated on the top of the box with an intensity of 1.2 LUX. Movements were monitored by a camera (Logitech) exactly located on the top of the arena. AVI files were than analyzed using ViewerII 5.1 software (BIOBSERVE GmbH). The field was divided in two areas, the center (210 mm) and the peripheral area. Total track length was assessed from the center of the animal body, while the number of visits in the center was counted when the four paws were located in the center area. Data were acquired for 10 minutes total and statistics were done comparing the first 5 minutes behavior.

Elevated plus maze (EPM) paradigm

The elevated plus maze was made of wood and composed of two light gray enclosed arms and two opened arms (230 mm each) extended at 90 degrees in the form of a plus, the center was considered the square area surrounded by the arms. The maze was elevated to 300 mm above the floor. Mice were placed in the center and their behavior was monitored for 10 minutes with a camera (Logitech) placed on the top of the maze. After every behavioral session the maze was cleaned with a solution (flugaten). This solution had a different smell from the ethanol or acetic acid used for cleaning the context for the fear conditioning and avoided contextual odor recall. Video tracking software (ViewerII 5.1 software, BIOBSERVE GmbH) was used to track mouse location. The visit to a compartment was considered only when the animal had all the four paws in one area. Time spent in the open arms was considered as inversely correlated with anxiety state, e.g. higher duration means low anxiety and vice versa.

For the optogenetic experiments, after connecting the optical fibers to the animal, we delivered constant light as described above for the open field assay.

Virus injections

For optical activation of $PKC\delta^+$ neurons, animals were injected into CEl with an AAV serotype 2/7 (Vector Core), containing a construct coding for ChR2-2A-eNpHR2.0-2A-Venus under the promotor EF1 at −1.4 mm posterior and ±2.9 mm lateral to bregma at a depth of −4 mm. Since

PKCδ$^+$ neurons expressed cyan fluorescence protein (CFP), to visualize the injection we co-injected also AAV serotype 2/1, containing a construct coding for FLEX-tdTomato under the promotor CAG. For the conditional knock-out, α5 floxed animals and controls (the wild types siblings) were bilaterally injected with an AAV serotype 2/1 virus expressing for CRE recombinase and GFP (Penn vector) under the promoter sequence CMV. Since this is not a conditional virus, bilateral injections were considered good when only CEA was infected in a bilateral manner.

Briefly, deeply anaesthetized animals were fixed in a stereotactic frame (Kopf Instruments) and the skin above the skull was cut. Glass pipettes (tip diameter 10–20 µm) connected to a Picospritzer III (Parker Hannifin Corporation) were lowered by a Micropositioner (Kopf Instruments) to the depth of 4 mm. About 300 nl were pressure injected into CEl.

Optogenetic experiments

For optogenetic experiments, Optic fibers with a diameter of 200 µm (Thorlabs GmbH) were inserted bilaterally above CEl at a depth of –3.5 mm. Optical connectors were composed of the optical fibers held by a screw. For the fear generalization experiment, mice were then placed into a behavioral context B and the optic fibers were connected by screwing the optical fibers connected to a blue laser (λ = 473 nm, 100 mW, Extreme Lasers). During retrieval day, the mice received a block of 8 CS$^-$ and 8 CS$^+$ and eight 30-s pulses of blue light were given for four of each tone. Light stimulation during CSs was changed for each animal to avoid artifact effects. The light started 50 ms before the first pip (what is pip?) and ended 50 ms after each pip. Freezing with and without light stimulation was quantified as previously described. After the experiment, optic fibers were removed and animals were perfused with PFA (4 %) for histological analysis of the injection site as described. The brain was removed and cut into 80 µm coronal slices.

For elevated plus maze and open field tests, optical fibers were connected to the implanted optical connectors and each mouse was monitored for 18-20 minutes while light was delivered 3 times for 3 minutes each time. After each light application, mouse behavior was monitored as well.

Immunohistochemistry

The mice were transcardially perfused with phosphate buffered saline followed by 4% paraformaldehyde (PFA) in phosphate buffered saline (PBS). Brains were post-fixed in PFA for 4 hours at 4°C and then transferred to 30% sucrose in PBS.

The brains were cut into 50 µm thick coronal slices on a vibratome (Leica Microsystems, Heerbrugg, Switzerland). Free-floating sections were rinsed in PBS. Subsequently, sections were incubated in blocking solution (20% bovine serum albumin (BSA) and 0.5% Triton X-100 in PBS (PBST)) for 2 hours. Then sections were incubated in blocking solution (3% BSA and 0.5% PBST) containing the primary polyclonal rabbit anti- GABAα5 antibody (5 µg/ml, gift from Dr. W. Sieghart, University of Vienna, Vienna, Austria) for 48 hours at 4 °C. Subsequently, sections were washed with PBS for three time (5 min each) and incubated for 4 hours at room temperature with fluorescent donkey anti-rabbit alexa fluor 594 (Invitrogen; 1:500 in 3% BSA and 0.5% PBST). Finally, immuno-labeled sections were rinsed three times with PBS, mounted on gelatin-coated slides, dehydrated and coverslipped. The brains from wild type and GABAα5 knockout mice were treated with the same staining procedures and imaged with the same settings under a LSM 700 microscope (Carl Zeiss AG, Germany).

Cre-regulated knockdown of alpha5 subunits

Four pairs of DNA oligos targeting the mouse α_5GABA$_A$R were designed using RNAi Explorer, and tested in HEK293T cells by cotransfecting the rat α_5 subunit with the knock-down constructs. Sequence no.2 (tccattgcacacaacatgac - NM_176942.4 (765-784)) showed the best knockdown (Fig 1a). For conditional expression, the shRNA construct was inserted into a modified lentilox 3.7 (pLL3.7) dsRed (pSICO) that contains loxP sites within the TATAbox sequence (Ventura, Meissner et al. 2004). The oligo for the shRNA was cloned into pSICO digested with Xho and Hpa. A scrambled control oligo (catacggtcaatcctcaaca) was also synthesized and constructed in the same vector. All constructs were verified by sequencing. To test conditional expression HEK293T cells were plated into 24-well plate with a density of 8.0×10^4 cells per well and were transfected with constructs expressing the rat α_5 subunit , α_5GABA$_A$R knock-down or the scrambled control and Cre at a ratio of 1:1:1. The cells were washed with PBS and lysed in 200 µl 1x sample buffer. Twenty microliters of each sample were used for SDS-PAGE and Western blots. The alpha 5 antibody (Novus) was diluted with the ratio of 1:1000.

Generation of conditional AAV Gabar5-shRNA constructs

The AAV shRNA constructs allow for conditional (Cre-Lox), stable expression of both short hairpin RNAs (shRNAs) for RNA interference under the promoter U6, and reporter protein tdTomato driven by the promoter EF1a. The sequences of both Gabar5-shRNA and control-shRNA were first synthesized with EcoRI/EcoRV restriction sites at each end and inserted into pBMH vector (Biomatik USA, LLC).

Gabra5-shRNA:

TGTCCATTGCACACAACATGACTTCAAGAGAGTCATGTTGTGTGCAATGGACTTTTTTC.

Control-shRNA:

TGCATACGGTCAATCCTCAACATTCAAGAGATGTTGAGGATTGACCGTATGCTTTTTT.

The pBMH-shRNA constructs were digested with EcoRI/EcoRV initially and the shRNA-containing segments were recycled and purified for ligation with pAAV-EF1-DIO-glyG-WPRE-pA (modified from the pAAV-EF1a-DIO-hChR2YFP, Deisseroth Lab, Stanford University) to insert the shRNA sequences after the second lox2711/loxP site.

Mouse U6 promoter was synthesized with EcoRI and EcoRV for inserting into pAAV-EF1a-tdTomato-WPRE-pA (a gift from Botond Roska lab, Friedrich Miescher Institute, Basel, Switzerland) to generate segment of mU6-Tdtomato, which later replaced the glycoprotein G (glyG) of pAAV-EF1a-DIO-glyG-shRNA-WPRE-pA backbone designed with Asc1 and Nhe1 restriction sites. The expression of both tdTomato and shRNA driven by EF1 and mU6 respectively is achieved at the same time upon Cre recombination (Fig.1). The constructs were sequenced before being amplified with endonuclease-free column (Macherey-nagel; Germany) and were further validated in cultured cells by co-transfecting a Cre construct (data now shown). Two AAVs (serotype9; Vector Core; University of Pennsylvania) for the expressions of Gabra5-shRNA (pAAV-EF1a-DIO-tdTomato-U6-Gabra5.shRNA) and control shRNA (pAAV-EF1a-DIO-tdTomato-U6-control.shRNA) were injected into the CeM of the PKCδ-Cre-EYFP transgenic animals, to ensure cell-type specific knockdown of alpha5 subunit in PKCδ-positive cells in CEl.

RESULTS

Role of tonic firing of PKCδ^+ neurons on anxiety and fear generalization

As previously reported, the plastic change of the tonic firing of PKCδ^+ neurons was correlated with fear generalization. Higher spontaneous firing statistically correlated with higher fear generalization (Ciocchi et al, 2010). Taken that fear conditioning increases the overall anxiety levels of the animal population tested and that this correlates with fear generalization (Figure 8), we hypothesized a causal role for PKCδ^+ neurons spontaneous firing in regulating anxiety levels and fear generalization.

Furthermore, we manipulated the spontaneous firing of PKCδ^+ neurons by performing optogenetic experiments *in vivo*. To gain genetic access to PKCδ^+ neurons, we used BAC transgenic mice expressing Cre recombinase and α subunit of a cyan fluorescent protein (CFP) (Haubensak et al, 2010).

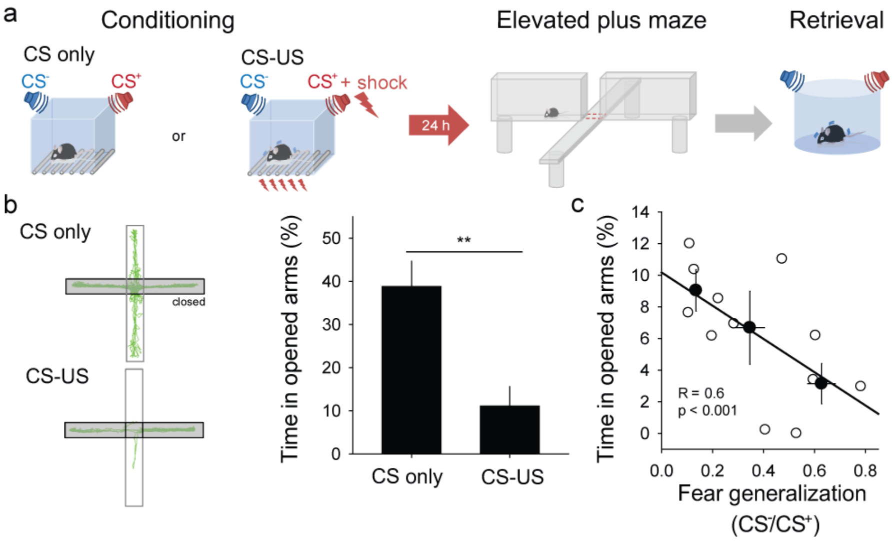

Figure 8. Fear conditioning on anxiety. a | Behavioral paradigms scheme. CS-US group of animals were conditioned to 5 CS$^+$ (red) paired with footshock (US) intermingled with 5 unpaired CS$^-$ (blue). CS only is the control group exposed only to the same context and to the two tones (CS$^+$ and CS$^-$) as described for the CS-US, but not to the footshock. Following 24 hours, the animals were tested in an elevated plus maze. Finally, only the CS-US group was put in the retrieval context and CS$^+$ and CS$^-$ were re-played. **b** | *left*, track of CS only and CS-US animals in an elevated plus maze; *right*, bar graph of the time spent in the opened arms in an elevated plus maze for the CS only and CS-US group. $^{**}p < 0.01$ by unpaired *t*-test. **c** | Correlation between time spent in the open arms versus fear generalization for the CS-US group. White dots are the values from each single animal while the black are averages of four animals at different fear generalization values (0-0.2; 0.2-0.5; 0.5-0.8). Linear regression values are indicated in the graph. All error bars indicate mean ± s.e.m.

We bilaterally injected a Cre- inducible Adeno- associated virus double floxed inverse ORF (DIO AAV virus) expressing *channelrhodopsin 2A* (ChR2A) or the enhanced proton pump (*archaerhodopsin*, Arch) in CEA of PKCδ Cre$^+$ animals. Following the injection, we bilaterally implanted opto-connectors about 500 µm above CEA in order to avoid damage upon insertion of optical fibers (Figure 10a and b).

Four to five weeks following the injection, blue light induced-ChR2 stimulation was effective in enhancing the firing of PKCδ^+ neurons while activation of Arch, with the yellow light wavelength, caused a decrease in extracellular firing *in vitro* (Figure 9).

After assessing the efficient time of ChR2 and Arch expression by measuring their impact on extracellular firing (figure 9), animals were subjected to anxiety and fear generalization paradigms (Figure 10).

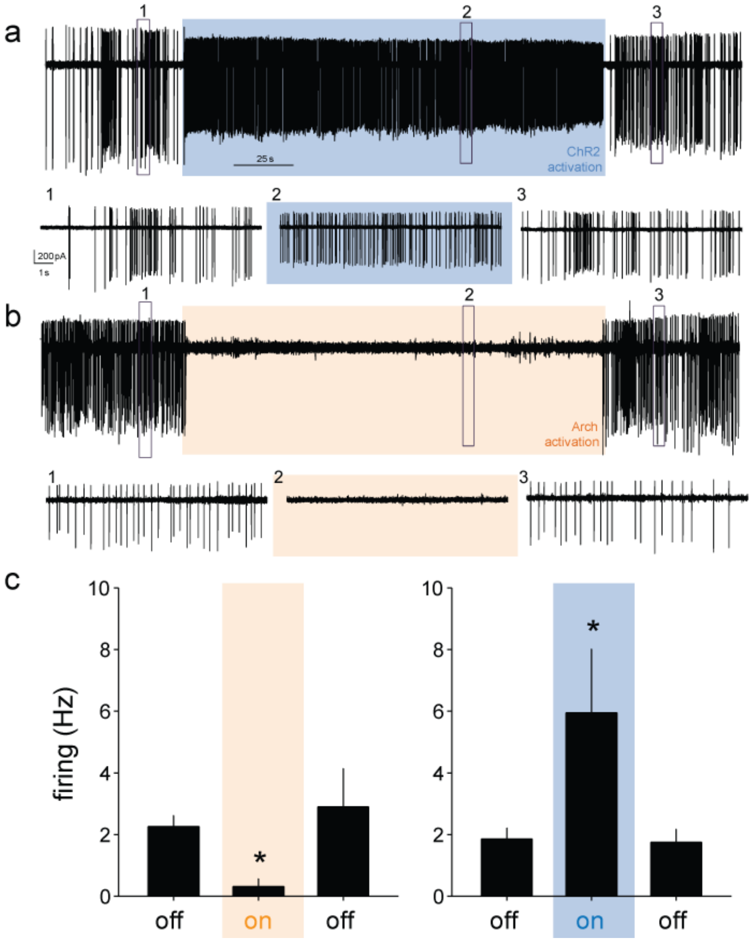

Figure 9. Light-evoked change in neuronal activity. a | *up*, Extracellular firing recording in *on-cell* from an infected PKCδ⁺ neuron with a AAV DIO-ChR2-2A-eNpHR-2A-Venus; the blue area shows the time of light activation that increase the firing; *down*, enlarged trace of the underlie areas 1, 2 and 3. **b** | same as **a**, but the only difference is that PKCδ⁺ neurons were infected with AAV FLEX-Arch-GFP and yellow light decreases their extracellular firing. **c** | Bar graph of the firing before (off), during (on) and after (off) light on (yellow for Arch, left graph, and blue for ChR2 activation). *$p < 0.05$ by paired t-test within off and on condition. All error bars indicate mean ± s.e.m.

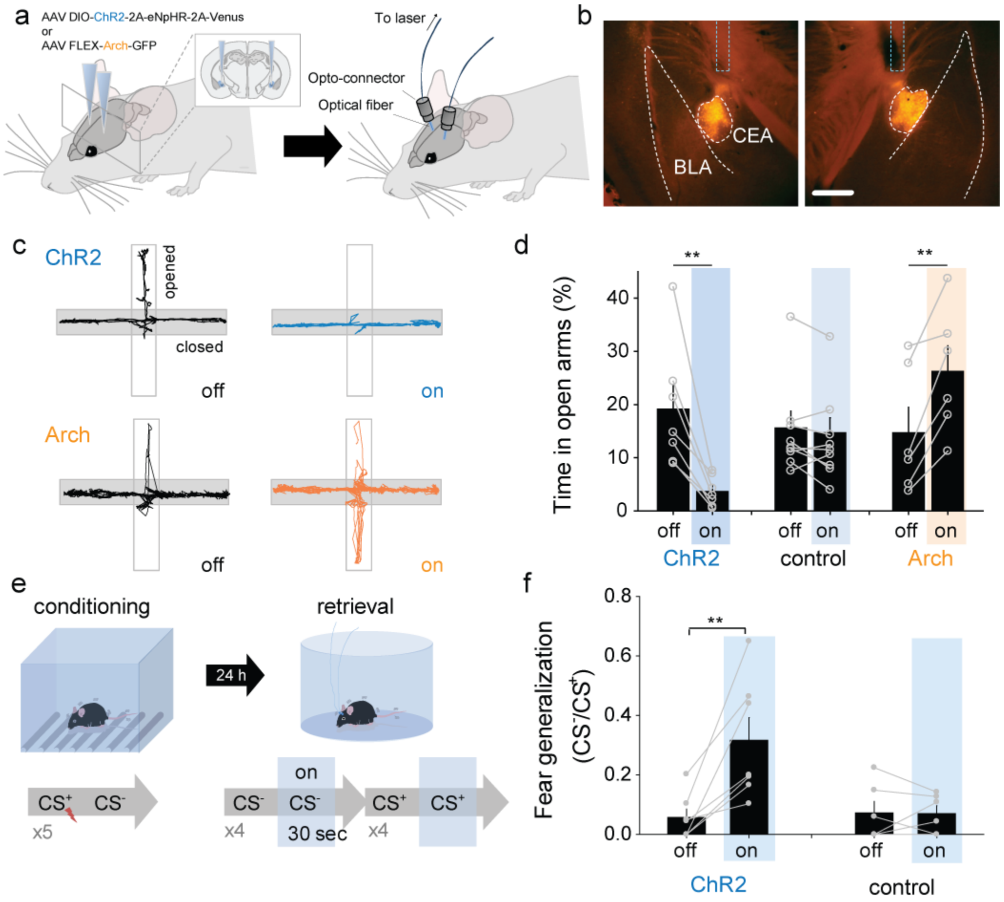

Figure 10. Spontaneous firing of PKCδ⁺ neurons controls fear generalization and anxiety. **a** | *left*, Schematic representation of virus injection; *right*, Schematic representation of a freely moving mouse bilaterally implanted with optical fibers. **b** | Coronal sections of a mouse brain indicating the location of amygdala and the bilateral injection of the conditional AAV virus expressing for td Tomato and ChR22A. White dashed lines indicated the border of BLA and CEA while the blue dashed line the insertion of the optical fibers. **c** | Elevated plus maze examples for the ChR2, control and Arch group of animals before and during light on. **d** | Bar graph of the time spent in the open arms (expressed in %) for the ChR2 (n = 8), control (n = 7) and Arch group (n = 7) of animals during light off and on. **e** | Scheme of the fear conditioning protocol and optogenetic protocol during retrieval. **f** | Bar graph of the fear generalization index during blue light off and on for the ChR2 group of PKCδ Cre$^+$ mice infected with conditional AAV virus expressing ChR22A and control animals not expressing ChR2A (n = 7 each group). $^{**}p<0.01$ by paired t-test. All error bars indicate mean ± s.e.m.

First, we used the elevated plus maze paradigm to assess the involvement of PKCδ^+ neurons on anxiety. It was found that activation with blue light, or inhibition with yellow light, of PKCδ$^+$ neurons either decreased or increased, respectively, the duration of time spent in the open arms. There was no effect on non-infected control animals (Figure 9c-d).

In order to confirm that these changes were clearly caused by the modulation of an anxiety-like behavior, we also performed the open field test. Activation of PKCδ^+ neurons upon blue light stimulation decreased the number of center crossings for the ChR2 group (normalized for the track length) without having any effect on control animals (non-infected animals). Furthermore, yellow light inhibition of PKCδ^+ neurons increased the number of center crossings per unit track length (Figure 11).

Since fear generalization correlates with anxiety, it could be predicted that activation of PKCδ^+ neurons not only enhanced anxiety levels but also fear to a "*neutral*" tone (CS$^-$) (Figure 8c).

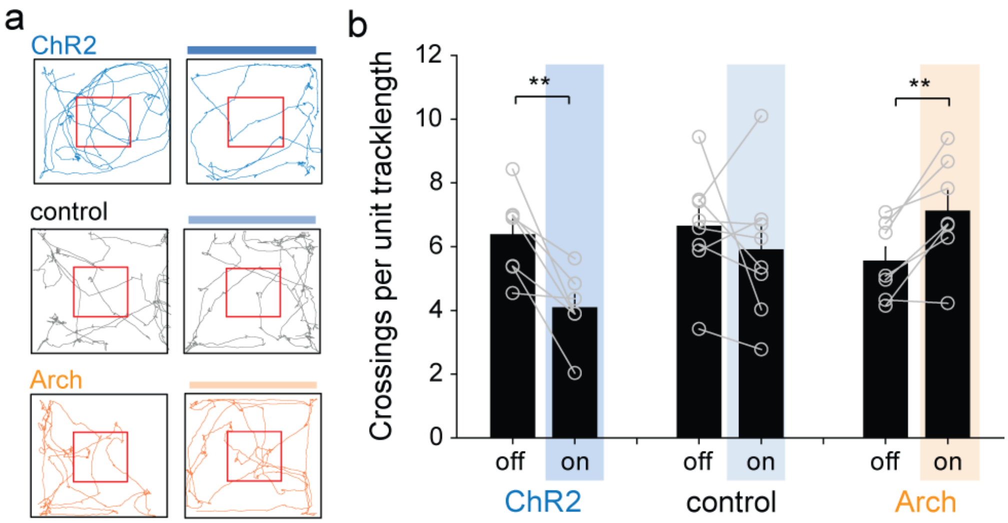

Figure 11. Light modulation on open field behavior. a | Animal track length examples in the open field arena for the ChR2, Control and Arch group. **b** | Before and After bar graph of the center crossing per unit track length of ChR2, Control and Arch group during light off and on. **$p < 0.01$ by paired t-test. All error bars indicate mean ± s.e.m.

To address this, we performed auditory fear conditioning giving five paired (CS$^+$) intermingled with five unpaired tones (CS$^-$). During retrieval, the animals were exposed to eight CS$^+$ and eight CS$^-$ in absence or presence of 30 s 373 nm light stimulation (four during light off and four during light on; Figure 10e). Tonic light-activation of PKCδ^+ neurons slightly enhanced the freezing to the CS$^+$ (light$_{off}$: 70.3 ± 8.7; light$_{on}$: 87.9 ± 8.7; $p < 0.05$ by paired t-test) and, with more pronounced effect, to the CS$^-$ (light$_{off}$: 5.2 ± 2.1; light$_{on}$: 28.2 ± 5.6; $p < 0.05$ by paired t-test). The overall effect was an increase in fear generalization index upon light activation while, in control animals, light did not have any considerable effect (Figure 10f).

These findings demonstrate that tonic activity of PKCδ^+ neurons is directly implicated in anxiety-like behavior and fear generalization to a *neutral* auditory stimulus.

The α_5GABA$_A$ extrasynaptic receptor controls the tonic firing of PKCδ$^+$ neurons

The optogenetic approach represents a powerful method to control neuronal excitability and its impact on behavior. However, this method does not completely mimic the physiological neuronal pattern involved in the generation of fear generalization and anxiety. Thus, it is critical to understand the plastic mechanism that modulate the tonic firing of PKC*δ*$^+$ neurons after fear conditioning and cause the observed enhancement of anxiety and fear generalization.

As previously mentioned, CEA is a neuronal network composed of 90% GABAergic neurons. CEA neurons are spontaneously active at about 6 Hz (Ciocchi et al., 2010). Furthermore, these neurons ensure high ambient GABA concentrations able to locally modulate the spontaneous firing of other CEA neurons. Interestingly, the GABAergic system is implicated in associative fear learning and anxiety (Brickley and Mody, 2011; Rudolph and Knoflach, 2011) and it is therefore a likely candidate in the observed tonic activity plastic changes induced by fear conditioning.

Since little is known about the GABAergic inhibition onto PKC*δ*$^+$ neurons, we performed whole-cell voltage- clamp recordings in acute brain slices using a CsCl-based internal solution (E_{Cl^-} = 0 mV),

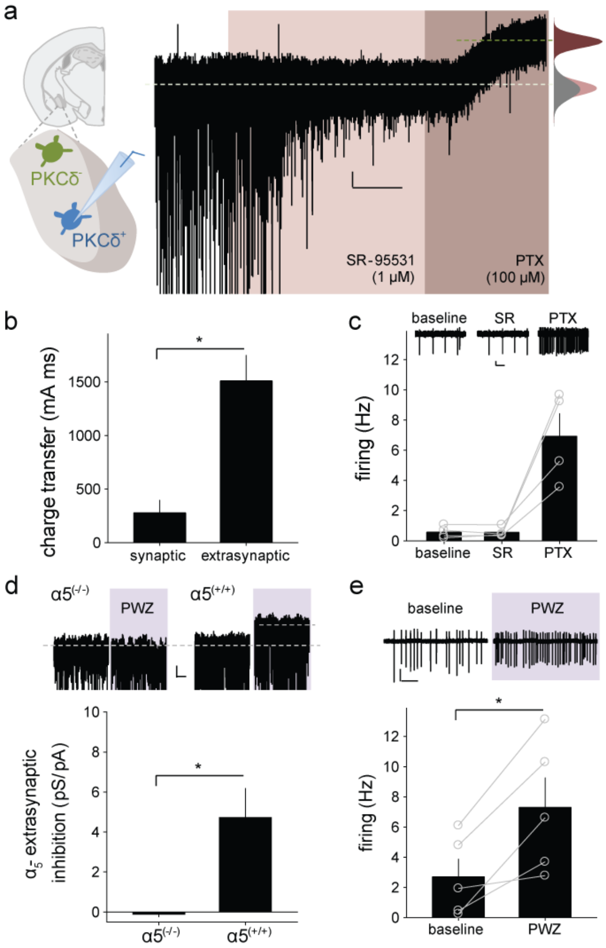

Figure 12. α_5-GABAAR- tonic inhibition controls the spontaneous firing of PKCδ$^+$ neurons. a | *left*, schematic representation of a coronal mouse brain slice and higher magnification of the two? neuronal populations identified in CEA; *right*, representative GABAergic current trace recorded from a PKCδ$^+$ neuron in vitro (scale bar: 5 pA, 2 min). Application of SR-95531 and PTX is indicated by the pink and brown rectangle, respectively. White dashed line indicates baseline holding current that fits with the average mean of two all-point histogram for baseline (gray) and SR-95531 (pink). PTX caused a shift of the holding current that is represented by the other dashed line that fits the average point of the Gaussian distribution shown in brown. This represents the tonic current. **b** | bar graph of the charge transfer for the synaptic versus extrasynaptic current (n = 6). *$p<0.05$ by paired t-test. **c** | *top*, spontaneous firing recorded in *on cell* from a PKCδ$^+$ neuron (scale bar: 10 pA, 500 ms); *lower*, bar graph of the spontaneous firing of PKCδ$^+$ neurons in baseline, during application of SR-95531 (SR) and PTX (n = 4). *$p < 0.05$ by one-sample t-test. **d** | *upper*, representative GABAergic current recordings from *α_5GABA$_A$R knock out x PKCδ$^+$ neurons* ($\alpha_5^{(-/-)}$) and *α_5GABA$_A$R wild type x PKCδ$^+$ neurons* ($\alpha_5^{(+/+)}$) (scale bar: 10 pA, 10 s). Violet square represent the application of PWZ-029 (1 μM, PWZ); *lower*, bar graph of the α_5GABA$_A$R extrasynaptic inhibition (expressed in pS/pF) for $\alpha_5^{(-/-)}$ and $\alpha_5^{(+/+)}$ neurons (n = 4). *$p<0.05$ by unpaired t-test. **e** | *top*, spontaneous firing recorded in *on cell* of a PKCδ$^+$ neuron before and during the application of PWZ (violet rectangle) (scale bar: 200 pA, 500 ms); *lower*, Bar graph of the spontaneous firing of PKCδ$^+$ neurons in baseline and during PWZ application (n = 5). *$p<0.05$ by paired t-test. All error bars indicate mean ± s.e.m.

clamping the neurons at -70 mV in order to reduce leak current noise. In addition, CNQX (10 μM) and APV (10 μM), AMPA and NMDA receptors blockers respectively, were used in order to selectively study spontaneous inhibitory postsynaptic currents (sIPSCs). This method allowed us to understand the presynaptic general and non-specific spontaneous inhibition received by the patched neuron.

GABAergic extrasynaptic inhibition was observed from PKCδ^+ neurons (applying 100 μM picrotoxin, PTX) and, importantly, was significantly not blocked by 1 μM SR95531 (SR, or gabazine), a competitive GABA$_A$R antagonist, which decreased or abolished the sIPSCs (Figure 12a). In addition, we found, as expected, that the inhibitory charge transfer of the extrasynaptic component was 5-fold higher than the synaptic one (Figure 12b). Thus, these pharmacological tools are indispensable in dissecting the extrasynaptic versus synaptic current and understanding their differential roles in neuronal excitability, as has already been shown (Semyanov et al, 2003).

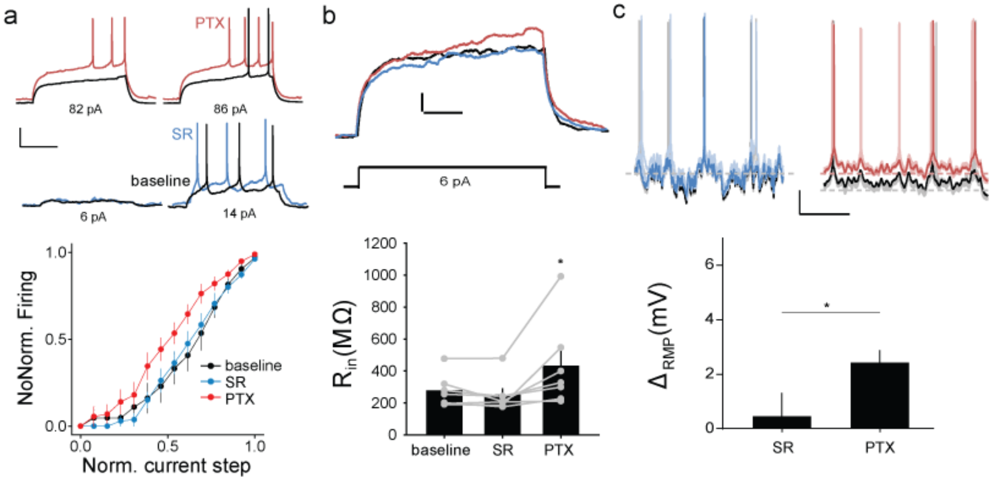

Figure 13. Extrasynaptic inhibition on neuronal excitability. a | *Top trace* shows the effect of PTX (100 μM, red trace) on baseline (black trace) while the *down trace* shows the effect of gabazine (SR, 1 μM, blue trace) on baseline. *Lower,* Input- output function of PKCδ$^+$ neurons before and during SR (blue), and PTX (red) of the normalized evoked firing *versus* the current steps. The functions are superimposed with baseline (in black). **b** | Two different subthreshold voltage changes in baseline, SR and PTX elicited by somatic current injections (6 pA). *Lown*, bar graph of the input resistance (R_{in}) expressed in MΩ in baseline and applying SR, and subsequently PTX. $^*p < 0.05$ by paired t-test. **c** | *Top traces* elicited by white current noise injections in baseline (black), SR (blue) and PTX (red). *Down*, bar graph of the change in resting membrane potential versus baseline in presence of SR and PTX. $^*p < 0.05$ by unpaired t-test. All error bars indicate mean ± s.e.m.

To address the role of the tonic component on neuronal excitability, we used extracellular loose cell-attached recordings (LCA) in order to leave intact the chloride gradient of PKCδ^+ neurons. PTX (100 μM), but not SR (1 μM), enhanced the tonic firing of PKCδ^+ neurons (Figure 12c).

Furthermore, The I/O curve was studied by giving current steps of increasing amplitude and analyzing the number of action potentials produced. The data showed that blocking the tonic current, but not the phasic current, significantly increased the input resistance and caused a subtractive shift of the I/O function in PKCδ^+ neurons (Figure 13a and b).

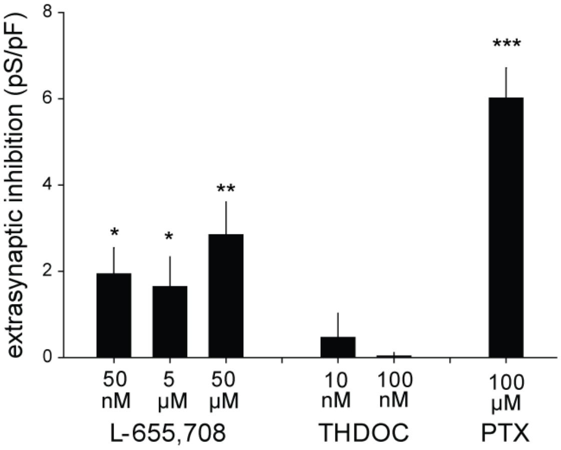

Figure 14. Extrasynaptic inhibition of PKCδ^+ neurons. Bar graph of the extrasynaptic inhibition partially blocked by the α_5GABA$_A$R inverse agonist L-655,708 at three different concentrations (50 nM, n = 6; 5 µM, n = 9; 50 µM, n = 9), THDOC (10 nM, n = 8; 100 nM, n = 8) and PTX (100 µM, n = 14). $^*p < 0.05$, ** $p < 0.01$, $^{***}p < 0.001$ by one-sample t-test. All error bars indicate mean ± s.e.m.

In addition, we used a white noise current step in order to reliably evoke spikes that could be followed after many trials in *whole cell* configuration. PTX, but not SR, depolarized the resting membrane potential and increased the number of evoked spikes (Figure 13c).

These data indicate that extrasynaptic current is present in the central amygdala and is important in controlling neuronal excitability and neuronal sensitivity to external inputs (see also supplementary figure 6-7).

In order to determine the composition of the GABA$_A$ receptor subunit responsible for the extrasynaptic inhibition, we performed a pharmacological approach *in vitro* by using L-655,708 and PWZ-029, two inverse agonist specific for the α5-containing receptors (Caraiscos et al., 2004; Savić et al, 2008). PWZ-029 (1 µM) decreased the extrasynaptic inhibition of PKCδ^+ neurons (α_5GABA$_A$R$^{(+/+)}$ *x* PKCδ^+) without having an effect on α_5GABA$_A$R knock-out PKCδ^+ neurons (α_5GABA$_A$R$^{(-/-)}$ *x* PKCδ^+) (Figure 12d).

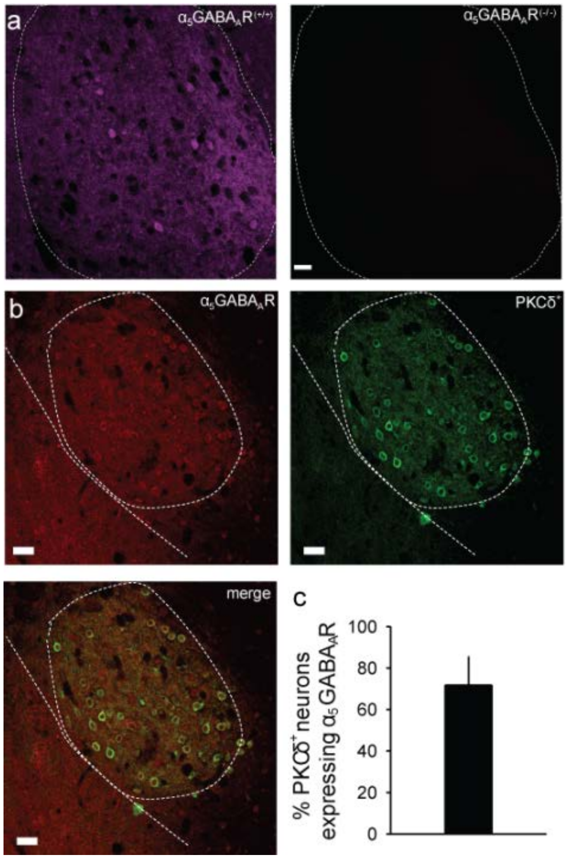

Figure 15. Localization of α_5GABA$_A$R in CEA and on PKCδ^+ neurons. a | α_5GABA$_A$R staining of CEA in wild type (α_5GABA$_A$R$^{(+/+)}$) and KO animals (α_5GABA$_A$R$^{(-/-)}$). **b** | α_5GABA$_A$R (red), GFP staining (green, PKCδ^+) and merge picture in CEA region of PKCδ Cre$^+$ animals. White bar: 20 µm. **c** | Bar graph of the percentage of PKCδ^+ neurons expressing α_5GABA$_A$R (n = 3). All error bars indicate mean ± s.e.m.

L-655,708, at three different concentrations, decreased the extrasynaptic inhibition of PKCδ^+ neurons but also that of the other two CEA neuronal subpopulations (Figure 14) as observed for PWZ-029. THDOC (a neurosteroid selective for δ-containing GABA$_A$ receptors, 10 nM and 100 nM) did not have a considerable effect (Figure 14).

Furthermore, immunohistochemical staining confirmed the presence of α_5GABA$_A$Rs in CEA neurons, whereas staining was absent in the control, constitutive α_5 knock-out, animals (α_5GABA$_A$R$^{(-/-)}$). Further, GFP staining in PKC*δ* CRE$^+$ animals showed that the α_5 subunit is co-localized in PKC*δ*$^-$ neurons (Figure 15). PWZ-029 (1 µM), which blocked extrasynaptic inhibition, significantly enhanced the firing frequency of PKCδ^+ neurons recorded in LCA mode (Figure 12e).

Extrasynaptic inhibition mediated by α_5GABA$_A$Rs is also been found in other CEA neurons (supplementary figure 8).

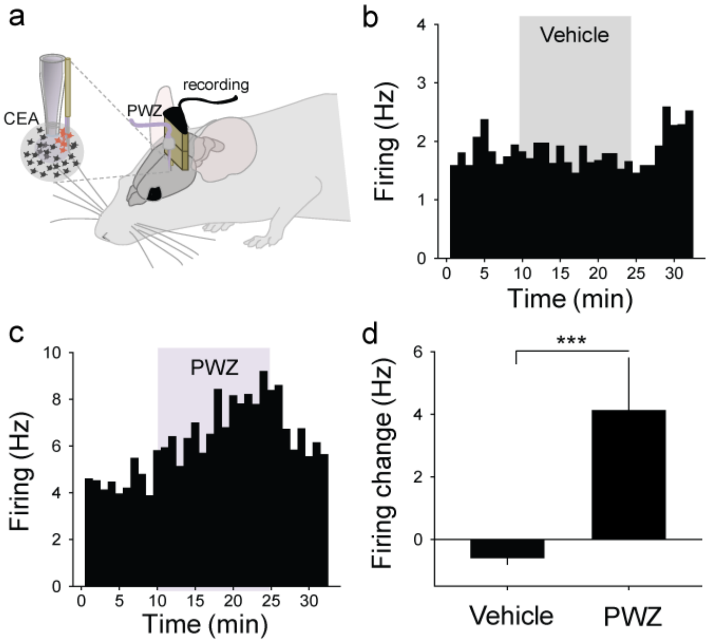

Figure 16. Extrasynaptic inhibition *in vivo*. a | Schematic representation of the canulae use to perfuse PWZ-029 (PWZ) and electrode implantation (recording) into CEA (enlarged area). The electrode records the extracellular firing of the cells next to the wire (shown in red). **b** | time course of the firing (expressed in Hz) of an example single unit. After 10 minutes baseline, vehicle was applied (grey area) and followed by washout. **c** | time course of the firing (expressed in Hz) of an example single unit. After 10 minutes baseline, PWZ was applied (violet area) and followed by washout. **d** | Bar graph of the firing change from baseline induced by vehicle (n = 12) and PWZ (n = 6). ***$p < 0.001$ by unpaired t-test. All error bars indicate mean ± s.e.m.

The slice preparation procedure we use lesions most of the synaptic contacts, thereby limiting the physiological ambient GABA concentration. Therefore, we combined localized infusion of PWZ-029 into the central amygdala with single unit recording to verify the effect of α_5GABA$_A$Rs blockage on the tonic firing of CEA neurons *in vivo*.

A pharmacological canulae was attached to an electrode, comprising 16 wires, and implanted into the CEA (Figure 16a). After 10 minutes of baseline recording, PWZ-029 (10 µM) was applied for 10 minutes and caused a reversible increase in firing of identified CEA neurons. The effect of PWZ-029 on the basal firing of CEA neurons was not observed following infusion of DMSO (vehicle group) (Figure 16b-c).

Overall, extrasynaptic inhibition recorded from PKCδ^+ neurons can be pharmacologically isolated from phasic inhibition and it is predominantly controlled by α_5GABA$_A$Rs. Tonic inhibition, as observed for other neuronal populations, sets the signal-to-noise ratio of PKCδ^+ neurons by modulating their excitability.

Plasticity of the α_5GABA$_A$R extrasynaptic inhibition

Given that fear conditioning induced changes in the tonic activity of CEl$_{off}$ neurons and correlates with fear generalization, a next important question is whether this tonic current is modulated by experience. This question can be addressed by using an ex vivo approach. We fear conditioned mice (CS-US) by placing them into the fear context where five CS$^+$ were paired with a footshock (US) and intermingled with five unpaired CS$^-$. The following day (retrieval), animals were placed into the extinction context and four CS$^+$ and four CS$^-$ were replayed. The animals froze about 60% of the time during the CS$^+$, whereas very low freezing levels were observed during the CS$^-$. Control animals (CS only) were treated in the same manner but were not exposed to the US and they did not freeze during exposure of the tones (Figure 17a). Animals were then euthanized and slices were prepared 20-30 minutes later. Recordings were obtained 2 hours after fear conditioning and a decrease of the extrasynaptic normalized conductance in PKCδ^+ neurons was observed for the CS-US animals. The

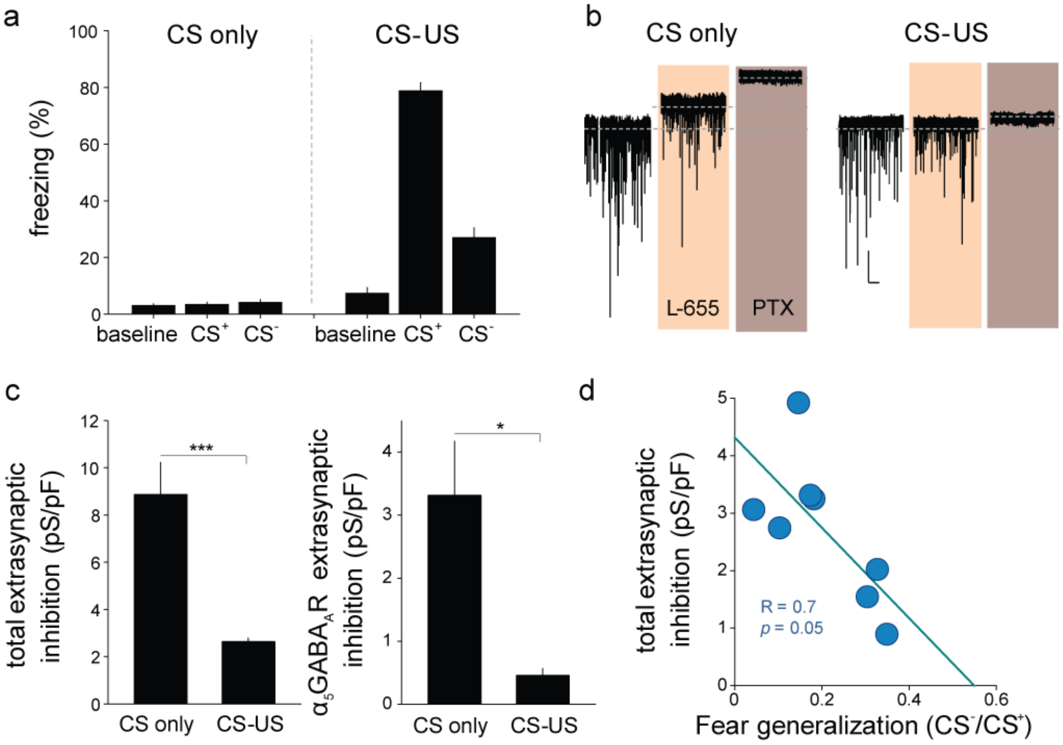

Figure 17. Plastic decrease of the exstrasynaptic inhibition induced by fear conditioning. a | Bar graph of the freezing levels during baseline, CS$^-$ and CS$^+$ for the control (CS only) and fear conditioned (CS-US) group (n = 8 each). **b** | Representative traces of sIPSCs in baseline, with application of L-655,708 (50 µM, yellow area) and PTX (100 µM, brown area). Scale bar: 50 pA, 10 s. **c** | Bar graphs of the total and α_5GABA$_A$R extrasynaptic inhibition (expressed in pS/pF) blocked with PTX (n = 14 for CS only; n = 26 for CS-US) and L-655,708 (n = 14 for CS only; n = 28 for CS-US), respectively.*p < 0.05, ***p < 0.001 by unpaired t-test. **d** | Linear correlation between the total extrasynaptic inhibition and fear generalization. The values are obtaining by fitting each dot (representing each animal and the average of the extrasynaptic inhibition values for each animal) with the linear regression function. All error bars indicate mean ± s.e.m.

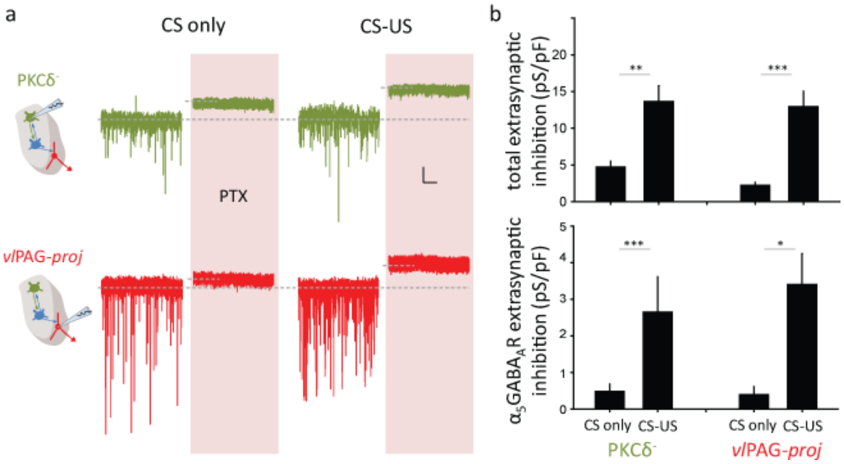

effect of L-655,708 was consistent with the change in total extrasynaptic inhibition. When the tonic current was decreased, L-655,708 had little or no effect (Figure 17b-c).

Figure 18. Fear related plastic changes of extrasynaptic inhibition of PKCδ$^-$ and *vl*PAG-projecting neurons. a | Compressed sIPSCs traces showing the effect of PTX application (pink bar) on the tonic current for PKCδ$^-$ (green) and *vl*PAG-projecting neurons (red) in CS only and CS-US group (scale bar: 25 pA, 10 s). **b |** *Top*, bar graph of the total extrasynaptic inhibition for PKCδ$^-$ ($n = 8$ CS only; $n = 12$ CS-US) and *vl*PAG-projecting neurons ($n = 6$ for CS only and CS-US) in CS only and CS-US group. *$p < 0.05$, **$p < 0.001$, ***$p < 0.001$ by unpaired t-test. All error bars indicate mean ± s.e.m.

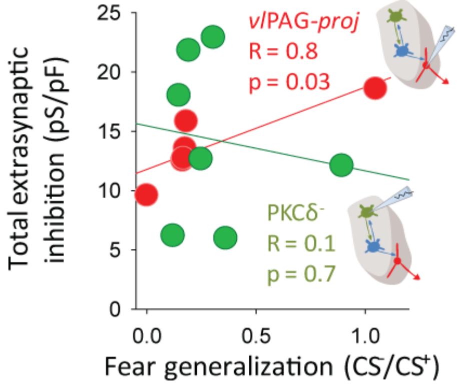

Figure 18. Relationship between extrasynaptic inhibition of different CEA neuronal subtypes and fear generalization. XY graph showing in the y axis normalized extrasynaptic inhibition recorded from PKCδ^- (green) and *vl*PAG-projecting neurons (red) and in the x axis the fear generalization. The values of the linear regression are shown in the graph for each neuronal sub-group.

As we showed previously, *in vivo* results indicate that CEl$_{\text{off}}$ neurons are those that solely increase their tonic firing after fear conditioning. In order to understand whether the plastic decrease observed for extrasynaptic inhibition was restricted to PKCδ^+ neurons, we recorded GABAergic sIPSCs from two other CEA neuronal populations: PKCδ^- and *vl*PAG-projecting neurons. Interestingly, we observed that fear conditioning enhanced the total and the α$_5$GABA$_A$R mediated extrasynaptic inhibition recorded from PKCδ^- and *vl*PAG-projecting CEm neurons (figure 18). Enhanced extrasynaptic inhibition was found to be associated with higher baseline sIPSC frequency recorded from these two neuronal populations. In PKCδ^- neurons, the sIPSC frequency was significantly enhanced (1.6 ± 0.4 Hz in CS only group and 2.7 ± 0.4 Hz in CS-US group, *$p < 0.05$ by unpaired t-test) similarly to that for *vl*PAG-projecting neurons (1.6 ± 0.4 Hz in CS only group and 2.7 ± 0.4 Hz in CS-US group, *$p < 0.05$ by unpaired t-test) (supplementary figure 16). The decrease in the extrasynaptic inhibition of PKCδ^+ neurons was not caused by a decrease in presynaptic inhibition because the sIPSC frequency recorded from these neurons did not significantly change in both behavioral groups (1.683 ± 0.187 (n = 26) for CS only; 1.363 ± 0.145 (n = 36) for CS-US group; $p > 0.05$ by unpaired t-test, data not shown) (supplementary figure 16).

As already discussed, the tonic firing of CEl_{off} neurons correlated with fear generalization to an unpaired tone (Ciocchi et al., 2010). Further, extrasynaptic inhibition modulates the tonic firing of $PKC\delta^+$ neurons and decreased after fear conditioning. Therefore, we checked whether plastic changes of the extrasynaptic inhibition relate to different levels of fear generalization. It was found that extrasynaptic inhibition of $PKC\delta^+$ inversely correlates with the fear generalization index (Figure 17d). Notably, a correlation between the extrasynaptic inhibition of *vl*PAG-projecting neurons and fear generalization but not for $PKC\delta^-$ neurons was observed (Figure 19).

Overall, these experiments showed that the extrasynaptic inhibition rapidly changed after fear induction because of a change of α_5GABA_AR component in specific neuronal subpopulation of CEA. It is likely that plastic changes of the extrasynaptic inhibition controlling the spontaneous firing of $PKC\delta^+$ neurons (considered CEl_{off} neurons) serve as a mechanism regulating fear generalization and anxiety. This assumption is confirmed by our data showing that the total extrasynaptic inhibition of $PKC\delta^+$ neurons was found to be inversely correlated with the fear generalization index (Figure 16d).

Role of α_5GABA$_A$R on anxiety and fear generalization

In order to find a causal role of the α_5GABA$_A$R inhibition on behavioral expression of fear generalization and anxiety, we created a conditional adeno-associated virus (AAV) encoding an shRNA against α_5GABA$_A$R to downregulate its expression selectively in virus-targeted PKCδ$^+$ neurons.

First, four pairs of siRNA DNA oligos targeting the mouse α_5GABA$_A$R were designed and tested in HEK293T cells by co-transfecting the rat α_5GABA$_A$R with the knock-down constructs. siRNA 5-2 (tccattgcacacaacatgac - NM_176942.4 (765-784)) showed the best knockdown (Figure 19a).

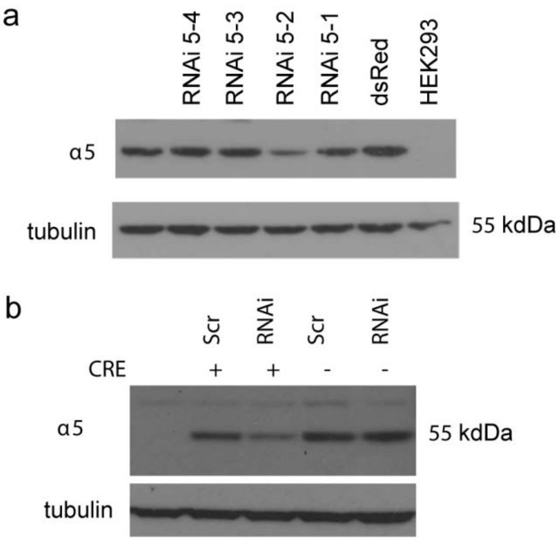

Figure 19. Cre-regulated knockdown of alpha 5 subunits. **a** | shown are western blots from HEK293 cells transfected with rat alpha5 subunit and four different siRNA oligonucleotides (siRNA 5.1 to siRNAi 5.4; lanes 2-5). dsRed was co-transfected to mark transfected cells. Lane1 show cells transfected with alpha5 alone, lane6 shows cells transfected with dsRed alone and lane7 are non-transfected cells. Alpha tubulin was used as the loading control. Blots were probed with an alpha5 antibody. **b** | siRNA5.2 or a scrambled oligo (Scr) was cloned into a floxed lentilox and HEK 293 cells with transfected with or without CRE recombinase. Transfected HEK293 cells were harvested 3 days after transfection and western blots probed with alpha5 antibody.

In order to assess the selective Cre-dependent expression of siRNA, we transiently transfected P19 cells with CMV-CRE-eGFP and EF1-DIO-U6-tdTomato-RNAi knock down plasmids.

Subsequently, after packaging, the conditional AAV virus expressing Tdtomato and siRNA was bilaterally injected into CEA of PKC*δ* Cre$^+$ animals (Figure 19a). Four to five weeks later the selective expression on PKC*δ*$^+$ neurons of the virus with Tdtomato was assessed using immuno-labeling. The infection rate of the virus to PKC*δ*$^+$ neurons was 88.97% ± 1.793 (n = 3) and Tdtomato expression was not observed in PKC*δ*$^-$ neurons and was restricted to CEA (Figure 20b).

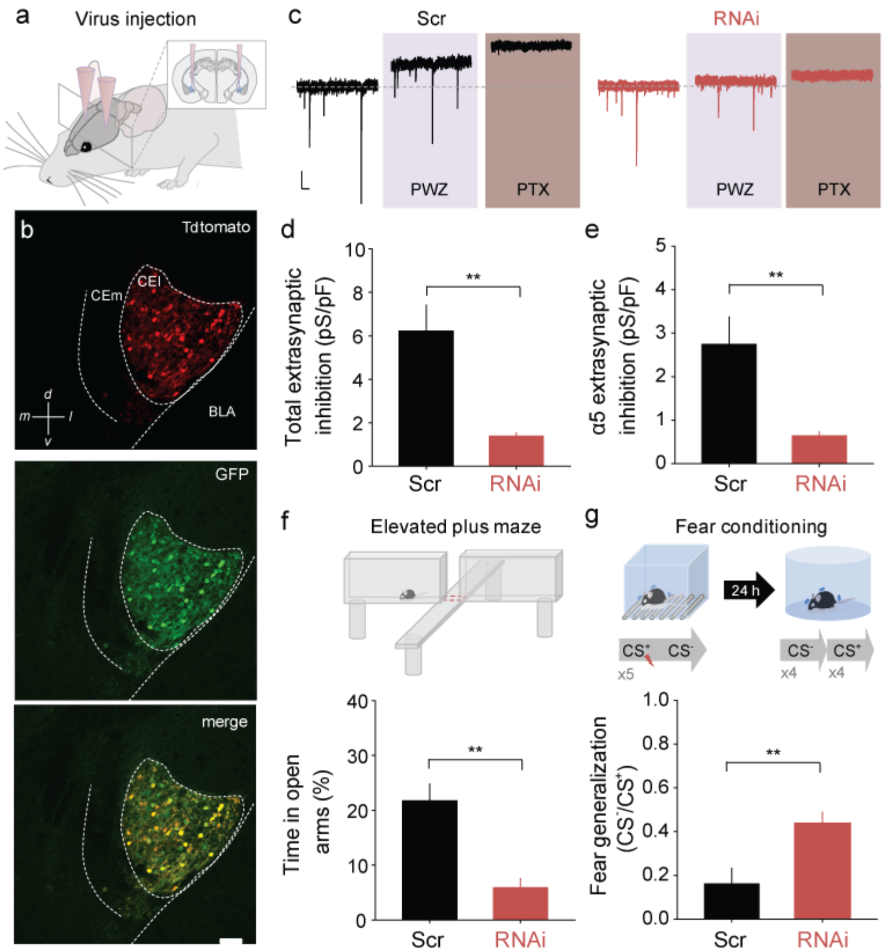

Figure 20. α_5GABA$_A$R inhibition of PKCδ^+ neurons controls fear generalization and anxiety. a | Schematic representation of the bilateral virus injection into CEA of a PKC*δ* Cre$^+$ animal. The virus is a conditional AAV expressing Tdtomato and siRNA under the U6 promoter. b | Immuno-labeling of 50 µm thick coronal slices focusing on CEA using antibody against Tdtomato (*red*, top), GFP (*green*, intermediate) and merge (*yellow*, bottom). BLA, CEl and CEm nucleus are indicated. Orientation bar: *m*, medial; *d*, dorsal; *l*, lateral; *v*, ventral. Scale white bar: 50 µm. **c** | Representative traces of sIPSCs recorded from PKCδ^+ neurons of the Scr (scramble, black) and α_5GABA$_A$R siRNA groups (red). Application of PWZ and PTX are indicated by the violet and brown box, respectively. Scale Bar: 20 pA, 15 s. **d** | Bar graph showing the total extrasynaptic inhibition blocked by PTX (100 µM) of the Scr and RNAi group (Scr, n = 7; RNAi, n = 8). **e** | Bar graph showing the α_5GABA$_A$R extrasynaptic inhibition blocked by PWZ-029 (1 µM, PWZ) of the Scr and RNAi group (Scr, n = 7; RNAi, n = 8). **f** | *Top*, Schematic representation of the elevated plus maze. *lower*, Bar graph showing the time spent in the open arms (expressed in percentage) for the Scr and α_5GABA$_A$R siRNA group (Scr, n = 7; RNAi, n = 7). **g** | *Top*, Schematic representation of the discriminatory auditory fear conditioning. In day 1 the mouse is placed in the conditioning context (cubic box) and receives five CSs followed by a shock (CS$^+$) intermingle with five unpaired CSs (CS$^-$). In day 2, 24 hours later, the animal is placed in the extinction context and four CS$^-$, four CS$^+$ are replayed in block (gray arrow). *lower*, Bar graph showing the fear generalization ratio for the Scr and α_5GABA$_A$R siRNA groups (Scr, n = 5; α_5GABA$_A$R siRNA, n = 5). $^{**}p < 0.01$ by unpaired t-test. All error bars indicate mean ± s.e.m.

sIPSC recordings from PKCδ^+ neurons were performed to assess the effect of down-regulation of the α_5GABA$_A$R (Figure 20c-e). It was found that knock-down of α_5GABA$_A$R, relative to control, significantly decreased the total extrasynaptic inhibition and the α_5GABA$_A$R extrasynaptic inhibition, which were blocked by PTX (100 µM) and PWZ-029 (1 µM), respectively (Figure 20c-e).

In contrast, the baseline amplitude of sIPSCs between scramble and α_5GABA$_A$R siRNA groups was not significantly changed (44.7 ± 16.9 pA, $n = 7$, for the Scr; 48.3 ± 13.6 pA, $n = 9$, for the α_5GABA$_A$R siRNA; $p > 0.05$ by unpaired t-test). There was also no difference in sIPSC frequency between the two groups (1.6 ± 0.6 pA, $n = 7$, for the Scr; 1.3 ± 0.3 pA, $n = 9$, for the α_5GABA$_A$R siRNA; $p > 0.05$ by unpaired t-test).

Finally, we used conditional knock-down to confirm the involvement of the α_5GABA$_A$Rs in fear generalization and anxiety by comparing the scramble (Scr) versus α_5GABA$_A$R siRNA groups.

Interestingly, animals with knock-down of α_5GABA$_A$R presented higher fear generalization, in comparison to controls. This was caused by an enhancement of freezing levels to the CS$^-$ in the auditory fear conditioning paradigm (Scr, CS$^-$(%): 10.7 ± 4.9; α_5GABA$_A$R siRNA, CS$^-$(%): 28.3 ± 4.0; $p < 0, 05$ by unpaired; Figure 20g). α_5GABA$_A$R siRNA -expressing animals, also exhibited a significant decrease in the time spent in the open arms of the elevated plus maze (Fig. 20f). Finally, monitoring the open field behavior, the conditional α_5GABA$_A$R knock-down group showed lower values of normalized crossing to the center, 8.9 ± 0.3, versus the control Scr group, 4.6 ± 0.7 ($p < 0.05$ by unpaired t-test, data not shown).

Together, these findings show that the decrease in extrasynaptic inhibition induced by fear conditioning is primarily caused by a down-regulation of α_5GABA$_A$Rs extrasynaptic inhibition in PKCδ^+ neurons. In addition, they confirm that α_5GABA$_A$Rs expressed in PKCδ^+ neurons are essential for the change of anxiety induced by auditory fear conditioning and maintenance of fear generalization.

SUPPLEMENTARY MATERIAL

CEA microcircuitry

Morphology of CEA neurons

The attractiveness of using BAC transgenic mice expressing Cre recombinase and the α subunit of a cyan fluorescent protein (CFP) is that we could study different morphological and physiological properties of PKCδ^+ neurons and other defined neuronal subpopulations of the CEA (Haubensak et al, 2010).

While performing electrophysiological recordings, we filled the neurons with biocytin (1%) that was previously mixed with the patch pipette internal solution. After a period of about 20 minutes, which allowed neuronal filling, we retracted the pipette and fixed the slice in 4% PFA and 0.5% picric acid. Subsequently, after performing a DAB staining, we were able to visualize and reconstruct CEA neurons.

PKCδ^- were considered the neurons located in CEl and not expressing CFP, while *vl*PAG projecting

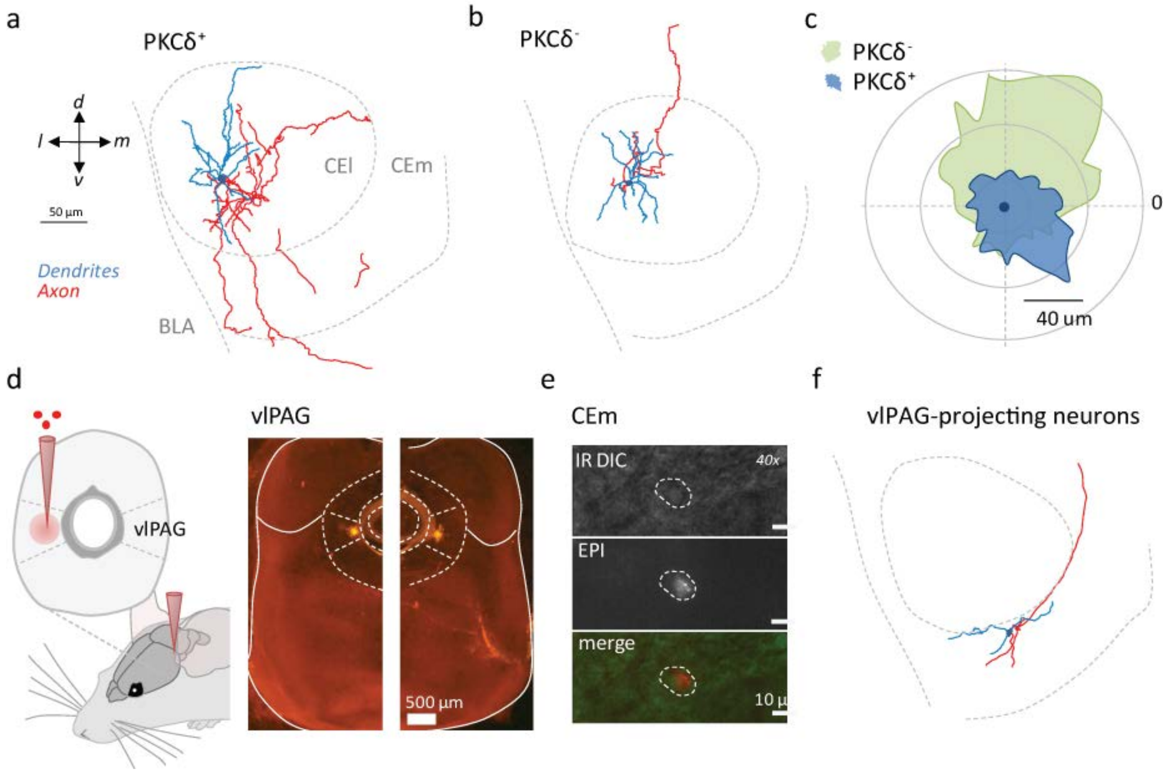

Supplementary figure 1. a | reconstruction of a representative PKCδ^+ neuron located in the CEl area. Red is the axon while in blue the dendrites. Orientation bar: *d*, dorsal; *v*, ventral; *m*, medial; *l*, lateral. **b** | reconstruction of a representative PKCδ^- neuron located in CEl area. **c** | polar plot of PKCδ^+ (n = 15, blue) and PKCδ^- neuron (n = 10, light green) located in CEl area. **d** | *Left*, schematic representation of red retro beads bilaterally injected into *vl*PAG. *Right*, fixed brainstem slice bilaterally injected with red retro beads in *vl*PAG. **e** | localization of red retro beads into the soma of CEm neurons visualized with an upright microscope. **f** | reconstruction of a representative vlPAG projecting neuron located in CEm area.

CEm neurons were identified by injecting fluorescent red beads into *vl*PAG and after 2-5 days checking the deposit of these microspheres in the soma of CEm neurons. The representative traces showed the different location of the recorded neurons from CEA. PKCδ^- (n = 15) and PKCδ^+ neurons (n = 10) were located in CEl and showed an average of 4.2 ± 0.3 and 4.3 ± 0.4, respectively, mainly aspiny dendrites located only in CEl area. The difference between these two CEl neuronal types lay on their axonal projection. In fact, 100% of PKCδ^+ neurons, compared to 20% of PKCδ^- neurons, projected toward a ventro-medial direction (to CEm area). The other PKCδ^- neurons strongly projected toward a dorso-medial direction where striatal structures are located. Both neuronal subtypes strongly and locally innervate the CEl nucleus. On the other hand, *vl*PAG-projecting neurons are smaller neurons located in CEm area. They have a lower number of dendrites (2.6 ± 0.2) in comparison with the other two neuronal subtypes of CEl described above. Dendrites are located in CEm right next to the border with CEl. Interestingly, their axons never cross this border (supplementary figure 1).

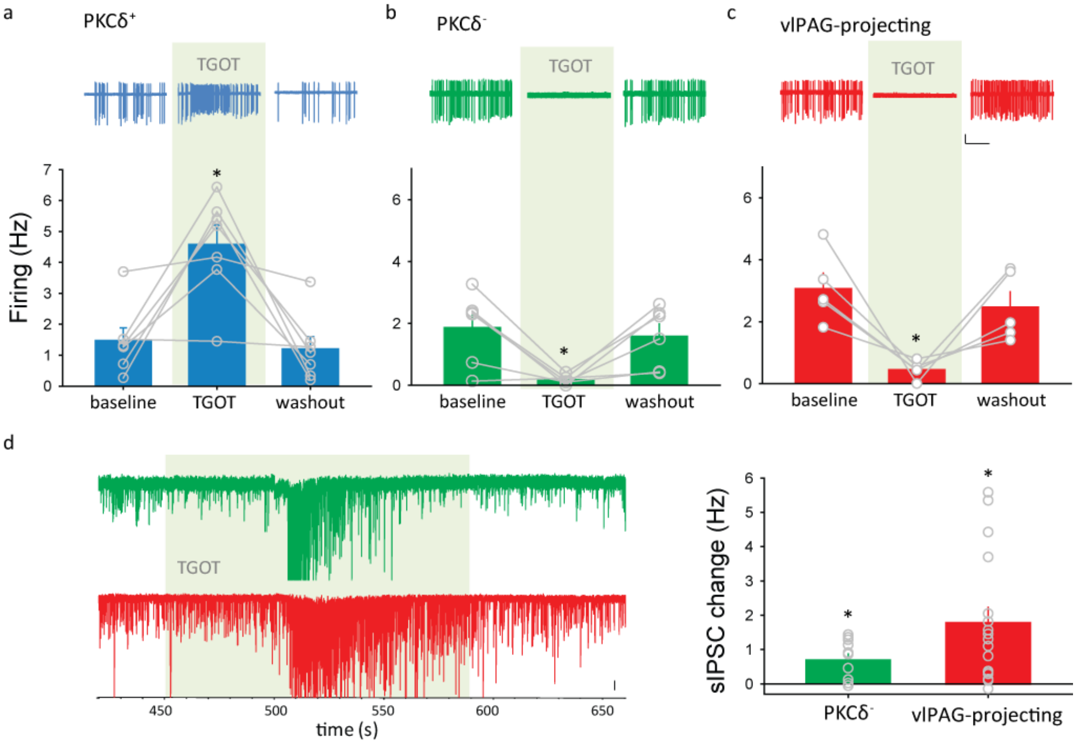

Supplementary figure 2. Pharmacological approach to study CEA microcircuitry. a | *Upper*, extracellular recording of the firing of PKCδ^+ neurons before during and after bath-application of 0.2 µM TGOT. *Lower*, bar graph of the firing in baseline, TGOT and washout. $^*p < 0.05$ by One-Way ANOVA followed by Bonferroni Post-hoc test. **b** and **c** | same as **a** but for PKCδ^- and *vl*PAG-projecting neurons, respectively. Scale bar: 200 pA, 5 s. TGOT caused a significant decrease of neuronal firing for both neuronal populations ($^*p < 0.05$ by One-Way ANOVA followed by Bonferroni Post-hoc test). **d** | *Left*, Recording of sIPSCs from PKCδ^+ neurons before during and after bath-application of 0.2 µM TGOT (light green bar). *Right*, Bar graph of the sIPSC frequency change induced by TGOT in PKCδ^- and *vl*PAG-projecting neurons. $^*p < 0.05$ by one-sample t-test *versus* control. All error bars indicate mean ± s.e.m.

Connectivity of CEA neurons

We assessed the presence of connectivity between PKCδ^+ and PKCδ^- or *vl*PAG-projecting neurons using pharmacological, optogenetic and multiple electrode recording approaches.

Since 80% of PKCδ^+ neurons expressed oxytocin receptors, connectivity can be studied using a pharmacological approach employing an agonist of this receptor (such as [Thr^4,Gly^7]-oxytocin or TGOT). Application of TGOT significantly enhanced the extracellular firing of about 80% of PKCδ^+ neurons (n = 7, supplementary figure 2a) while temporally inhibiting PKCδ^- and *vl*PAG-projecting neurons (n = 6 each cell type, supplementary figure 2).

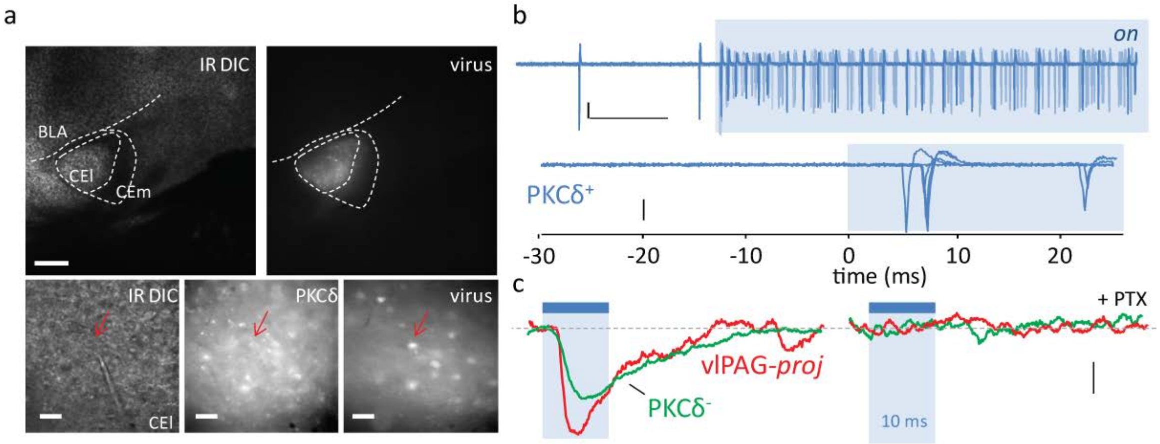

Supplementary figure 3. Optogenetic approach to study CEA microcircuitry. a | Image from the upright microscope in normal light (IR DIC) and with the green fluorescence protein (GFP) filter in order to visualize the virus injection specific in CEA. Scale bar: 250 µm. The smaller squares show higher magnification (40x) of normal light (IR DIC), with CFP filter (to visualize PKCδ^+ neurons, PKCδ) and with the GFP filter (to visualize the infected neurons, virus). Scale bar: 20 µm. **c** | *Left*, Light-evoked IPSCs (light blue bar, 10 ms) onto PKCδ^- and *vl*PAG-projecting neurons. *Right*, same cells but with 100 µM PTX application.

In order to demonstrate that the increased firing triggered GABA release onto PKCδ^- and *vl*PAG-projecting neurons, we recorded sIPSCs from these two neuronal populations in *whole cell* configuration using a CsCl-based internal solution in presence of AMPA and NMDA blockers (V_{hold}= -70 mV). We found a significant, reversible increase of sIPSC frequency onto PKCδ^- and *vl*PAG-projecting neurons upon TGOT bath-application of about 1-2 Hz ($p < 0.05$ by sample t-test, supplementary figure 2d). The effect of TGOT on sIPSC frequency did not

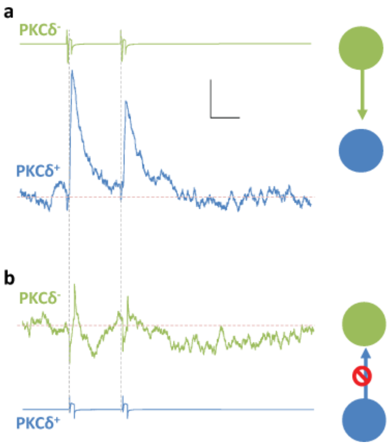

Supplementary figure 4.

significantly different in PKCδ^- and *vl*PAG-projecting neurons ($p > 0.05$ by unpaired t-test). Additionally, we performed optogenetic experiments in slices precisely targeting PKCδ^+ neurons with conditional AAV viruses that express ChR2 in these neurons (figure 9, and supplementary figure 3a-b). Light-evoked firing of PKCδ^+ neurons enhanced monosynaptic GABAergic IPSCs onto 40% of PKCδ^- and 60% of *vl*PAG-projecting neurons (supplementary figure 3c).

The latest methods assessed the inhibitory effect of GABAergic PKCδ^+ neurons onto two neuronal subclasses of CEA network. Furthermore, we performed multiple electrode recordings to assess whether PKCδ^- neurons are directly connected to PKCδ^+ neurons. We found that one PKCδ^- neuron (light green, supplementary figure 4b) out of three was connected to one PKCδ^+ neurons (blue) while no connection was observed between PKCδ^+ and PKCδ^- neurons (figure on the left).

It is clear that PKCδ^+ neurons form local GABAergic synapses onto CEA neurons, however it is unclear whether they can be classified as rely neurons. In order to study their possible long-range projections, we bilaterally injected (red triangular lines, supplementary figure 5a) a Cre- inducible Adeno- associated virus double floxed inverse ORF (DIO AAV virus) expressing *Tdtomato* in CEA of PKCδ Cre$^+$ animals. After about one month following injection, we verified the infection in CEA

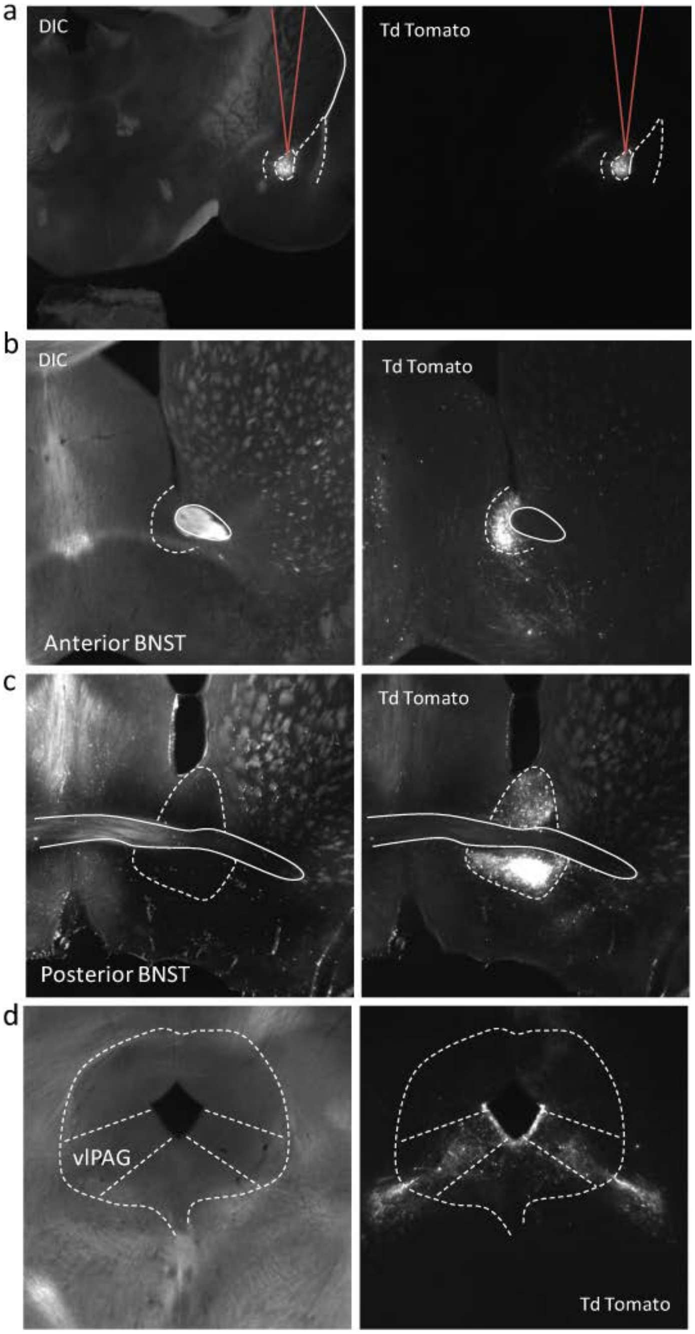

Supplementary figure 5. Projections of PKCδ^+ neurons. (a) *Left*, DIC image of CEA. *Right*, fluorescent image showing the injection site of the conditional virus expressing Tdtomato in CEA. (b), ((c) and (d) sae as (a) but for anterio, posterior BNST and vlPAG.

(supplementary figure 5a) and checked the presence of axonal innervation of PKCδ^+ neurons in different brain areas involved in the expression of fear and anxiety. Interestingly, we found that the axons of PKCδ^+ neurons were primarily found in the anterior and posterior BNST and *vl*PAG, two areas involved in fear and anxiety expression (supplementary figure 5b-d).

Overall, our results show that PKCδ^+ neurons form local GABAergic connections and can also project to distant brain areas. The functional role of these long-range projections is unknown.

Pharmacology of GABAergic inhibition of CEA neurons

Extrasynaptic inhibition in CEA

Since little is known about the GABAergic transmission onto specific neuronal types of CEA, we also examined the GABAergic inhibition of PKCδ⁻ and *vl*PAG-projecting CEm neurons using *whole cell* voltage clamp recordings in acute brain slices. Cells were clamped at -70 mV and a CsCl-based internal solution was used ($E_{Cl^-} = 0$ mV). This method allowed us to understand the general and non-specific inhibition received by the patched neuron.

GABAergic tonic current was found in all three types of neurons (applying 100 µM picrotoxin) with the largest normalized conductance in PKCδ⁻ cells in naive animals. GABAergic tonic current was not blocked by 1 µM SR95531 (gabazine), which decreased or abolished spontaneous inhibitory postsynaptic currents (sIPSCs) (supplementary figure 6).

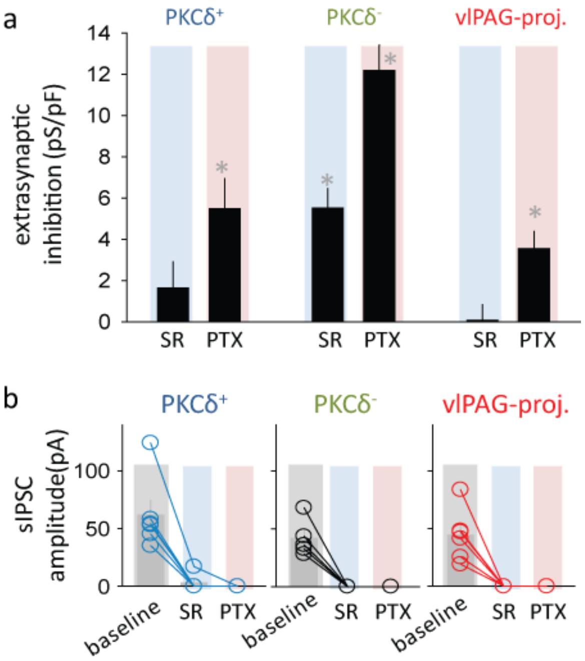

Supplementary figure 6. Extrasynaptic inhibition in CEA neurons. a | Bar graph of the normalized extrasynaptic inhibition blocked by gabazine (SR) and picrotoxin (PTX) for the three neuronal populations of CEA. **b** | Bar graph of the sIPSC amplitude in baseline, SR and PTX for the three neuronal populations. Each line correspond to the recording from one cell. All error bars indicate mean ± s.e.m.

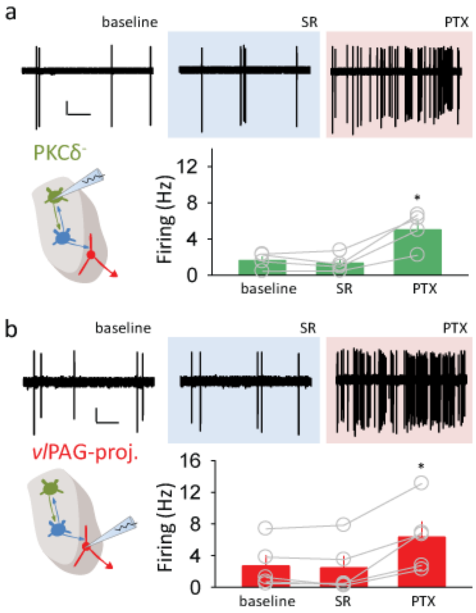

Supplementary figure 7. Role of extrasynaptic inhibition on firing of CEA neurons. a | *Upper*, representative trace of the extracellular firing of a PKCδ⁻ neuron in baseline, with SR and PTX application. Lower left, schematic representation of the CEA microcircuitry showing the specific targeting of PKCδ⁻ neurons (green). *Lower right*, bar graph of the firing frequency (expressed in Hz) in baseline, SR and PTX. **b** same as **a** but for *vl*PAG-projecting neurons. PTX have a significant effect on increasing firing. *p < 0.05 by paired t-test. All error bars indicate mean ± s.e.m.

To further characterize the effect of extrasynaptic versus synaptic current, extracellular loose cell-attached

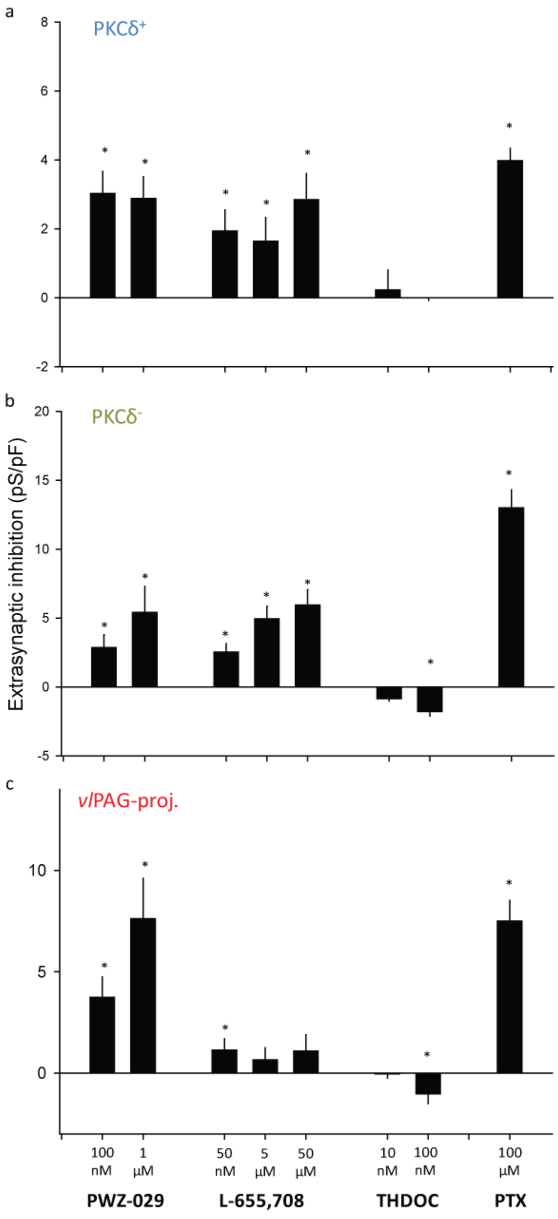

Supplementary Figure 8. Extrasynaptic inhibition of CEA neurons. a | Bar graph of the normalized values of extrasynaptic inhibition of PKCδ^{+} neurons modulated by: 100 nM and 1 µM PWZ-029 (n = 5-6); 50 nM, 5 and 50 µM L-655,708 (n = 6-9); 10 and 100 nM THDOC (n = 8); 100 µM PTX (n = 10). **b** | Bar graph of the normalized values of extrasynaptic inhibition of PKCδ^{-} neurons modulated by: 100 nM and 1 µM PWZ-029 (n = 5-6); 50 nM, 5 and 50 µM L-655,708 (n = 5-6); 10 and 100 nM THDOC (n = 7); 100 µM PTX (n = 10). **c** | Bar graph of the normalized values of extrasynaptic inhibition of *vl*PAG-projecting neurons modulated by: 100 nM and 1 µM PWZ-029 (n = 5-6); 50 nM, 5 and 50 µM L-655,708 (n = 7-11); 10 and 100 nM THDOC (n = 8); 100 µM PTX (n = 23). *$p < 0.05$ by sample t-test. All error bars indicate mean ± s.e.m.

recordings (LCA) were performed in order to leave intact the chloride gradient of the three neuronal types. Only PTX was able to enhance the firing of PKCδ^{-} and *vl*PAG-projecting CEm neurons. These data strongly indicate that extrasynaptic current is present in CEA and is important in controlling neuronal excitability (figure 12, supplementary figure 7).

In order to determine the composition of the GABA$_A$ receptor subunit responsible for the extrasynaptic inhibition, we used different concentrations of L-655,708 and PWZ-029 (obtained from J. Cook, UWisconsin), two inverse agonists specific for the α5-containing receptors, and THDOC, a neurosteroid selective for δ-containing receptors, at 10 nM and 100 nM. L-655,708 and PWZ-029 decreased the tonic current in all three neuronal types examined while 100 nM THDOC had a small but considerable effect only on PKCδ^{-} and *vl*PAG-projecting CEm neurons (supplementary figure 8). Notably, about 57% of the extrasynaptic inhibition recorded from PKCδ^{+} neurons is affected by 100 nM THDOC.

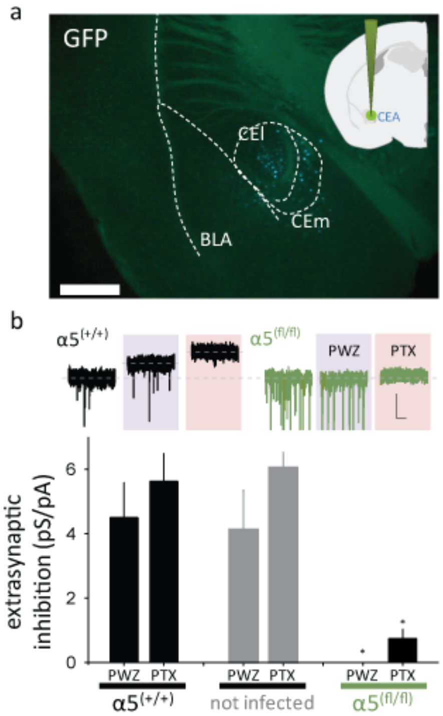

Supplementary figure 9. α_5GABA$_A$R meditated inhibition in CEA. **a** | Image using a GFP filter of a right coronal brain section showing CEA infected (antero-posterior location is -1.58 mm) with AAV expressing Cre recombinase and GFP tag (blue). BLA and CEA (CEl and CEm) structures are indicated by the dashed white line. Scale bar: 500 μM. Top right show a schematic representation of the injection. **b** | Bar graph of the extrasynaptic inhibition blocked by 1 μM PWZ-029 (PWZ, gray bar) and 100 μM PTX (pink bar) recorded from CEA neurons infected with the virus in a wild type (n = 5, α5$^{(+/+)}$), alpha5-floxed (n = 6, α5$^{(fl/fl)}$) and not infected (n = 6) in alpha5-floxed animals. $^*p < 0.05$ by One-way ANOVA followed by Bonferroni *Post-hoc* test. All error bars indicate mean ± s.e.m.

In order to further confirm the participation of the α_5GABA$_A$Rs in the generation of the extracellular inhibition in CEA neurons, we used α_5GABA$_A$R-floxed animals to create a conditional knock-out mouse upon localized injection of an adeno-associated virus (AAV) expressing the protein Cre recombinase, and GFP to mark the infected cells in CEA. After injection, we waited 4 weeks for efficient ablation of the α_5GABA$_A$R in infected CEA neurons and recorded GABAergic currents before and during bath-application of PWZ-028 (1 μM) from infected and non-infected neurons in both the α_5GABA$_A$R-floxed animals and from infected neurons in controls animals (littermates of α_5GABA$_A$R-floxed animals). PWZ-029 and PTX blocked the extrasynaptic inhibition in infected neurons of control and in non-infected neurons of α_5GABA$_A$R-floxed animals. On the other hand, these compounds did not have any significant effect on infected neurons of the α_5GABA$_A$R-floxed animals (Supplementary figure 9). PWZ-029 significantly enhanced the firing frequency of CEA neurons (Supplementary figure 10).

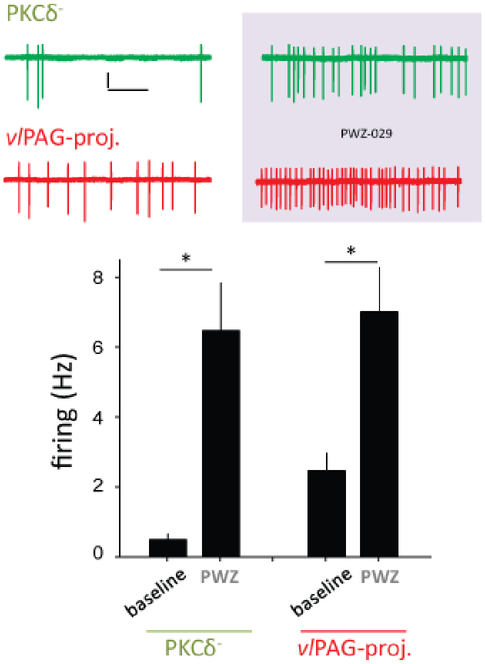

Supplementary figure 10. Role of α_5GABA$_A$R on firing of CEA neurons. *Top* | representative traces of the extracellular firing recorded in loose-cell attached mode from the soma of PKCδ$^-$ (green) and *vl*PAG-projecting neurons (red) in baseline and presence of 1 μM PWZ-029 (gray bar). *Down* | Bar graph of the firing frequency (Hz) for the two neuronal populations in baseline and PWZ (n = 5 each group). $^*p < 0.05$ by paired t-test. All error bars indicate mean ± s.e.m.

GABAergic synaptic events of PKCδ^+ neurons

From our results, it is likely that α_5GABA$_A$Rs mediated the tonic current of PKCδ^+ neurons of central amygdala. We therefore analyzed spontaneous inhibitory post-synaptic currents (sIPSCs) in order to understand whether α_5GABA$_A$Rs are responsible also for the inhibitory synaptic transmission.

Application of L-655,708 (50 nM, 5 and 50 μM) did not have any considerable effect on sIPSC amplitude and frequency of PKCδ^+ neurons. In addition, PWZ-029 (1 μM) did not consistently change sIPSC amplitude and frequency of wild type and α_5GABA$_A$Rs constitutive knock outs in PKCδ^+ neurons ($p > 0.05$ by unpaired t-test).

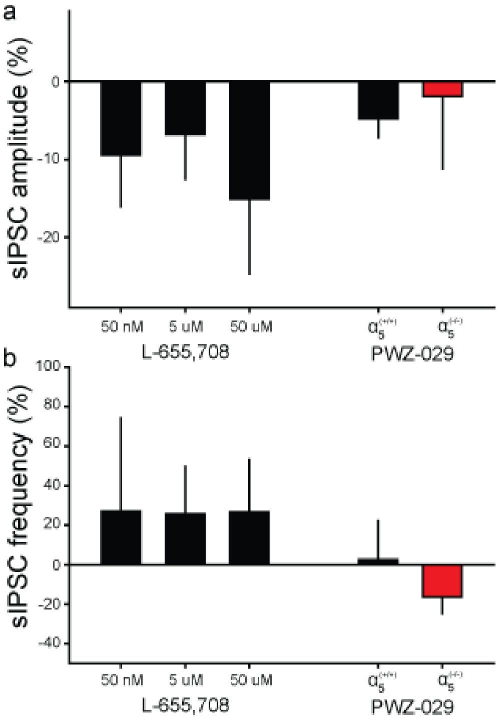

Supplemenatry figure 11. sIPSCs are not constituted by α_5GABA$_A$R. a | Bar graph of the sIPSCs amplitude change (%) upon bath-application of L-655,708 (50 nM, 5 and 50 μM) and PWZ-029 (1 μM) on wild types and constitutive knock outs in PKCδ^+ neurons ($\alpha_5^{(+/+)}$ in black, $\alpha_5^{(-/-)}$ in red). **b** | same as a but for the sIPSC frequency change (%). All these values are not statistically significant. All error bars indicate mean ± s.e.m.

Interestingly, application of zolpidem, a benzodiazepine selective for α_1GABA$_A$Rs at low concentrations, did not have a consistent effect on the extrasynaptic inhibition (20 nM, 0.2 ± 0.2 pS/pF; 100 nM, 0.1 ± 0.4 pS/pF; 300 nM, 0.04 ± 0.7 pS/pF; n = 7, $p > 0.05$ by one sample t-test versus control) but only on the decay time of sIPSCs in PKCδ^+ neurons (20 nM, 5.3 ± 2.1 %; 100 nM, 5.9 ± 2.9 pS/pF; 300 nM, 12.6 ± 2.0 pS/pF; n = 7, $p < 0.05$ by one sample t-test versus control).

Role of spillover on the extrasynaptic inhibition

GABA spillover is likely to maintain an activity-dependent activation of extrasynaptic GABA$_A$Rs. We examined whether blockage of presynaptic activity would influence this tonic conductance recorded from the defined CEA neurons using tetrodotoxin (1 μM TTX). TTX caused a consistent blockage of the extrasynaptic inhibition only in PKCδ^- and *vl*PAG-projecting CEm but not in PKCδ^+ neurons (supplementary figure 12a-b). However, analyzing the change of sIPSC frequency induced by TTX and plotting it against the extrasynaptic inhibition blocked by abolition of presynaptic release, we found a significant inverse linear correlation in all the neuronal populations considered (supplementary figure 12c-e). The interpretation of these data is that GABA spillover is fundamental in the maintenance of the extrasynaptic inhibition of PKCδ^+ neurons and the other CEA neurons.

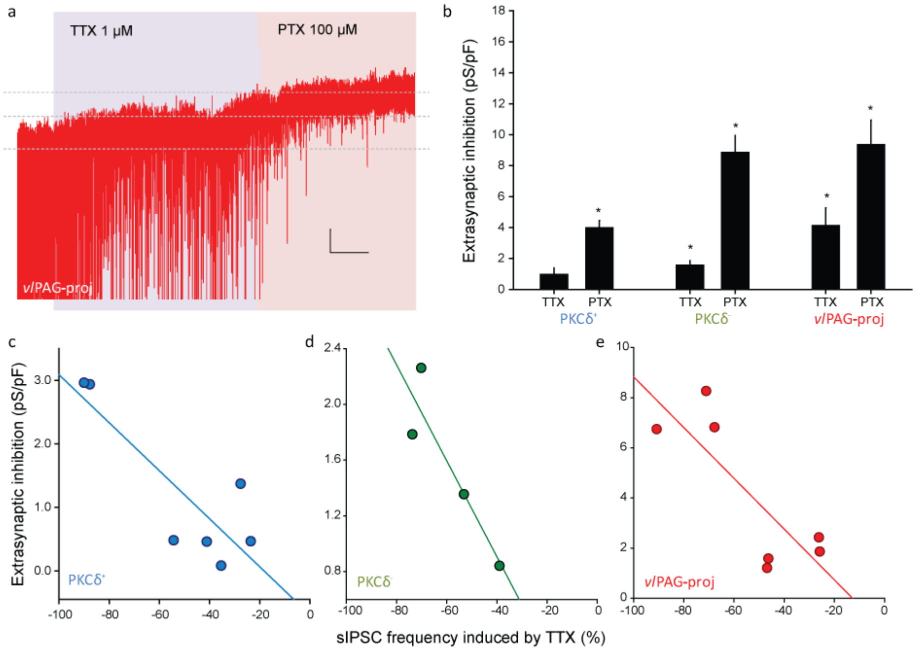

Supplementary figure 12. Role of spillover on extrasynaptic inhibition. a | Example trace of a *vl*PAG-projecting CEm neurons showing the bath-application of tetrodotoxin, TTX, and picrotoxin, PTX. Scale bar: 20 pA, 5 min. **b** | Bar graph of the extrasynaptic inhibition (pS/pF) blocked by TTX and PTX in the three different CEA neuronal subtypes (PKCδ^+: n = 7; PKCδ^-: n = 4; vlPAG-projecting: n = 7). *p < 0.05 by one sample t-test. All error bars indicate mean ± s.e.m. **c**, **d** and **e** | Linear regression between the effect of TTX on sIPSC amplitude (%) versus its effect on the extrasynaptic inhibition (pS/pF) for PKCδ^+ (R = 0.8), PKCδ^- (R = 0.9) and *vl*PAG-projecting (R = 0.8), respectively. All linear regressions are significant (p < 0.05).

Spontaneous gating of the GABA$_A$R-mediated extrasynaptic inhibition

Herein, we showed that extrasynaptic inhibition onto PKCδ^+ neurons is slightly sensitive to 1 µM gabazine (supplementary figure 6). Higher saturating concentrations of gabazine (50 µM) produced a significant blockage of the extrasynaptic inhibition that was lower than the effect of 100 µM picrotoxin (gabazine: 1.86 ± 0.8 pS/pF; picrotoxin: 4.9 ± 1.1 pS/pF; $p < 0.05$ by unpaired t-test between the two groups).

Several studies reported that tonically active GABA$_A$ receptors are gabazine–insensitive in hippocampal neurons (Bai et al, 2001). Gabazine, in contrast to picrotoxin, inhibits the GABA$_A$R in the presence of exogenous GABA or enhanced ambient GABA concentrations (Overstreet and Westbrook, 2001; Stell et al, 2003). It is likely that the extrasynaptic GABA$_A$R mediating inhibition

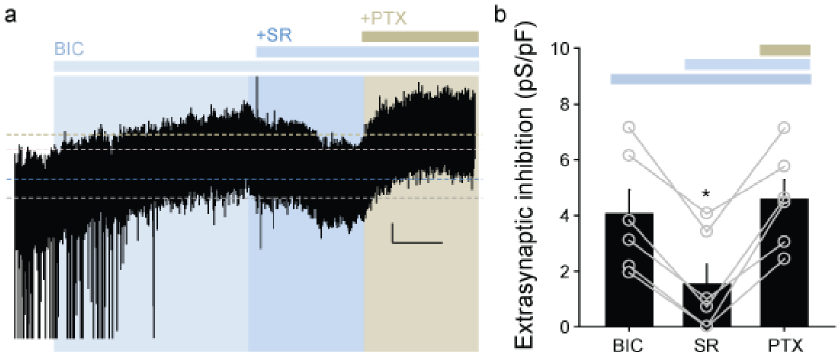

Supplementary figure 13. Spontaneous gating of the extrasynaptic GABA$_A$R of PKCδ^+ neurons. **a** | Representative GABAergic trace recorded from PKCδ^+ neurons showing the effect of bicuculline (20 µM, BIC), gabazine (20 µM, SR) and picrotoxin (100 µM, PTX) on the holding current (dashed lines). Solid lines and areas show the drug bath-application. Scale bar: 5 pA, 2 min. **b** | Bar graph of the extrasynaptic inhibition (pS/pF) in presence of bicuculline, (BIC), bicuculline + gabazine (SR) and bicuculline + gabazine + picrotoxin (PTX). Each gray line represent one recording, n = 6. $^*p < 0.05$ by One-Way ANOVA followed by repeated measurements. All error bars indicate mean ± s.e.m.

of PKCδ^+ neurons does not require GABA because they possess spontaneous gating properties. We used another competitive antagonist, 20 µM bicuculline (BIC), which is also known for having an inverse agonist effect on GABA$_A$Rs. Bicuculline blocks GABA$_A$R without exogeneous GABA and also competes with gabazine on the GABA binding pocket of the GABA$_A$R. Saturating concentrations of bicuculline caused a decrease of the extrasynaptic inhibition. Co-application of bicuculline with gabazine (20 µM) decreased its effect on the extrasynaptic inhibition. Finally, picrotoxin, a GABA$_A$R non-competitive antagonist, reversed the effect of gabazine and blocked the extrasynaptic inhibition to the same extent as bicuculline (supplementary figure 13). These data suggest that the extrasynaptic inhibition of PKCδ^+ neurons is mediated by spontaneously active GABA$_A$Rs.

Role of central amygdala GABAergic inhibition on fear and anxiety

Associative learning on the GABAergic inhibition of CEA neurons

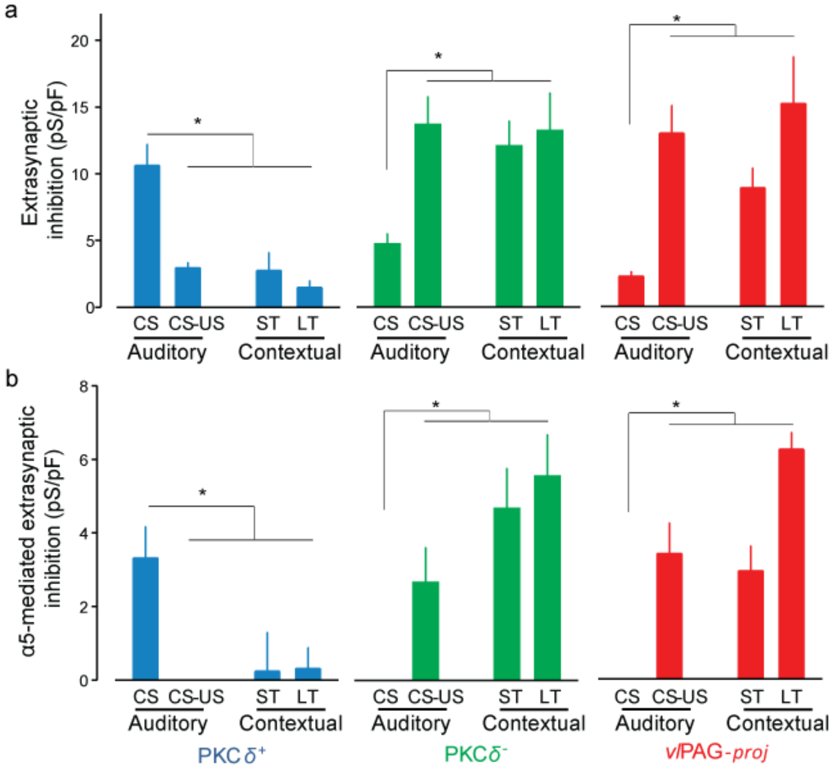

Supplementary figure 14. Contextual fear conditioning on CEA extrasynaptic inhibition. a | bar graph of the total extrasynaptic inhibition (blocked with 100 μM PTX) recorded from PKCδ^+ (*blue*), PKCδ^- (*green*) and *vl*PAG-projecting CEm neurons (*red*). In each single panel is shown the auditory fear conditioning (auditory) with CS (control) and CS-US (fear conditioned) group and the contextual fear conditioning (contextual) with ST (short term, recordings were done right after conditioning) and LT (long term, recordings were done 24 hours after conditioning). Statistical *n* for PKCδ^+ neurons: CS (14), CS-US (26), ST (7), LT (6); Statistical *n* for PKCδ^- neurons: CS (8), CS-US (12), ST (6), LT (6); Statistical *n* for *vl*PAG-projecting CEm neurons: CS (6), CS-US (6), ST (10), LT (7). **b** | Same as **a** but for the *α*5 mediated extrasynaptic inhibition blocked by 50 nM L-655,708 in the three neuronal subtypes. *$p < 0.05$ by One-Way ANOVA followed by Bonferroni *Post-hoc* test. All error bars indicate mean ± s.e.m.

In order to understand whether other forms of associative learning can cause plastic changes of the α_5-mediated inhibition, we recorded GABAergic current from the defined CEA neuronal population 24 hours after contextual fear conditioning (LT).

Contextual fear conditioning (contextual), as shown for auditory fear conditioning (auditory), induced a similar long term change of the total and α_5GABA$_A$R-dependent extrasynaptic inhibition in the three CEA cell-types (LT, supplemetary figure 14). Interestingly, this form of extrasynaptic inhibition in the three defined CEA neurons was observed also when we recorded immediately following fear conditioning (ST), suggesting its fast induction. Overall, these experiments showed that the extrasynaptic inhibition changed after fear because of a change of the α_5GABA$_A$R component in a specific neuronal subpopulation of CEA.

Extrasynaptic inhibition is not affected in constitutive alpha5 KO

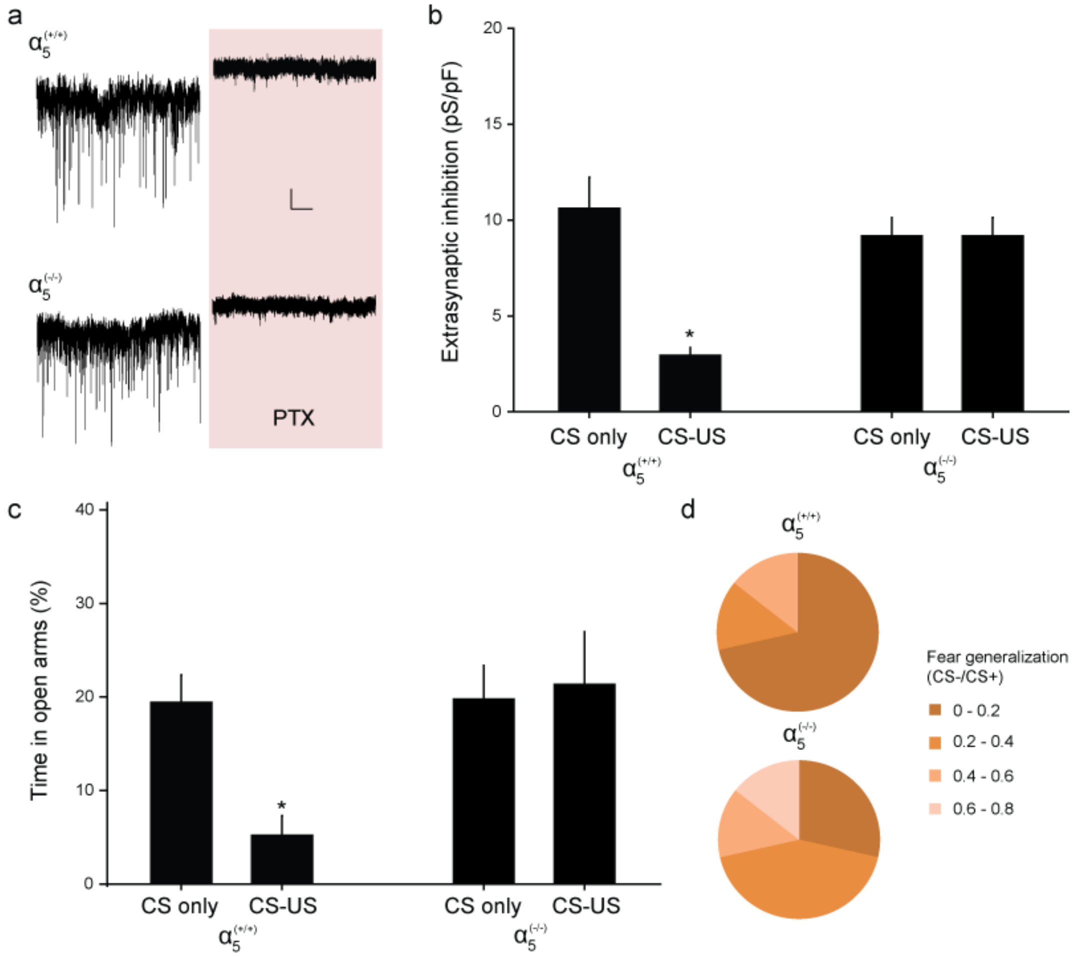

Supplementary figure 15. Auditory fear conditioning on residual tonic inhibition in α_5GABA$_A$R$^{(-/-)}$ *x* PKCδ Cre$^+$ animals. a | Representative traces of the PTX-sensitive tonic inhibition recorded from identified PKCδ^+ neurons in α_5GABA$_A$R wild type ($\alpha_5^{(+/+)}$) and α_5GABA$_A$R knock out ($\alpha_5^{(-/-)}$) PKCδ Cre$^+$ animals. Bath-application of PTX (100 μM) is shown by the pink area. Scale bar: 20 pA, 10 s. **b** | Bar graph of the extrasynaptic inhibition blocked by PTX application in recorded from identified PKCδ^+ neurons in α_5GABA$_A$R wild type ($\alpha_5^{(+/+)}$) and α_5GABA$_A$R knock out ($\alpha_5^{(-/-)}$) PKCδ Cre$^+$ animals. The animals in CS only were only exposed to the tones while the CS-US is the fear conditioned group. Statistical *n* for $\alpha_5^{(+/+)}$ PKCδ^+ neurons: CS (14), CS-US (26) while the statistical *n* for $\alpha_5^{(-/-)}$ PKCδ^+ neurons: CS (5), CS-US (5). **c** | bar graph of the time spent in the open arms (%) in α_5GABA$_A$R wild type ($\alpha_5^{(+/+)}$) and α_5GABA$_A$R knock out ($\alpha_5^{(-/-)}$) PKCδ Cre$^+$ animals after CS only or CS associated with shock exposure (CS-US). **d** | Pie chart showing the number of α_5GABA$_A$R wild type (n = 7,$\alpha_5^{(+/+)}$) and knock out (n = 7, $\alpha_5^{(-/-)}$) PKCδ Cre$^+$ animals that fear generalized at different values (0-0.2, 0.2-0.4, 0.4-0.6, 0.6-0.8). All error bars indicate mean ± s.e.m.

As mentioned in the main results, in order to confirm that PKCδ^+ neurons expressed α_5GABA$_A$Rs, we crossed PKCδ Cre$^+$ with α_5GABA$_A$R-floxed animals and obtained an animal constitutive for α_5GABA$_A$R knock-out in all PKCδ Cre$^+$ neurons (α_5GABA$_A$R$^{(-/-)}$ *x* PKCδ^+). PWZ-029 (1 μM) did not block the extrasynaptic inhibition (figure 12) while a residual compensatory extrasynaptic inhibition was observed by bath-application of PTX (supplementary figure 15a-b, $\alpha_5^{(-/-)}$ CS only).

Interestingly, the residual tonic inhibition, which was PTX-sensitive, recorded from $\alpha_5GABA_AR^{(-/-)}$ *x* $PKC\delta^+$ neurons of CEA did not change after auditory fear conditioning (supplementary figure 15). Further, to understand the importance of the plastic decrease which the α_5GABA_ARs extrasynaptic inhibition in $PKC\delta^+$ neurons overcome, we tested $\alpha_5GABA_AR^{(-/-)}$ *x* PKC*δ* Cre^+ animals in the elevated plus maze 24 hours after an auditory fear conditioning session. Interestingly, the constitutive knock outs did not decrease the time spent in the open arms after fear conditioning as observed in control $\alpha_5GABA_AR^{(+/+)}$ *x* PKC*δ* Cre^+ animals. Additionally, it we observed a higher number of $\alpha_5GABA_AR^{(-/-)}$ *x* PKC*δ* Cre^+ animals with elevated fear generalization ratios in comparison to the control $\alpha_5GABA_AR^{(+/+)}$ *x* PKC*δ* Cre^+ animals (supplementary figure 15d).

Overall, this suggests that α_5GABA_ARs expressed in $PKC\delta^+$ neurons are essential for the observed plastic decrease induced by fear conditioning and the maintenance of anxiety and fear generalization at physiological levels.

Associative learning on GABAergic synaptic events

As showed, we observed a decrease and increase of the extrasynaptic inhibition of $PKC\delta^+$ and the other CEA neurons, respectively. This plastic change could be also caused by a change of presynaptic GABA release rather than a change in extrasynaptic protein Composition. No change in sIPSC frequency was found between CS only and CS-US groups recorded from $PKC\delta^+$ neurons.

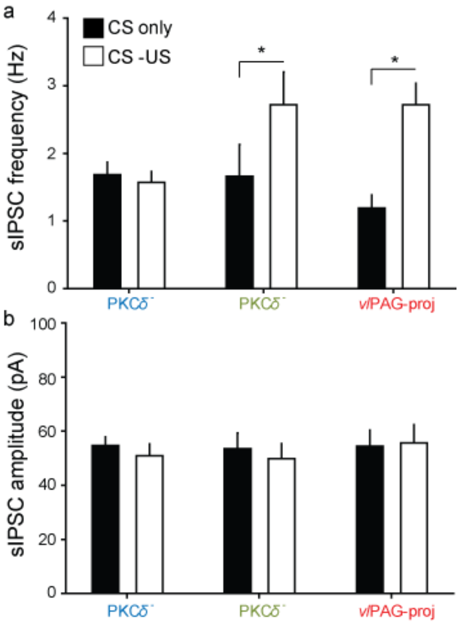

Supplementary figure 16. Role of sIPSCs on extrasynaptic inhibition plasticity. a | Bar graph of the sIPSC frequency recorded in baseline from the three neuronal subtypes in CS only and CS-US group. **b** | Bar graph of the sIPSC amplitude recorded in baseline from the three neuronal subtypes in CS only and CS-US group. The three neuronal subtypes are: $PKC\delta^+$ (CS only, n = 26; CS-US, n = 36), $PKC\delta^-$ (CS only, n = 12; CS-US, n = 12) and *vl*PAG-projecting CEm neurons (CS only, n = 14; CS-US, n = 14). $^*p < 0.05$ by unpaired t-test. All error bars indicate mean ± s.e.m.

Role of α_5GABA$_A$R mediated inhibition in CEA on anxiety

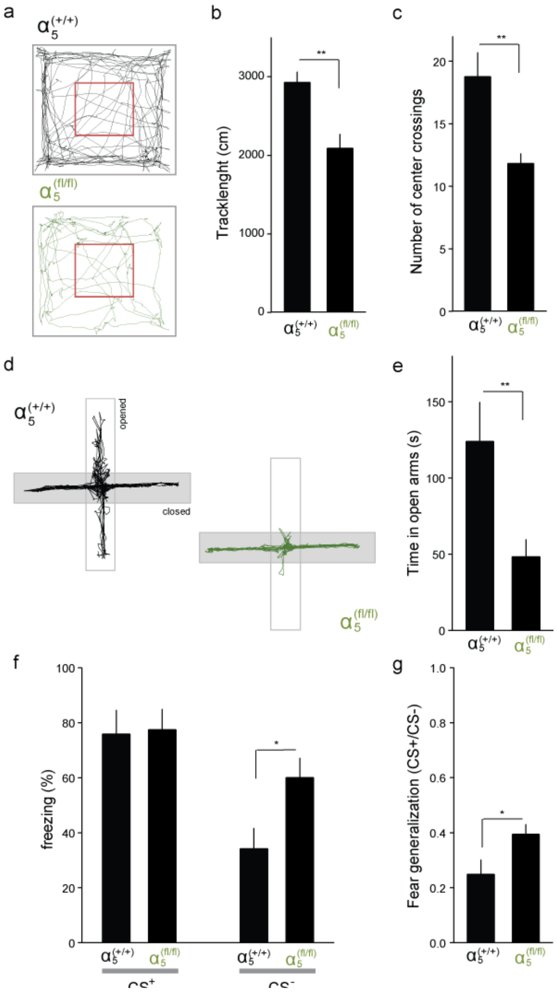

Supplementary figure 17. Role of α_5GABA$_A$R on anxiety and fear generalization. a | representative open field track of a control (black $\alpha_5^{(+/+)}$) and α_5GABA$_A$R-floxed (green $\alpha_5^{(fl/fl)}$) animals. Both groups were bilaterally injected into CEA with an AAV virus expressing Cre recombinase and GFP tag. **b** | Bar graph of the track length (cm) for $\alpha_5^{(+/+)}$ (n = 12) and $\alpha_5^{(fl/fl)}$ (n = 10) animals. **c** | Bar graph of the number of crossing to the center for $\alpha_5^{(+/+)}$ (n = 12) and $\alpha_5^{(fl/fl)}$ (n = 10) animals. **d** | representative elevated plus maze track of a control $\alpha_5^{(+/+)}$ and α_5GABA$_A$R-floxed $\alpha_5^{(fl/fl)}$ animal. The open (white) and close arms (grey) are indicated. **e** | Bar graph of the time spent in the open arms (%)for $\alpha_5^{(+/+)}$ (n = 9) and $\alpha_5^{(fl/fl)}$ (n = 13) group. **f** | Bar graph of the freezing levels (%) for both $\alpha_5^{(+/+)}$ (n = 8) and $\alpha_5^{(fl/fl)}$ (n = 8) group exposed to the CS$^+$ and CS$^-$ during retrieval day (24 hours after auditory fear conditioning). **g** | Bar graph of the fear generalization (CS$^-$/CS$^+$) for both $\alpha_5^{(+/+)}$ (n = 8) and $\alpha_5^{(fl/fl)}$ (n = 8) group. *$p < 0.05$, **$p < 0.01$ by unpaired t-test. All error bars indicate mean ± s.e.m.

Finally, we used genetic models to confirm the involvement of the α_5GABA$_A$Rs in the anxiety and fear generalization behavioral states. First, we bilaterally injected an AAV virus expressing CRE recombinase and GFP into CEA of α_5GABA$_A$R-floxed animals and control animals. This infection was localized to CEA and infections in the nearby areas were discarded from the α_5GABA$_A$R-floxed animal group. Animals were exposed to the open field arena and their behavior was recorded for 10 minutes. Interestingly, the conditional KO ($\alpha_5^{(fl/fl)}$) animals had lower values of track length and visits in the center in comparison with the control ($\alpha_5^{(+/+)}$). The $\alpha_5^{(fl/fl)}$ animals showed also a decrease in the duration of time spent in the open arms of an elevated plus maze. In addition, α_5GABA$_A$R-floxed animals, in comparison with the control group, had a higher generalization index caused by an enhancement of freezing levels to the CS$^-$ (supplementary figure 17).

In summary, lack of α_5GABA$_A$Rs in the central amygdala enhanced anxiety and fear generalization levels.

Role of tonic firing on tone responsiveness

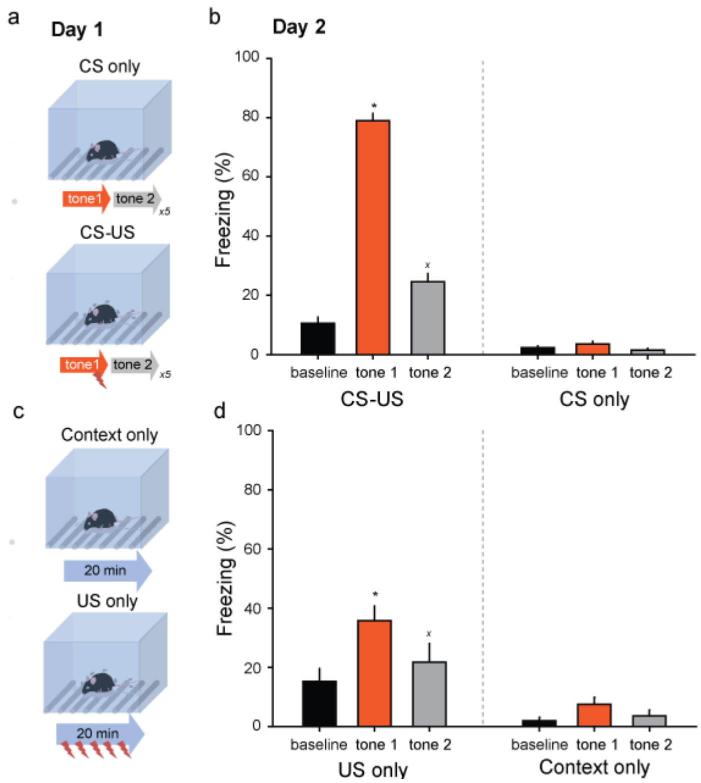

Supplementary figure 18. Auditory and Contextual fear conditioning on the freezing to a neutral tone. a | Schematic representation of day 1 for the CS only and CS-US group. CS only group were exposed to the conditioning context, five intermingled tone 1 (7.5 kHz, red) and tone 2 (white noise, grey). Animals of the CS-US group were fear conditioned with five tones 1 paired with a footshock intermingled to unpaired tones 2. **b** | Bar graph of the freezing levels (%) in a new extinction context in day 2 of the CS-US (n = 40) and CS only (n = 11) groups during baseline, tone 1 and tone 2. The grey dashed line divided the two groups. $^{*}p < 0.05$, $^{x}p < 0.05$ by One-Way ANOVA followed by Tukey test between one condition (tone 1 or tone 2) and respectively with each one of the other conditions (baseline in CS-US; baseline, tone 1 and tone 2 in CS only). All error bars indicate mean ± s.e.m.

Auditory fear conditioning strengthened the freezing to a conditional cue paired with a footshock (supplementary figure 18b). Further, as expected, the paired *tone 1* elicited higher levels of freezing in comparison to an unconditioned *tone 2* in an extinction context (supplementary figure 18a-b). Classically, it is known that the plastic long term potentiation of thalamo-cortical inputs carrying the *tone 1* occurs in lateral amygdala. However, it was found that this occurs also in central amygdala with conditioned auditory inputs (Samson and Pare, 2005; Ciocchi et al, 2010; Li et al, 2013; Penzo et al, 2014). It is hypothesized that the potentiation of specific thalamo-cortical inputs (in this case the *tone 1*) to $\mathrm{CEl_{on}}$ neurons would temporarily inhibit $\mathrm{CEl_{off}}$ neurons (PKCδ expressing) causing a dis-inhibition of CEm output neurons and the observed high levels of freezing to the conditioned acoustic cue (Ciocchi et al, 2010).

Interestingly, an unpaired *tone 2* enhanced the level of freezing in the CS-US in comparison to the CS only group (supplementary figure 18b). A plausible hypothesis for this is that enhanced tonic firing of PKCδ^{+} neurons induced by auditory fear conditioning would amplify tone responsiveness and the observed fear generalization to the unpaired acoustic stimulus (figure 8). However, it can be argued also that generalization of auditory information is caused by a long term potentiation of auditory afferents onto these neurons and enhanced transmission to an unpaired tone. Thus, we performed contextual fear conditioning in order to enhance the plasticity of multiple sensorial pathways carrying contextual information rather than to only a single specific acoustic stimulus. The second day (day 2), we placed the animal in a novel environment to avoid freezing elicited by the context and checked whether novel auditory tones elicit consistent freezing responses in a novel environment (supplementary figure 18c-d). Furthermore, two novel tones (tone 1 or tone 2) significantly enhanced the level of freezing in comparison to a control group (contextual only) (supplementary figure 18d). The results show that fear conditioning caused a plastic amplification of unconditioned stimuli.

Previously, we have shown that contextual fear conditioning decreased the extrasynaptic inhibition of PKCδ^+ neurons as found for auditory fear conditioning (supplementary figure 11). This reflected an enhancement of their spontaneous firing and an increase in signal-to noise ratio to acoustic cues. Subsequently, to further confirm that the enhancement of the freezing to an unpaired *novel* tone was induced by an increase of the tonic firing of PKCδ^+ neurons, we performed contextual fear conditioning using PKCδ Cre$^+$ animals previously injected with a AAV viruses expressing either ChR2 or Arch and implanted with optical connectors. The second day, light-induced ChR2 activation or Arch inhibition of PKCδ^+ neurons enhanced or decreased, respectively, the freezing to a novel unpaired *tone 1*. Light delivery alone did not alter freezing (supplementary figure 19).

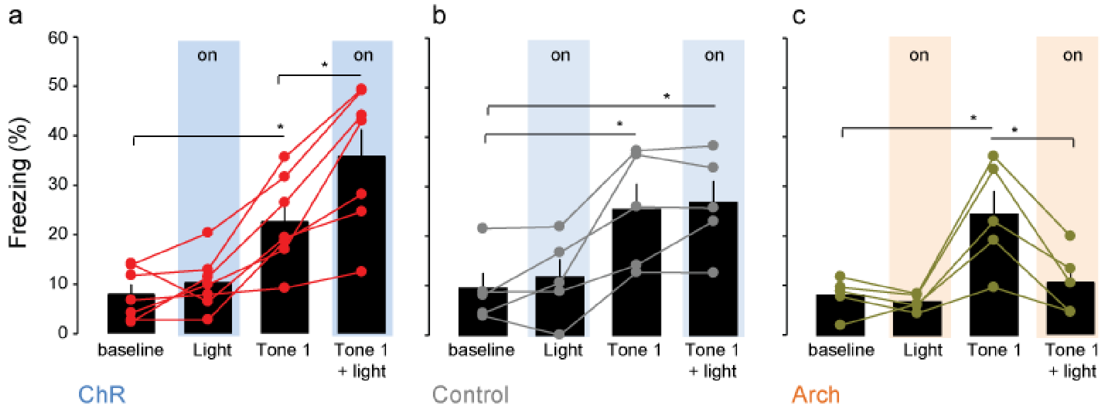

Supplementary figure 19. Modulation of a novel tone by the tonic activity of PKCδ^+ neurons. a | Bar graph of the freezing levels (%) one day after contextual fear conditioning in the extinction context of baseline, in presence of light only (light), during the tone 1 (7.5 kHz) and light combined with the tone 1 (tone 1 + light) (n = 7). The blue bar indicates the light application (on). **b** | Same as **a** but for control animals not expressing ChR or Arch (n = 5). **b** | Same as **a** but for the Arch group. (n = 5). *$p < 0.05$ by paired t-test versus the condition indicated by the line. All error bars indicate mean ± s.e.m.

These findings demonstrate that tonic activity of PKCδ^+ neurons is implicated in fear generalization to a "*known*" and *novel* auditory stimulus.

DISCUSSION

Our findings demonstrate that traumatic experiences plastically tune a form of extracellular inhibition in a defined neuronal population of the central nucleus of amygdale, thereby having important consequences on anxiety and fear generalization.

Fear conditioning induced changes in tonic firing of PKCδ^+ neurons, which was found to be controlled by extrasynaptic α_5GABA$_A$R–mediated inhibition. Furthermore, this particular tonic inhibition of PKCδ^+ neurons was decreased after fear conditioning and correlated with fear generalization. Finally, local genetic reduction of α_5GABA$_A$R expression in PKCδ^+ neurons enhanced anxiety and fear generalization to an unconditioned stimulus.

We found that a defined central amygdala neuronal population constitutively expressing the PKCδ marker was directly involved in anxiety modulation. PKCδ-expressing neurons located in central amygdala were found to be part of the CEl$_{off}$ neuronal population using the combination of single unit recordings with pharmacogenetic silencing (Haubensak et al., 2010). To achieve specific targeting and manipulation of CEl$_{off}$ neurons, we used transgenic PKCδ Cre$^+$ animals. It is noteworthy in this regard that PKCδ-expressing neurons seem to have peculiar properties in comparison with other defined neuronal populations of the central amygdala. They do not overlap with *somatostatin* and *corticotrophin-releasing factor* expressing neuron found in this amygdala nucleus (Haubensak et al. 2010, Li, Penzo et al. 2013). In addition, the majority of PKCδ-expressing neurons also express *oxytocin receptors* and they are selectively activated by its agonist (supplementary figure 2, Haubensak et al., 2010). Finally, the morphology and the axonal projections of PKCδ-expressing neurons differ from two other neuronal populations located in the central amygdala (supplementary figure 1). Thus, the use of this particular Cre line ensured a selective physiological means to target a defined neuronal population to assay its effect on certain behavioral emotional responses.

The involvement of CEA on anxiogenesis has already been shown by numerous studies in rats and humans (Jellestad et al. 1986, Adamec and Shallow 1998, Tye et al. 2011, Etkin et al. 2009). However, the direct physiological role of specific CEA neuronal subtypes on anxiety-like behavior remained unclear. Herein, we found that tonic bidirectional optogenetic modulation of the spontaneous firing of PKCδ^+ neurons modulated anxiety-like behavior in mice. In particular, light-evoked enhancement of spontaneous firing augmented anxiety-like behavior while a decrease was observed when these neurons were selectively inhibited *in vivo*.

Anxiety has been described as a sustained generalized emotional response to an unknown and/or less predictable threat accompanied by increased arousal and vigilance. Anxiety can last for an extended period of time (Davis, Walker et al. 2010). During this period, sensory stimuli can trigger a higher level of fear response in order to escape/defend from potential threats (Duvarci,, Bauer and Pare 2009). For this reason, we tested whether the tonic firing of a defined CEA population was responsible, not only to enhance general anxiety to ambiguous contextual information, but also fear responses to *unpaired* or *novel* acoustic stimuli. Fear generalization to an unconditional stimulus was increased by the spontaneous firing enhancement of PKCδ^+ neurons. Additionally, contextual fear conditioning enhanced freezing responses to novel cues.

It can be hypothesized that an enhancement of awareness to unpredictable threatening events causes higher anxiety and uncontrollable fear responses. Accordingly, modulating the firing of PKCδ^+ neurons with optogenetic manipulations, we were able to show also that freezing responses induced by *novel* stimuli, never heard before retrieval, could be controlled by enhancing or diminishing their spontaneous firing. Interesting, unpaired light activation, or inhibition, of PKCδ^+ neurons did not have a significant impact on contextual freezing (supplementary figure 18, 19). Moreover, a salient stimulus is required in order to elicit higher levels of fear responses induced by PKCδ^+ neurons. These data show that define neuronal population of CEA control the anxiety and fear reaction to sensory stimuli. Considering the strict correlation between anxiety and fear generalization, it is reasonable to consider PKCδ^+ neurons as a tuning station for multiple sensorial inputs. Furthermore, the tonic signal modulation of these particular neuronal subtypes influenced discrete cues and, in addition, a broader range of unpredicted and uncontrollable contextual inputs leading to higher anxiety states.

It is fundamental to elucidate the mechanisms by which PKCδ-expressing neurons of the central amygdala carry multiple sensorial stimuli and convey them to other brain structures. PKCδ^+ neurons receive inhibitory inputs during the encoding of a conditioned cue related to fear conditioning. In fact, it is known that CEl$_{off}$ neurons expressing PKCδ are phasically inhibited by GABAergic inputs from CEl$_{on}$ neurons (supplementary figure 4) carrying CS-evoked stimuli *in vivo*. Thus, input discrimination results from the change in intrinsic spontaneous firing which enhances the signal-to-noise ratio of CS-evoked responses in CEl$_{\text{off}}$ PKCδ-expressing neurons (Ciocchi et al. 2010).

PKCδ^+ neurons are GABAergic cell types and inhibit postsynaptic neurons located in CEl (PKCδ^-) and those in CEm projecting to *vl*PAG area (Supplementary figure 2, 3; Haubensak et al. 2010). A possible role of PKCδ^+ neurons on setting the tonic firing of CEm output neurons comes from *in vivo* studies (Ciocchi et al., 2010). The tonic activity of CEm neurons decreased after fear conditioning and inversely correlates with fear generalization *in vivo* (Ciocchi et al., 2010). Given that fear conditioning induced the opposite effect on the tonic firing of CEl$_{\text{off}}$ neurons, it can be speculated that the latter population increases GABA release and tonically inhibits CEm neurons after fear conditioning. Consequently, an enhanced GABA tone diminishes the signal-to-noise ratio of CS-evoked phasic firing carried by thalamo-cortical and BLA afferents onto CEm neurons. Moreover, it is yet to be determined whether PKCδ^+ neurons impact behavioral outcomes through the modulation of CEm output neurons and/or sending long range projections to other brain areas fundamental in the direct expression of anxiety, such as BNST or *vl*PAG (supplementary figure 5; Jolkkonen and Pitkanen 1998).

In addition to inhibitory afferents, the diverse plastic nature of BLA inputs onto specific CEA neurons is beginning to be understood. However, it is still not known whether BLA inputs carry multi-sensorial inputs to PKCδ^+ neurons. It is likely that CEA PKCδ^+ neurons that do not express somatostatin also receive glutamatergic inputs from BLA which are decreased by fear conditioning (Li et al., 2013). Interestingly, it was found that specific activation of BLA glutamatergic afferents in CEA, using a codon-optimized channelrodopsin, leads to an acute reversible anxiolytic effect. Moreover, BLA inputs selectively activate an unidentified neuronal cell type in CEl (Tye et al, 2011). It is likely, considering the proposed CEA microcircuitry model (Ciocchi et al., 2010), that BLA inputs could preferentially activate presynaptic CEl$_{\text{on}}$ neurons. As a result, constant GABA release from CEl$_{\text{on}}$ neurons would inhibit CEl$_{\text{off}}$ neurons expressing PKCδ, thereby causing the observed anxiolytic outcome. Overall, we found a precise anxiogenic role for PKCδ^+ neurons of CEA that exacerbate salient sensorial inputs. The role for the neuronal inputs and outputs, which carry the fearful information encoded by PKCδ^+ neurons, is important to be determined.

The optogenetic approach helped us in define the role of PKCδ-expressing neurons on fear and anxiety behavior. Although this is a powerful method, it was critical to elucidate the intrinsic mechanism regulating neuronal spontaneous firing. It was found that PKCδ-expressing neurons of the central amygdala are equipped with a peculiar type of GABA$_A$R that guarantees strong extrasynaptic inhibition. This constant form of inhibition is mediated by unsynchronized spontaneous firing of GABAergic CEA neurons at about 6 Hz (Supplementary figure 12; Ciocchi et al. 2010). Interestingly, extrasynaptic inhibition of PKCδ-expressing neurons is also regulated by the spontaneous gating of GABA$_A$R. Consequently, this leads to a constant activation of extrasynaptic inhibition which causes a continuous control of spontaneous neuronal firing which is observed in all the CEA neuronal types. Extrasynaptic inhibition ensures low input resistance and hyperpolarized resting membrane potentials. Additionally, inhibition of spontaneous GABAergic synaptic events does not consistently contribute to cellular excitability. This suggests that phasic inhibition must be synchronized in order to temporarily inhibit the neuron, as has already been shown (Crowley et al., 2009; Farrant and Nusser, et al., 2005).

Extrasynaptic inhibition has been demonstrated to be important in filtering unsynchronized glutamatergic information that is not associated with sensory stimulation *in vivo*. This ensures a reliable relay of sensory-evoked mossy fiber signals (Chadderton et al., 2004). Tonic inhibition of PKCδ^+ neurons therefore might filter out sparse glutamatergic inputs that are not associated with any functional coding. Furthermore, it was hypothesized that a constant inhibitory tone onto PKCδ^+ neurons balances the sensitivity to CS-evoked responses by maintaining fine tuning of the signal-to-noise ratio important in input selectivity and, consequently, ambiguity to an unpredicted stimulus carried in CEA (Ciocchi et al., 2010).

After uncovering a potential mechanism controlling cellular excitability, we used a series of electrophysiological, pharmacological and genetic approaches to causally relate the role of the extrasynaptic inhibition of PKCδ^+ neurons to fear generalization.

First, we examined the subunit composition of the GABA$_A$R subtype involved in the generation of the extrasynaptic inhibition of PKCδ^+ neurons. It was found to be predominantly mediated by α_5 and not δ-containing GABA$_A$Rs. Further, knocking out the α_5-containing GABA$_A$R selectively in PKCδ^+ neurons completely abolished the inverse agonist blockage of the tonic current. Partial inhibition of the α_5-containing GABA$_A$Rs regulated predominantly the extrasynaptic inhibition of PKCδ^+ neurons since it did not have a considerable effect on the amplitude and frequency of synaptic responses.

Immunohistochemical data demonstrated the expression of the α_5-containing GABA$_A$R in PKCδ^+ neurons and their complete absence in the constitutive knock out. THDOC, a neurosteroid that selectively activates δ-containing GABA$_A$Rs, did not have any considerable effect on the tonic current in PKCδ^+ neurons.

It was previously shown that α_5GABA$_A$Rs are expressed in CEA and are mostly present in neurons not expressing the *corticotrophin-releasing factor receptor 1* (Pirker et al. 2000, Herman et al. 2013). However, since a peculiar form of tonic inhibition was described in CEA mediated by α_1-containing GABA$_A$Rs located in *corticotrophin-releasing factor receptor 1* expressing neurons (Herman et al. 2013). We therefore tested the effect of nanomolar concentrations of zolpidem, a benzodiazepine which activates these receptors, on PKCδ^+ neurons. Zolpidem had only a considerable effect on the decay of sIPSCs but not on the extrasynaptic inhibition. This finding suggests that α_1-containing GABA$_A$Rs mostly contribute to the synaptic events recorded from PKCδ^+ neurons of CEA. The fact that we did not observe an effect of the α_1-containing GABA$_A$R in these neurons may be due to the partial overlap between the *corticotrophin-releasing factor receptor 1* and PKCδ expression of central amygdala neurons.

Another important feature of our findings is that we discovered a functional role for α_5GABA$_A$Rs in PKCδ^+ neurons in encoding a certain behavioral outcome. First, selective inhibition of the α_5 receptor enhanced the tonic firing of PKCδ^+ neurons *in vitro*. Single unit recordings combined with pharmacological application of PWZ-029, an inverse agonist of α_5GABA$_A$Rs, in freely moving animals demonstrated their role in regulating the spontaneous firing of CEA neurons. Consequently, it is likely that extrasynaptic inhibition sets the signal-to-noise ratio of presynaptic inputs onto these neurons, which therefore has important consequences on behavioral outcomes. Accordingly, α_5GABA$_A$R-mediated inhibition is down-regulated by classical fear conditioning specifically in PKCδ^+ neurons while it is enhanced in the two other CEA neuronal populations. This plastic change did not affect the residual compensatory tonic current recorded from PKCδ^+ neurons in constitutive α_5GABA$_A$R knock-out animals. Indeed, the fear conditioning-induced plastic decrease of the α_5GABA$_A$R-mediated inhibition in PKCδ^+ neurons was inversely correlated with fear generalization of the animal. Finally, the ablation of α_5GABA$_A$R specifically in PKCδ^+ neurons increased the anxiety state and fear generalization to an unconditional sensory stimulus.

Generally, our novel findings strongly support the hypothesis that a variable plastic decrease of α_5GABA$_A$R-mediating extrasynaptic inhibition in a specific sub-population of CEA neurons is associated with anxiety and fear generalization. A traumatic experience caused plastic changes in this defined extrasynaptic inhibition, via reduced tonic firing of CEA PKCδ^+ neurons, and induced a behavioral shift towards an anxiety phenotype. Consequently, specific post-traumatic decreases in α_5 containing GABA$_A$Rs levels could enhance the excitability of PKCδ^+ neurons and increase GABA tone onto postsynaptic neurons (such as, PKCδ^- and *vl*PAG-projecting CEm neurons; figure 15, supplementary figure 2, 16). This mechanism would allow the precise tuning of single-to-noise ratio of CS-evoked responses in CEm output neurons involved in freezing responses (for instance projecting to *vl*PAG). Interestingly, the extrasynaptic inhibition of *vl*PAG-projecting CEm neurons is enhanced after fear conditioning and directly correlates with fear generalization. In addition, these plastic changes are also associated with enhanced levels of presynaptic GABA release onto *vl*PAG-projecting CEm neurons (supplementary figure 16).

Associative sensory learning was observed to mediate the plasticity of the tonic inhibition in other neuronal subtypes of the barrel cortex (Uban-Cleko et al. 2010). However, we observed for the first time that auditory and contextual fear conditioning rapidly decreases the α_5GABA$_A$R-mediated inhibition of PKCδ^+ neurons, which predicts fear generalization. A fascinating hypothesis is that plasticity of the α_5GABA$_A$R could be important in the development of anxiety disorders. Supporting this finding, numerous studies have shown an association of the α_5GABA$_A$R with anxiety disorders in rodents and humans (Navarro et al. 2002, Heldt and Ressler 2007, Delong et al. 2007, Craddock et al. 2010, Tasan et al. 2011). Our findings could help in understanding the etiology and individual predisposition to pathological anxiety disorders. Therefore, it is fundamental to elucidate molecular and genetic mechanisms that predict the nature of the response variance observed for the plasticity of extrasynaptic inhibition following trauma and its role in anxiety behavior (Yehuda and LeDoux 2007).

Down-regulation of α_5GABA$_A$-mediated inhibition found in PKCδ^+ neurons can be caused by decreased expression of the receptor, after fear conditioning, selectively in CEA (Heldt and Ressler 2007). It is noteworthy that a mouse model of *increased trait anxiety* exhibited decreased α_5-containing GABA$_A$Rs transcription in CEA (Tasan et al. 2011). It is probable that plastic changes induced by trauma increase the internalization and degradation of the α_5 containing $GABA_ARs$. Consequently, this enhances feedback mechanisms favoring transcriptional downregulation and ultimately protein level diminution specifically in CEA PKCδ^+ neurons.

One could further speculate that activity-mediated plasticity of the tonic inhibition could be initiated by an instructive signal causing a massive calcium influx (Luscher et al. 2011). Interestingly, parabrachial nucleus glutamatergic afferents densely innervate CEA (Shimada et al. 1992, Carter et al. 2013). This nucleus is part of the *spinoparabrachioamygdaloid tract* which is important in transmitting somatic and visceral noxious stimuli, for instance the electric shock inputs (US). Thus, pain signals, initiated by activation of specific NMDA receptors located in CEA, could directly cause a massive calcium influx into PKCδ-expressing neurons that is important in fear memory acquisition (Rodrigues et al. 2001). Finally, calcium-related signals could activate clathrin- and dynamin-dependent endocytosis mechanisms involved in $GABA_AR$ internalization (Luscher et al. 2011). Specific signaling events involved in the internalization of the α_5GABA_AR could be caused by the PI/PKC pathway. It is interesting then that the various PKC isoforms yield differential phosphorylation of the $GABA_ARs$ subtypes and, consequently, have unique impacts on receptor regulation (Song and Messing, 2005). Furthermore, high expression of the PKCδ protein found in specific cell types of CEl could have a peculiar effect on plasticity and trafficking of the α_5GABA_AR in CEA.

Another fascinating possibility is that ambient GABA could be the cause of the decrease of α_5GABA_AR-mediated tonic inhibition following fear conditioning. Notably, mice deficient for the 65 kD isoform of the GABA synthesizing enzyme glutamic acid decarboxylase (GAD65), which is strongly expressed in CEA (Poulin et al. 2008), exhibit reduced extracellular GABA levels and generalization of unconditioned fear responses (Stork et al. 2000, Bergado-Acosta et al. 2008). However, these experiments used global constitutive knockout mice and did not show a specific plastic change of GAD65 in defined neurons of amygdala. Long term plastic changes of transporters and glutamate decarboxylase enzymes regulating ambient GABA are not likely because the mRNA of GAD67, GAD65 and the GABA transporter 1 (GAT1) was not affected by fear conditioning (Heldt and Ressler 2007).

It is likely that PKCδ-expressing neurons located in central amygdala adjust the plastic GABAergic tone onto *vl*PAG-projecting CEm neurons involved in freezing expression. This is helped by a peculiar form of trauma-induced α_5GABA$_A$R plasticity that occurs only in PKCδ-expressing neurons of central amygdala.

Overall, our results demonstrate that PKCδ^+ neurons not only transmit phasic information important to gate cue-induced fear but also tonic signals regulating fear generalization and anxiety. Regulation of the tonic firing rate of PKCδ^+ neurons may represent a general mechanism by which anxiety states are modulated by fear conditioning but also by drugs of abuse (ethanol), social interactions (oxytocin) and inflammatory processes mediated by interleukin that are known to control anxiety states. Our work points to an important link between α_5GABA$_A$R-mediated tonic inhibition specifically expressed in a defined neuronal sub-population of the central amygdala and the predisposition to develop anxiety following trauma experience.

Ade, K. K., M. J. Janssen, et al. (2008). "Differential tonic GABA conductances in striatal medium spiny neurons." J Neurosci **28**(5): 1185-97.

Adolphs, R. (2013). "The biology of fear." Curr Biol **23**(2): R79-93.

Alldred, M. J., J. Mulder-Rosi, et al. (2005). "Distinct gamma2 subunit domains mediate clustering and synaptic function of postsynaptic GABAA receptors and gephyrin." J Neurosci **25**(3): 594-603.

Bai, D., G. Zhu, et al. (2001). "Distinct functional and pharmacological properties of tonic and quantal inhibitory postsynaptic currents mediated by gamma-aminobutyric acid(A) receptors in hippocampal neurons." Mol Pharmacol **59**(4): 814-24.

Balleine, B. W. and S. Killcross (2006). "Parallel incentive processing: an integrated view of amygdala function." Trends Neurosci **29**(5): 272-9.

Bedford, F. K., J. T. Kittler, et al. (2001). "GABA(A) receptor cell surface number and subunit stability are regulated by the ubiquitin-like protein Plic-1." Nat Neurosci **4**(9): 908-16.

Biro, A. A., N. B. Holderith, et al. (2006). "Release probability-dependent scaling of the postsynaptic responses at single hippocampal GABAergic synapses." J Neurosci **26**(48): 12487-96.

Blanchard, E. B., J. M. Lackner, et al. (2008). "The role of stress in symptom exacerbation among IBS patients." J Psychosom Res **64**(2): 119-28.

Bouret, S., A. Duvel, et al. (2003). "Phasic activation of locus ceruleus neurons by the central nucleus of the amygdala." J Neurosci **23**(8): 3491-7.

Bradley, C. A., C. Taghibiglou, et al. (2008). "Mechanisms involved in the reduction of GABAA receptor alpha1-subunit expression caused by the epilepsy mutation A322D in the trafficking-competent receptor." J Biol Chem **283**(32): 22043-50.

Brickley, S. G., S. G. Cull-Candy, et al. (1996). "Development of a tonic form of synaptic inhibition in rat cerebellar granule cells resulting from persistent activation of GABAA receptors." J Physiol **497 (Pt 3)**: 753-9.

Brickley, S. G. and I. Mody (2012). "Extrasynaptic GABA(A) receptors: their function in the CNS and implications for disease." Neuron **73**(1): 23-34.

Brunig, I., E. Scotti, et al. (2002). "Intact sorting, targeting, and clustering of gamma-aminobutyric acid A receptor subtypes in hippocampal neurons in vitro." J Comp Neurol **443**(1): 43-55.

Caraiscos, V. B., E. M. Elliott, et al. (2004). "Tonic inhibition in mouse hippocampal CA1 pyramidal neurons is mediated by alpha5 subunit-containing gamma-aminobutyric acid type A receptors." Proc Natl Acad Sci U S A **101**(10): 3662-7.

Cassel, W. A., K. M. Weidenheim, et al. (1986). "Malignant melanoma. Inflammatory mononuclear cell infiltrates in cerebral metastases during concurrent therapy with viral oncolysate." Cancer **57**(7): 1302-12.

Cassell, M. D., L. J. Freedman, et al. (1999). "The intrinsic organization of the central extended amygdala." Ann N Y Acad Sci **877**: 217-41.

Cassell, M. D., T. S. Gray, et al. (1986). "Neuronal architecture in the rat central nucleus of the amygdala: a cytological, hodological, and immunocytochemical study." J Comp Neurol **246**(4): 478-99.

Chadderton, P., T. W. Margrie, et al. (2004). "Integration of quanta in cerebellar granule cells during sensory processing." Nature **428**(6985): 856-60.

Chambers, M. S., J. R. Atack, et al. (2004). "An orally bioavailable, functionally selective inverse agonist at the benzodiazepine site of GABAA alpha5 receptors with cognition enhancing properties." J Med Chem **47**(24): 5829-32.

Chen, Z. W. and R. W. Olsen (2007). "GABAA receptor associated proteins: a key factor regulating GABAA receptor function." J Neurochem **100**(2): 279-94.

Chieng, B. and M. J. Christie (2010). "Somatostatin and nociceptin inhibit neurons in the central nucleus of amygdala that project to the periaqueductal grey." Neuropharmacology **59**(6): 425-30.

Chieng, B. C., M. J. Christie, et al. (2006). "Characterization of neurons in the rat central nucleus of the amygdala: cellular physiology, morphology, and opioid sensitivity." J Comp Neurol **497**(6): 910-27.

Ciocchi, S., C. Herry, et al. (2010). "Encoding of conditioned fear in central amygdala inhibitory circuits." Nature **468**(7321): 277-82.

Ciriello, J., M. P. Rosas-Arellano, et al. (2003). "Identification of neurons containing orexin-B (hypocretin-2) immunoreactivity in limbic structures." Brain Res **967**(1-2): 123-31.

Citri, A. and R. C. Malenka (2008). "Synaptic plasticity: multiple forms, functions, and mechanisms." Neuropsychopharmacology **33**(1): 18-41.

Cobb, S. R., E. H. Buhl, et al. (1995). "Synchronization of neuronal activity in hippocampus by individual GABAergic interneurons." Nature **378**(6552): 75-8.

Collins, D. R. and D. Pare (2000). "Differential fear conditioning induces reciprocal changes in the sensory responses of lateral amygdala neurons to the CS(+) and CS(-)." Learn Mem **7**(2): 97-103.

Collinson, N., F. M. Kuenzi, et al. (2002). "Enhanced learning and memory and altered GABAergic synaptic transmission in mice lacking the alpha 5 subunit of the GABAA receptor." J Neurosci **22**(13): 5572-80.

Connolly, C. N., B. J. Krishek, et al. (1996). "Assembly and cell surface expression of heteromeric and homomeric gamma-aminobutyric acid type A receptors." J Biol Chem **271**(1): 89-96.

Craddock, N., L. Jones, et al. (2010). "Strong genetic evidence for a selective influence of GABAA receptors on a component of the bipolar disorder phenotype." Mol Psychiatry **15**(2): 146-53.

Crestani, F., R. Assandri, et al. (2002). "Contribution of the alpha1-GABA(A) receptor subtype to the pharmacological actions of benzodiazepine site inverse agonists." Neuropharmacology **43**(4): 679-84.

Crestani, F., R. Keist, et al. (2002). "Trace fear conditioning involves hippocampal alpha5 GABA(A) receptors." Proc Natl Acad Sci U S A **99**(13): 8980-5.

Davis, M., D. L. Walker, et al. (2010). "Phasic vs sustained fear in rats and humans: role of the extended amygdala in fear vs anxiety." Neuropsychopharmacology **35**(1): 105-35.

Delgado, J. M., H. E. Rosvold, et al. (1956). "Evoking conditioned fear by electrical stimulation of subcortical structures in the monkey brain." J Comp Physiol Psychol **49**(4): 373-80.

Delong, R. (2007). "GABA(A) receptor alpha5 subunit as a candidate gene for autism and bipolar disorder: a proposed endophenotype with parent-of-origin and gain-of-function features,with or without oculocutaneous albinism." Autism **11**(2): 135-47.

Dias, B. G., S. B. Banerjee, et al. (2013). "Towards new approaches to disorders of fear and anxiety." Curr Opin Neurobiol **23**(3): 346-52.

Dong, Y. L., Y. Fukazawa, et al. (2010). "Differential postsynaptic compartments in the laterocapsular division of the central nucleus of amygdala for afferents from the parabrachial nucleus and the basolateral nucleus in the rat." J Comp Neurol **518**(23): 4771-91.

Doyere, V., G. E. Schafe, et al. (2003). "Long-term potentiation in freely moving rats reveals asymmetries in thalamic and cortical inputs to the lateral amygdala." Eur J Neurosci **17**(12): 2703-15.

Duley, A. R., C. H. Hillman, et al. (2007). "Sensorimotor gating and anxiety: prepulse inhibition following acute exercise." Int J Psychophysiol **64**(2): 157-64.

Dumont, E. C., M. Martina, et al. (2002). "Physiological properties of central amygdala neurons: species differences." Eur J Neurosci **15**(3): 545-52.

Duvarci, S., E. P. Bauer, et al. (2009). "The bed nucleus of the stria terminalis mediates inter-individual variations in anxiety and fear." J Neurosci **29**(33): 10357-61.

Eccles, J. (1965). "The Synapse." Sci Am **212**: 56-66.

Ehrlich, I., Y. Humeau, et al. (2009). "Amygdala inhibitory circuits and the control of fear memory." Neuron **62**(6): 757-71.

Essrich, C., M. Lorez, et al. (1998). "Postsynaptic clustering of major GABAA receptor subtypes requires the gamma 2 subunit and gephyrin." Nat Neurosci **1**(7): 563-71.

Etkin, A., K. E. Prater, et al. (2009). "Disrupted amygdalar subregion functional connectivity and evidence of a compensatory network in generalized anxiety disorder." Arch Gen Psychiatry **66**(12): 1361-72.

Fanselow, M. S. and A. M. Poulos (2005). "The neuroscience of mammalian associative learning." Annu Rev Psychol **56**: 207-34.

Farrant, M. and Z. Nusser (2005). "Variations on an inhibitory theme: phasic and tonic activation of GABA(A) receptors." Nat Rev Neurosci **6**(3): 215-29.

Fishell, G. and B. Rudy (2011). "Mechanisms of inhibition within the telencephalon: "where the wild things are"." Annu Rev Neurosci **34**: 535-67.

Fisher, A. S., R. J. Stewart, et al. (2007). "Disruption of noradrenergic transmission and the behavioural response to a novel environment in NK1R-/- mice." Eur J Neurosci **25**(4): 1195-204.

Freund, T. F. and G. Buzsaki (1996). "Interneurons of the hippocampus." Hippocampus **6**(4): 347-470.

Galarreta, M. and S. Hestrin (2001). "Spike transmission and synchrony detection in networks of GABAergic interneurons." Science **292**(5525): 2295-9.

Gallagher, M. J., L. Ding, et al. (2007). "The GABAA receptor alpha1 subunit epilepsy mutation A322D inhibits transmembrane helix formation and causes proteasomal degradation." Proc Natl Acad Sci U S A **104**(32): 12999-3004.

Glykys, J., E. O. Mann, et al. (2008). "Which GABA(A) receptor subunits are necessary for tonic inhibition in the hippocampus?" J Neurosci **28**(6): 1421-6.

Goosens, K. A. and S. Maren (2001). "Contextual and auditory fear conditioning are mediated by the lateral, basal, and central amygdaloid nuclei in rats." Learn Mem **8**(3): 148-55.

Goosens, K. A. and S. Maren (2003). "Pretraining NMDA receptor blockade in the basolateral complex, but not the central nucleus, of the amygdala prevents savings of conditional fear." Behav Neurosci **117**(4): 738-50.

Gozzi, A., A. Jain, et al. (2010). "A neural switch for active and passive fear." Neuron **67**(4): 656-66.

Gray, T. S., M. D. Cassell, et al. (1984). "Distribution of pro-opiomelanocortin-derived peptides and enkephalins in the rat central nucleus of the amygdala." Brain Res **306**(1-2): 354-8.

Gulledge, A. T. and G. J. Stuart (2003). "Excitatory actions of GABA in the cortex." Neuron **37**(2): 299-309.

Handley, S. L. and S. Mithani (1984). "Effects of alpha-adrenoceptor agonists and antagonists in a maze-exploration model of 'fear'-motivated behaviour." Naunyn Schmiedebergs Arch Pharmacol **327**(1): 1-5.

Harris, J. A. and R. F. Westbrook (1998). "Evidence that GABA transmission mediates context-specific extinction of learned fear." Psychopharmacology (Berl) **140**(1): 105-15.

Haubensak, W., P. S. Kunwar, et al. (2010). "Genetic dissection of an amygdala microcircuit that gates conditioned fear." Nature **468**(7321): 270-6.

Hauser, J., U. Rudolph, et al. (2005). "Hippocampal alpha5 subunit-containing GABAA receptors modulate the expression of prepulse inhibition." Mol Psychiatry **10**(2): 201-7.

Heldt, S. A. and K. J. Ressler (2007). "Training-induced changes in the expression of GABAA-associated genes in the amygdala after the acquisition and extinction of Pavlovian fear." Eur J Neurosci **26**(12): 3631-44.

Herman, M. A., C. Contet, et al. (2013). "Novel subunit-specific tonic GABA currents and differential effects of ethanol in the central amygdala of CRF receptor-1 reporter mice." J Neurosci **33**(8): 3284-98.

Herry, C., S. Ciocchi, et al. (2008). "Switching on and off fear by distinct neuronal circuits." Nature **454**(7204): 600-6.

Honkaniemi, J. (1992). "Colocalization of peptide- and tyrosine hydroxylase-like immunoreactivities with Fos-immunoreactive neurons in rat central amygdaloid nucleus after immobilization stress." Brain Res **598**(1-2): 107-13.

Hopkins, D. A. and G. Holstege (1978). "Amygdaloid projections to the mesencephalon, pons and medulla oblongata in the cat." Exp Brain Res **32**(4): 529-47.

Huang, Y. Y. and E. R. Kandel (1998). "Postsynaptic induction and PKA-dependent expression of LTP in the lateral amygdala." Neuron **21**(1): 169-78.

Huber, D., P. Veinante, et al. (2005). "Vasopressin and oxytocin excite distinct neuronal populations in the central amygdala." Science **308**(5719): 245-8.

Jellestad, F. K., A. Markowska, et al. (1986). "Behavioral effects after ibotenic acid, 6-OHDA and electrolytic lesions in the central amygdala nucleus of the rat." Physiol Behav **37**(6): 855-62.

Jolkkonen, E. and A. Pitkanen (1998). "Intrinsic connections of the rat amygdaloid complex: projections originating in the central nucleus." J Comp Neurol **395**(1): 53-72.

Jonas, P., J. Bischofberger, et al. (2004). "Interneuron Diversity series: Fast in, fast out--temporal and spatial signal processing in hippocampal interneurons." Trends Neurosci **27**(1): 30-40.

Kalin, N. H., S. E. Shelton, et al. (2004). "The role of the central nucleus of the amygdala in mediating fear and anxiety in the primate." J Neurosci **24**(24): 5506-15.

Kandel, E. R. and W. A. Spencer (1968). "Cellular neurophysiological approaches in the study of learning." Physiol Rev **48**(1): 65-134.

Kaneda, M., M. Farrant, et al. (1995). "Whole-cell and single-channel currents activated by GABA and glycine in granule cells of the rat cerebellum." J Physiol **485 (Pt 2)**: 419-35.

Kasugai, Y., J. D. Swinny, et al. (2010). "Quantitative localisation of synaptic and extrasynaptic GABAA receptor subunits on hippocampal pyramidal cells by freeze-fracture replica immunolabelling." Eur J Neurosci **32**(11): 1868-88.

Knobloch, H. S., A. Charlet, et al. (2012). "Evoked axonal oxytocin release in the central amygdala attenuates fear response." Neuron **73**(3): 553-66.

Krettek, J. E. and J. L. Price (1978). "Amygdaloid projections to subcortical structures within the basal forebrain and brainstem in the rat and cat." J Comp Neurol **178**(2): 225-54.

Krettek, J. E. and J. L. Price (1978). "A description of the amygdaloid complex in the rat and cat with observations on intra-amygdaloid axonal connections." J Comp Neurol **178**(2): 255-80.

LeDoux, J. E. (2000). "Emotion circuits in the brain." Annu Rev Neurosci **23**: 155-84.

LeDoux, J. E., C. R. Farb, et al. (1991). "Overlapping projections to the amygdala and striatum from auditory processing areas of the thalamus and cortex." Neurosci Lett **134**(1): 139-44.

Li, H., M. A. Penzo, et al. (2013). "Experience-dependent modification of a central amygdala fear circuit." Nat Neurosci **16**(3): 332-9.

Likhtik, E., J. M. Stujenske, et al. (2014). "Prefrontal entrainment of amygdala activity signals safety in learned fear and innate anxiety." Nat Neurosci **17**(1): 106-13.

Luscher, B., T. Fuchs, et al. (2011). "GABAA receptor trafficking-mediated plasticity of inhibitory synapses." Neuron **70**(3): 385-409.

Luscher, B. and C. A. Keller (2004). "Regulation of GABAA receptor trafficking, channel activity, and functional plasticity of inhibitory synapses." Pharmacol Ther **102**(3): 195-221.

Lydiard, R. B. (2003). "The role of GABA in anxiety disorders." J Clin Psychiatry **64 Suppl 3**: 21-7.

Lynch, G. S., T. Dunwiddie, et al. (1977). "Heterosynaptic depression: a postsynaptic correlate of long-term potentiation." Nature **266**(5604): 737-9.

Malenka, R. C. and M. F. Bear (2004). "LTP and LTD: an embarrassment of riches." Neuron **44**(1): 5-21.

Malizia, A. L. (2002). "Receptor binding and drug modulation in anxiety." Eur Neuropsychopharmacol **12**(6): 567-74.

Maren, S. (2001). "Neurobiology of Pavlovian fear conditioning." Annu Rev Neurosci **24**: 897-931.

Marks, M. and P. de Silva (1994). "The 'match/mismatch' model of fear: empirical status and clinical implications." Behav Res Ther **32**(7): 759-70.

Marsden, K. C., J. B. Beattie, et al. (2007). "NMDA receptor activation potentiates inhibitory transmission through GABA receptor-associated protein-dependent exocytosis of GABA(A) receptors." J Neurosci **27**(52): 14326-37.

Martin, S. J., P. D. Grimwood, et al. (2000). "Synaptic plasticity and memory: an evaluation of the hypothesis." Annu Rev Neurosci **23**: 649-711.

Martina, M., S. Royer, et al. (1999). "Physiological properties of central medial and central lateral amygdala neurons." J Neurophysiol **82**(4): 1843-54.

McCartney, M. R., T. Z. Deeb, et al. (2007). "Tonically active GABAA receptors in hippocampal pyramidal neurons exhibit constitutive GABA-independent gating." Mol Pharmacol **71**(2): 539-48.

McDonald, A. J. (1992). "Projection neurons of the basolateral amygdala: a correlative Golgi and retrograde tract tracing study." Brain Res Bull **28**(2): 179-85.

McGaugh, J. L. (2004). "Memory reconsolidation hypothesis revived but restrained: theoretical comment on Biedenkapp and Rudy (2004)." Behav Neurosci **118**(5): 1140-2.

McKernan, M. G. and P. Shinnick-Gallagher (1997). "Fear conditioning induces a lasting potentiation of synaptic currents in vitro." Nature **390**(6660): 607-11.

Menard, J. and D. Treit (1999). "Effects of centrally administered anxiolytic compounds in animal models of anxiety." Neurosci Biobehav Rev **23**(4): 591-613.

Mitchell, S. J. and R. A. Silver (2003). "Shunting inhibition modulates neuronal gain during synaptic excitation." Neuron **38**(3): 433-45.

Montgomery, K. C. and M. Segall (1955). "Discrimination learning based upon the exploratory drive." J Comp Physiol Psychol **48**(3): 225-8.

Navarro, J. F., E. Buron, et al. (2002). "Anxiogenic-like activity of L-655,708, a selective ligand for the benzodiazepine site of GABA(A) receptors which contain the alpha-5 subunit, in the elevated plus-maze test." Prog Neuropsychopharmacol Biol Psychiatry **26**(7-8): 1389-92.

Nie, Z., P. Schweitzer, et al. (2004). "Ethanol augments GABAergic transmission in the central amygdala via CRF1 receptors." Science **303**(5663): 1512-4.

Nieh, E. H., S. Y. Kim, et al. (2013). "Optogenetic dissection of neural circuits underlying emotional valence and motivated behaviors." Brain Res **1511**: 73-92.

Nusser, Z. and I. Mody (2002). "Selective modulation of tonic and phasic inhibitions in dentate gyrus granule cells." J Neurophysiol **87**(5): 2624-8.

Ottersen, O. P. and Y. Ben-Ari (1979). "Afferent connections to the amygdaloid complex of the rat and cat. I. Projections from the thalamus." J Comp Neurol **187**(2): 401-24.

Pape, H. C. and D. Pare (2010). "Plastic synaptic networks of the amygdala for the acquisition, expression, and extinction of conditioned fear." Physiol Rev **90**(2): 419-63.

Pascoe, J. P. and B. S. Kapp (1985). "Electrophysiological characteristics of amygdaloid central nucleus neurons during Pavlovian fear conditioning in the rabbit." Behav Brain Res **16**(2-3): 117-33.

Pellow, S., P. Chopin, et al. (1985). "Validation of open:closed arm entries in an elevated plus-maze as a measure of anxiety in the rat." J Neurosci Methods **14**(3): 149-67.

Penzo, M. A., V. Robert, et al. (2014). "Fear conditioning potentiates synaptic transmission onto long-range projection neurons in the lateral subdivision of central amygdala." J Neurosci **34**(7): 2432-7.

Perez-Orive, J., O. Mazor, et al. (2002). "Oscillations and sparsening of odor representations in the mushroom body." Science **297**(5580): 359-65.

Porcello, D. M., M. M. Huntsman, et al. (2003). "Intact synaptic GABAergic inhibition and altered neurosteroid modulation of thalamic relay neurons in mice lacking delta subunit." J Neurophysiol **89**(3): 1378-86.

Pouille, F. and M. Scanziani (2001). "Enforcement of temporal fidelity in pyramidal cells by somatic feed-forward inhibition." Science **293**(5532): 1159-63.

Quirk, G. J., J. L. Armony, et al. (1997). "Fear conditioning enhances different temporal components of tone-evoked spike trains in auditory cortex and lateral amygdala." Neuron **19**(3): 613-24.

Quirk, G. J., C. Repa, et al. (1995). "Fear conditioning enhances short-latency auditory responses of lateral amygdala neurons: parallel recordings in the freely behaving rat." Neuron **15**(5): 1029-39.

Rabinak, C. A. and S. Maren (2008). "Associative structure of fear memory after basolateral amygdala lesions in rats." Behav Neurosci **122**(6): 1284-94.

Roberts, G. W., P. L. Woodhams, et al. (1982). "Distribution of neuropeptides in the limbic system of the rat: the amygdaloid complex." Neuroscience **7**(1): 99-131.

Rogan, M. T. and J. E. LeDoux (1995). "LTP is accompanied by commensurate enhancement of auditory-evoked responses in a fear conditioning circuit." Neuron **15**(1): 127-36.

Rogan, M. T., U. V. Staubli, et al. (1997). "Fear conditioning induces associative long-term potentiation in the amygdala." Nature **390**(6660): 604-7.

Rossi, D. J., M. Hamann, et al. (2003). "Multiple modes of GABAergic inhibition of rat cerebellar granule cells." J Physiol **548**(Pt 1): 97-110.

Rowland, A. M., J. E. Richmond, et al. (2006). "Presynaptic terminals independently regulate synaptic clustering and autophagy of GABAA receptors in Caenorhabditis elegans." J Neurosci **26**(6): 1711-20.

Rudolph, U. and F. Knoflach (2011). "Beyond classical benzodiazepines: novel therapeutic potential of GABAA receptor subtypes." Nat Rev Drug Discov **10**(9): 685-97.

Rudolph, U. and H. Mohler (2006). "GABA-based therapeutic approaches: GABAA receptor subtype functions." Curr Opin Pharmacol **6**(1): 18-23.

Samson, R. D., S. Duvarci, et al. (2005). "Synaptic plasticity in the central nucleus of the amygdala." Rev Neurosci **16**(4): 287-302.

Samson, R. D. and D. Pare (2005). "Activity-dependent synaptic plasticity in the central nucleus of the amygdala." J Neurosci **25**(7): 1847-55.

Semyanov, A., M. C. Walker, et al. (2003). "GABA uptake regulates cortical excitability via cell type-specific tonic inhibition." Nat Neurosci **6**(5): 484-90.

Serwanski, D. R., C. P. Miralles, et al. (2006). "Synaptic and nonsynaptic localization of GABAA receptors containing the alpha5 subunit in the rat brain." J Comp Neurol **499**(3): 458-70.

Shen, H., Q. H. Gong, et al. (2007). "Reversal of neurosteroid effects at alpha4beta2delta GABAA receptors triggers anxiety at puberty." Nat Neurosci **10**(4): 469-77.

Shen, H., N. Sabaliauskas, et al. (2010). "A critical role for alpha4betadelta GABAA receptors in shaping learning deficits at puberty in mice." Science **327**(5972): 1515-8.

Shimada, S., S. Inagaki, et al. (1992). "Synaptic contacts between CGRP-immunoreactive terminals and enkephalin-immunoreactive neurons in the central amygdaloid nucleus of the rat." Neurosci Lett **134**(2): 243-6.

Shin, L. M. and I. Liberzon (2010). "The neurocircuitry of fear, stress, and anxiety disorders." Neuropsychopharmacology **35**(1): 169-91.

Silver, R. A., S. F. Traynelis, et al. (1992). "Rapid-time-course miniature and evoked excitatory currents at cerebellar synapses in situ." Nature **355**(6356): 163-6.

Sjostrom, P. J., E. A. Rancz, et al. (2008). "Dendritic excitability and synaptic plasticity." Physiol Rev **88**(2): 769-840.

Somogyi, P. and T. Klausberger (2005). "Defined types of cortical interneurone structure space and spike timing in the hippocampus." J Physiol **562**(Pt 1): 9-26.

Spampanato, C., S. De Maria, et al. (2012). "Simvastatin inhibits cancer cell growth by inducing apoptosis correlated to activation of Bax and down-regulation of BCL-2 gene expression." Int J Oncol **40**(4): 935-41.

Stell, B. M. and I. Mody (2002). "Receptors with different affinities mediate phasic and tonic GABA(A) conductances in hippocampal neurons." J Neurosci **22**(10): RC223.

Sternfeld, F., R. W. Carling, et al. (2004). "Selective, orally active gamma-aminobutyric acidA alpha5 receptor inverse agonists as cognition enhancers." J Med Chem **47**(9): 2176-9.

Sun, N., H. Yi, et al. (1994). "Evidence for a GABAergic interface between cortical afferents and brainstem projection neurons in the rat central extended amygdala." J Comp Neurol **340**(1): 43-64.

Swanson, L. W. and G. D. Petrovich (1998). "What is the amygdala?" Trends Neurosci **21**(8): 323-31.

Tasan, R. O., A. Bukovac, et al. (2011). "Altered GABA transmission in a mouse model of increased trait anxiety." Neuroscience **183**: 71-80.

Tooby, J. and L. Cosmides (1990). "On the universality of human nature and the uniqueness of the individual: the role of genetics and adaptation." J Pers **58**(1): 17-67.

Tsvetkov, E., W. A. Carlezon, et al. (2002). "Fear conditioning occludes LTP-induced presynaptic enhancement of synaptic transmission in the cortical pathway to the lateral amygdala." Neuron **34**(2): 289-300.

Tye, K. M., R. Prakash, et al. (2011). "Amygdala circuitry mediating reversible and bidirectional control of anxiety." Nature **471**(7338): 358-62.

Urban-Ciecko, J., M. Kossut, et al. (2010). "Sensory learning differentially affects GABAergic tonic currents in excitatory neurons and fast spiking interneurons in layer 4 of mouse barrel cortex." J Neurophysiol **104**(2): 746-54.

Veening, J. G., L. W. Swanson, et al. (1984). "The organization of projections from the central nucleus of the amygdala to brainstem sites involved in central autonomic regulation: a combined retrograde transport-immunohistochemical study." Brain Res **303**(2): 337-57.

Veinante, P. and M. J. Freund-Mercier (1995). "Histoautoradiographic detection of oxytocin- and vasopressin-binding sites in the amygdala of the rat." Adv Exp Med Biol **395**: 347-8.

Veinante, P. and M. J. Freund-Mercier (1997). "Distribution of oxytocin- and vasopressin-binding sites in the rat extended amygdala: a histoautoradiographic study." J Comp Neurol **383**(3): 305-25.

Veinante, P. and M. J. Freund-Mercier (1998). "Intrinsic and extrinsic connections of the rat central extended amygdala: an in vivo electrophysiological study of the central amygdaloid nucleus." Brain Res **794**(2): 188-98.

Ventura, A., A. Meissner, et al. (2004). "Cre-lox-regulated conditional RNA interference from transgenes." Proc Natl Acad Sci U S A **101**(28): 10380-5.

Viviani, D., A. Charlet, et al. (2011). "Oxytocin selectively gates fear responses through distinct outputs from the central amygdala." Science **333**(6038): 104-7.

Wall, M. J. and M. M. Usowicz (1997). "Development of action potential-dependent and independent spontaneous GABAA receptor-mediated currents in granule cells of postnatal rat cerebellum." Eur J Neurosci **9**(3): 533-48.

Wang, D. S., A. A. Zurek, et al. (2012). "Memory deficits induced by inflammation are regulated by alpha5-subunit-containing GABAA receptors." Cell Rep **2**(3): 488-96.

Waters, S. M. and J. E. Krause (2000). "Distribution of galanin-1, -2 and -3 receptor messenger RNAs in central and peripheral rat tissues." Neuroscience **95**(1): 265-71.

Weiskrantz, L. (1956). "Behavioral changes associated with ablation of the amygdaloid complex in monkeys." J Comp Physiol Psychol **49**(4): 381-91.

Wilensky, A. E., G. E. Schafe, et al. (2000). "The amygdala modulates memory consolidation of fear-motivated inhibitory avoidance learning but not classical fear conditioning." J Neurosci **20**(18): 7059-66.

Yamada, J., A. Okabe, et al. (2004). "Cl- uptake promoting depolarizing GABA actions in immature rat neocortical neurones is mediated by NKCC1." J Physiol **557**(Pt 3): 829-41.

Yee, B. K., J. Hauser, et al. (2004). "GABA receptors containing the alpha5 subunit mediate the trace effect in aversive and appetitive conditioning and extinction of conditioned fear." Eur J Neurosci **20**(7): 1928-36.

Yehuda, R. and J. LeDoux (2007). "Response variation following trauma: a translational neuroscience approach to understanding PTSD." Neuron **56**(1): 19-32.

Yu, B. and P. Shinnick-Gallagher (1998). "Corticotropin-releasing factor increases dihydropyridine- and neurotoxin-resistant calcium currents in neurons of the central amygdala." J Pharmacol Exp Ther **284**(1): 170-9.

Zarnowska, E. D., R. Keist, et al. (2009). "GABAA receptor alpha5 subunits contribute to GABAA,slow synaptic inhibition in mouse hippocampus." J Neurophysiol **101**(3): 1179-91.

Zimmerman, J. M., C. A. Rabinak, et al. (2007). "The central nucleus of the amygdala is essential for acquiring and expressing conditional fear after overtraining." Learn Mem **14**(9): 634-44.

Acknowledgements

I am very thankful to Andreas Lüthi for giving me the opportunity to run this fascinating project.

I am incredibly thankful to Lynda Demmou for successfully performing a technically hard task, the *in vivo* recordings in freely moving animals combined with pharmacology. Thanks Chun Xu for the immunohistochemistry and scientific discussions. Thanks Tingjia Lu for cloning the AAV shRNA. Thanks Alberto Loche for the advices you gave to Tingjia. Thank you to Yu Kasugai and Dr. Francesco Ferraguti (University of Innsbruck, Austria) for trying the alpha5 labelling using Freeze-fracture replica immuno-labeling. Thanks to Dr. J. Cook and Michael Poe, University of Wisconsin, for providing the alpha5-inverse agonists. Thanks Dr. U. Rudolph, McLean Hospital, for providing the alpha5 KO brains. Thanks to the Anderson lab for providing PKCδ Cre^{+} animals and making possible the study of a specific neuronal population of central amygdala. Thanks to Pankaj lab for providing the RNAi. Thanks to Silvia Arber and Monika Mielich for providing the CRE deleter mouse line.

A big thank goes also to Philip Tovote and Jonathan Fadok for behavioral technical advices and for spending time to discuss and build the great open field and fear conditioning setup. Phil, I still remember going to Jumbo and Inter-discount to buy all the material and finally building the open field setup! Jon, a big thank for patiently teaching me to perform single units in combination with optogenetic. Milica (Markovic), I am really thankful to you because I have learned brain injections, building and implanting opto-connectors. Thanks to Joao Bacelo for giving me the white noise protocol, analyses software, and for the scientific discussion. Thanks Jan Grundeman for writing the macros for studying the location of the animal along the time during retrieval baseline. Thanks Philippe Gastrein for the technical help you gave me on slice electrophysiology and DAB staining. Thanks Francois for the DAB staining and the scientific discussions. Grazie Stephane Ciocchi for helping me initially help with discussions and the papers you gave me to read. This project and all the

fine experiments were discussed during the lab meeting and outside with all the members of the Lüthi group. Thank you also for listening to my long lab meetings and giving me all the helpful feedbacks!

Thanks Mike Bidinosti, MAN, for correcting my thesis!!!

Outside the lab, I would like to thank all the people that I met in Basel and share all the fantastic moments. Zia Barbara, Silvietta, Pietro, Zia Alessia, Alberto, Striscia, Mike, Steffen, Francois, Jon, Phil, Lynda, Lema, Eli. Thanks to all my present and previous flatmates (Antonia, Mari, Jaime, Helena, Diane) for sharing friendship, dinners, guitar sessions and parties. All other friends that I met outside of Switzerland but that kept in touch with me despite the distance: David, Stefano, Mario, Matteo, Federica, Ziu Loi, Marcio, Mino, Riccio, Roby, Stefano.

Grazie Celine for being part of my life and helping me with the thesis printing and everything else!

Un grazie speciale va' a mio padre che nonostante le difficolta' e' riuscito a guidarmi. Grazie a te sono riuscito a capire che nella vita conta seguire le proprie passioni in modo serio e spensierato. Grazie anche a mia madre perche' il tuo ricordo mi ha spinto lontano e continuera' a farlo

Personal information

Name (First, Last Name):	Paolo, Botta
Date and place of birth:	June 5th, 1981; Cagliari, Italy
Marital status:	Single
Citizenship:	Italian
Work Address:	**Friedrich Miescher Institute for biochemical research** *Andreas Lüthi group* Maulbeerstrasse 66 4058 Basel, Switzerland Office 4.16 Phone (+41) 078 90 86 872
E-mail address:	paolo.botta@fmi.ch
Languages:	Fluent Italian and English; Intermediate Spanish; basic-intermediate German and basic Portuguese.

Education & professional experience

> September 2009 – May 2014

PhD student at the Neurobiology section of the Novartis FMI, Basel, Switzerland with 5.8/6 magna cum laude. Thesis title: **Modulating anxiety with extrasynaptic inhibition.** Advisor: Dr. Andreas Lüthi, PhD.

> October 2005 – June 2009

Research fellowship in the Department of Neurosciences, at the University of New Mexico, NM, U.S.A. Advisor: C. F. Valenzuela, M.D.-Ph.D.

> July 2005

M. Sc. in Neuropsychobiology, with full credits and honors (110/110 summa cum laude).
Thesis title: "**Pharmacological and electrophysiological characterization of thiocolchicoside on the GABAergic and glycinergic inhibitory transmission**". Advisor: E. Sanna, Ph.D. University of Cagliari, Italy.

> July 2003

B.Sc. in Experimental Biology, with full credits and honors (110/110 summa cum laude). Thesis title: "**Use of cold probes and immune colorimetric techniques to identify gene sequences codifying calcium – calmodulin expressed in Euphorbia Characias**".

Advisor: A. Padiglia Ph.D. University of Cagliari, Italy.

> July 2000

High School Diploma in "Industrial Chemistry" from the *Istituto Tecnico Industriale* "*M. GIUA*", Cagliari, Italy, with credits 80/100.

Technical experience

University of Cagliari, Italy

- Southern Blotting for the identification of nucleotide sequence encoding for EF – hand domains of calmodulin in Euphorbia characias, by the use of non-radioactive probes.
- HPLC for the biochemical characterization of different peptides from saliva.
- Expression of cloned $GABA_A$ receptors in Xenopus oocytes and two-electrode voltage clamp.
- Preparation of hippocampal primary cell cultures and their pharmacologic treatment.
- Whole-cell patch-clamp recordings from hippocampal cultured cells.

University of New Mexico, New Mexico, U.S.A.

- Whole-cell, loose-patch cell-attached, perforated - patch clamp recordings from cerebellar and hippocampal neurons in brain slices to record spontaneous and evoked glutamatergic, GABAergic, K^+ currents, action currents and potentials.
- Use of standard software for the data acquisition and analysis (Clampex 9.0; Clampfit 9.0; MiniAnalysis 6.0.3.; Graph Prism 4.0; Microsoft Office Excel 2003).
- Scientific writing and oral presentations

Friedrich Miescher Institute, Basel, Switzerland

- *Patch clamp recordings from amygdala in brain slices.*
- *Genotyping.*
- *Stereotaxical injections of retro-beads and viruses in localized regions of the brain.*
- *Optogenetic recordings in vitro for assessing circuit connectivity.*
- *Morphological reconstruction of neurons filled with Biocytin.*
- *Anxiety and fear conditioning paradigms in combination with optogenetical and genetical manipulations in vivo.*
- *Scientific writing and oral presentations.*

Awards

- Best PhD talk, joint PhD retreat FMI-VBC, Vienna 2013
- Best Poster, Inhibition in the CNS, Gordon Conference, Les Diableret, Switzerland, 2013

Papers

1. M. Carta, L. Murru, P. Botta, G. Talani, G. Sechi, P. De Riu, E. Sanna, G. Biggio. **The muscle relaxant thiocolchicoside is an antagonist of GABAA receptor function in the central nervous system.** Neuropharmacology, 2006, 51: 805 - 815.

2. Botta P, R. A. Radcliffe , M. Carta , M. Mameli , E. Daly , K. L. Floyd , R. A. Deitrich, C. F. Valenzuela. **Modulation of GABAA receptors in cerebellar granule neurons by ethanol: a review of genetic and electrophysiological studies.** Alcohol, 2007, 41: 187 – 199.

3. Botta P*, M. Mameli*, K. L. Floyd, R. A. Radcliffe, C. F. Valenzuela. **Ethanol sensitivity of GABAergic currents in cerebellar granule neurons is not increased by a single amino acid change (R100Q) in the alpha6 GABAA receptors subunit.** J. Pharm. Exp. Ther., 2007, 323 (2): 684 – 391. ** Equal contribution.*

4. M. Mameli*, P. Botta*, P. Zamudio, S. Zucca, C. F. Valenzuela. **Ethanol decreases Purkinje neuron excitability by increasing GABA release in rat cerebellar slices.** J. Pharm. Exp. Ther., 2008, 327 (3): 910 - 7. ** Equal contribution.*

5. A. Belmenguenai*, P. Botta*, J. T. Weber*, M. Carta, M. De Ruiter, C. I. De Zeeuw, C. F. Valenzuela, and C. Hansel. **Alcohol impairs long-term depression at the cerebellar parallel fiber-Purkinje cell synapse.** Journal of Neurophysiology, 2008, 100 (6): 3167 - 74. ** Equal contribution.*

6. Bullock WM, Bolognani F, Botta P, Valenzuela CF, Perrone-Bizzozero NI. **Schizophrenia-like GABAergic gene expression deficits in cerebellar Golgi cells from rats chronically exposed to low-dose phencyclidine.** Neurochem Int. 2009, 55 (8): 775 - 82.

7. Botta P, de Souza FM, Sangrey T, De Schutter E, Valenzuela CF. **Alcohol excites cerebellar Golgi cells by inhibiting the Na+/K+ ATPase.** Neuropsychopharmacology, 2010; 35(9):1984-96.

8. Van Skike CE, Botta P, Chin VS, Tokunaga S, McDaniel JM, Venard J, Diaz-Granados JL, Valenzuela CF, Matthews DB. **Behavioral effects of ethanol in cerebellum are age dependent: potential system and molecular mechanisms.** Alcohol Clin Exp Res. 2010; 34(12):2070-80.

9. Botta P, Simões de Souza FM, Sangrey T, De Shutters E, Valenzuela CF. **Excitation of rat cerebellar Golgi cells by ethanol: further characterization of the mechanism.** Alcohol Clin Exp Res. 2012; 36(4):616-24.

10. Botta P, Zucca A and Valenzuela CF. **Acute ethanol exposure inhibits silencing of cerebellar Golgi cell firing induced by granule cell axon input.** Frontiers in Integrative Neuroscience. 2014 Feb 6; 8:10.
11. *Eline Pecho-Vrieseling, *Claus Rieker, Sascha Fuchs, Dorothee Bleckmann, Maria Soledad Esposito, Paolo Botta, Chris Goldstein, Mario Bernhard, Ivan Galimberti, Matthias Müller, Andreas Lüthi, Silvia Arber,Tewis Bouwmeester, Herman van der Putten, Francesco Paolo Di Giorgio. **Synaptic transneuronal propagation of mutant huntingtin contributes to non-cell autonomous pathology in neurons.** Nature Neuroscience, 2014. Ahead to print.

Talks

1. **Effect of Ethanol on Cerebellar Circuitry**. February 2009, University of Lausanne, Lausanne, Switzerland; FMI, Basel, Switzerland; University College London, London; University of Bristol, Bristol, England.

2. **Tonic inhibition in central amygdala inhibitory circuits**. FMI Neuroscience Colloquia, October 2012, Basel, Switzerland.

3. **Tonic inhibition in central amygdala inhibitory circuits**. Gordon Research Seminar on Inhibition in the CNS. June 2013, Les Diablerets, Switzerland.

4. **Regulating anxiety with extrasynaptic inhibition**. FMI Annual Meeting, September 2013.

Posters-Communications

1. Mura A., Travaglione A., Satta S., Botta P., Pistis G., Pariglia A.. **Molecular analysis and primary structure of calmoduline gene from Euphorbia characias.** Rendiconti del Seminario della Facoltà di Scienze MMFFNN, XVI Congresso Società Italiana di Biochimica, Sezione Sardegna, p. 63, 2003.

2. Carta M., Bachis E., Botta P., Zucca S., Talani G., Murru L., Mascia M. P., Sanna E., Sechi G., Biggio G.. **Thiocolchicoside is an antagonist of the function of GABA$_A$ and Glycine Receptors.** Società Italiana di Farmacologia, 32° Congresso Nazionale. Napoli, 1 – 4 Giugno 2005.

3. M. Mameli, P.A. Zamudio, J.L. Sanderson, P. Botta, M. Carta and C.F. Valenzuela. **Effect of ethanol on GABAergic transmission in cerebellar Purkinje neurons.** 35th Society for Neuroscience Meeting, 11-16 November 2005, Washington DC, MD.

4. P. Botta, M. Mameli, C. F. Valenzuela. **Mechanism of the ethanol-induced increase of quantal GABA release at cerebellar Purkinje neurons.** 36th Society for Neuroscience Meeting, October 2006, Atlanta, Georgia.

5. P. Botta, M. Mameli, R.A. Radcliffe, K. Floyd, and C. F. Valenzuela. **Ethanol modulation of GABAergic transmission at cerebellar granule neurons.** 30th Research Society on Alcoholism, July 2007, Chicago, Illinois.

6. P. Botta, C. F. Valenzuela. **Ethanol increases the spontaneous firing of the cerebellar Golgi cells independently of glutamatergic and GABAergic ionotropic receptors.** 37th Society for Neuroscience Meeting, November 2007, San Diego, California.

7. A. Belmenguenai, P. Botta, J. T. Weber, M. Carta, M. De Ruiter, C. De Zeeuw, C. F. Valenzuela and C. Hansel. **Ethanol affects plasticity at cerebellar parallel fiber to Purkinje cell synapses.** 37th Society for Neuroscience Meeting, November 2007, San Diego, California.

8. P. Botta, C. F. Valenzuela. **Ethanol increases frequency and regularity of spontaneous firing via distinct mechanisms in cerebellar Golgi neurons.** 31st Research Society on Alcoholism, June/July 2008, Washington DC.

9. P. Botta, C. F. Valenzuela. **Ethanol increases spontaneous action potential firing frequency of cerebellar Golgi neurons via membrane depolarization.** 38th Society for Neuroscience Meeting, November 2008, Washington DC.

10. P. Botta, A. Lüthi. **Characterization of local neuronal connectivity in central amygdala**. PhD student Retreat, May 2011, Barcelona, Spain.

11. Paolo Botta, Chun Xu, Uwe Rudolph, Andreas Lüthi. **Tonic inhibition in central amygdala inhibitory circuits**. Federation of European neuroscience Societies. July 2012, Barcelona, Spain.

12. Paolo Botta, Lynda Demmou, Chun Xu, Uwe Rudolph, Andreas Lüthi. **Tonic inhibition in central amygdala inhibitory circuits**. Gordon Research Seminar and Conferences on Inhibition in the CNS. June 2013, Les Diablerets, Switzerland.

13. Paolo Botta, Lynda Demmou, Chun Xu, Uwe Rudolph, Andreas Lüthi. **Tonic inhibition in central amygdala inhibitory circuits**. Neurobiology of Synapses and their Dysfunction. October 2013, Stresa, Italy.

Journal Clubs

1. B. Sacchetti *et al.* **Long – term synaptic changes induced in the cerebellar cortex by fear conditioning**. Neuron, 2004, 42: 973 – 982. Presented at the University of New Mexico: November 10th, 2006.

2. E. A.Rancz and Hausser M. **Dendritic Ca^{2+} spikes are tunable triggers of cannabinoid release and short – term synaptic plasticity in cerebellar Purkinje neurons**. The Journal of Neuroscience, 2006, 26(20): 5428 – 5437. Presented at the University of New Mexico: June 29th, 2007.

3. J. Hartmann *et al.* **TRPC3 are required for synaptic transmission and motor coordination**. Neuron, 2008, 14; 59(3): 392 – 398. Presented at the University of New Mexico: August 29th, 2008.

4. Yizhar et al. **Neocortical excitation/inhibition balance in information processing and social dysfunction.** Nature, 2011. Presented at the FMI: September 2011.

5. Atasoy et al. **Deconstruction of a neural circuit for hunger.** Nature, 2012. Presented at the FMI: October 201

THE END

"We shall not cease from exploration, and the end of all our exploring will be to arrive where we started and know the place for the first time."

T. S. Eliot